



## 216715 NEWCOM<sup>++</sup>

### DR.10.2

#### Intermediate report on achievable performance limits of networks and on ways to achieve them

**Contractual Date of Delivery to the CEC:** T0+18

**Actual Date of Delivery to the CEC:** T0+18

**Editor(s):** George Iosifidis, Iordanis Koutsopoulos

**Participating institutions:** NKUA / IASA, RWTH, CNIT, CTTC, FTW, CNRS

**Contributors:** Giuseppa Alfano, Carles Anton, Chiara Buratti, Flavio Fabbri, Laura Galluccio, Paolo Giaccone, Maxime Guillaud, George Iosifidis, Iordanis Koutsopoulos, Javier Matamoros, Roberto Verdone

**Internal Reviewer(s):** Leandros Tassioulas (NKUA / IASA), Sergio Benedetto (POLITO)

**Workpackage number:** WPR.10: Network Theory

**Nature:** R

**Total Effort Spent:** 4 MM

**Dissemination Level:** Public

**Version:** 0.3

#### Abstract:

Deliverable DR.10.2 reports on recent research achievements pertaining to fundamental performance limits of networks and ways to achieve them. These limits are explored under the premise of autonomous networking. A first topic is modeling selfishness and cooperation in a network of autonomous nodes through a utility vs. cost approach. Such a model aims at understanding fundamental insights and design algorithms that guarantee cooperation and discourage selfishness. Massively dense sensor networks are an important class of networks where the study of performance limits will have impact on network operational objectives. We derive analytical models of area throughput and energy consumption in Wireless Sensor Networks (WSNs) and study the impact of connectivity on them. Further, in wireless sensor networks endowed with the task of estimation, we study opportunistic power allocation for energy conservation. We also study the impact of stochastic geometry on fading and interference in wireless networks. Chief among the network control mechanisms that shape performance limits is resource allocation and scheduling. We study message passing algorithms for performing scheduling in a decentralized fashion. We next dwell into distributed optimization and reputation inspired approaches to model resource allocation and content exchange in peer-to-peer autonomous networks. Finally, the deliverable contains a concise report of the status of the Joint Research Activities (JRAs) that are carried out among WP partners with an emphasis on summary of JRA efforts and the way forward.

**Keyword list:** Network Information Theory, Scaling Laws, Throughput and Energy Efficiency, Reputation Mechanisms, Scheduling Algorithms, Peer-to-peer Networks, Sensor Networks, Stochastic Geometry.

**TABLE OF CONTENTS**

<b>1</b>	<b>Introduction</b>	<b>4</b>
1.1	Glossary . . . . .	5
1.2	Acronyms . . . . .	7
<b>2</b>	<b>Cooperation and selfishness in wireless networks</b>	<b>8</b>
2.1	Introduction . . . . .	8
2.1.1	Background . . . . .	8
2.1.2	System Model . . . . .	8
2.1.3	Penalty Definition . . . . .	10
2.1.4	Distributed Algorithm . . . . .	11
2.2	Performance Results . . . . .	14
2.3	Conclusions and future work . . . . .	14
<b>3</b>	<b>Area Throughput and Energy Consumption for Clustered Wireless Sensor Networks</b>	<b>17</b>
3.1	Introduction . . . . .	17
3.2	Related Works . . . . .	17
3.3	System Model . . . . .	18
3.4	Derivation of Network Connectivity and Energy Consumption of Sensors . . . . .	19
3.4.1	Evaluating Audibility of Sensors . . . . .	19
3.4.2	MAC and Throughput Considerations . . . . .	19
3.4.3	Energy Considerations . . . . .	21
3.5	The Model of IEEE 802.15.4 . . . . .	21
3.6	Numerical Results . . . . .	23
<b>4</b>	<b>Opportunistic Power Allocation Schemes for Wireless Sensor Networks With One-bit of Feedback</b>	<b>26</b>
4.1	Introduction . . . . .	26
4.2	Signal Model . . . . .	27
4.3	Opportunistic Power Allocation: Protocol Description . . . . .	29
4.4	OPA for the minimization of distortion (OPA-D) . . . . .	30
4.4.1	Imperfect Channel State Information . . . . .	31
4.5	OPA for the minimization of transmit power (OPA-P) . . . . .	33
4.6	OPA for the Enhancement of Network Lifetime (OPA-LT) . . . . .	34
4.7	Summary . . . . .	35
<b>5</b>	<b>Message passing paradigm in Wireless Networks</b>	<b>37</b>
5.1	Introduction . . . . .	37
5.2	System Model . . . . .	37
5.3	Message passing for MWIS . . . . .	38
5.3.1	Convergence . . . . .	38
5.3.2	Asynchronous implementation . . . . .	39
5.4	Conclusion . . . . .	39
<b>6</b>	<b>Distributed Optimization and Reputation for Modeling Resource Allocation of Peer-to-peer Networks</b>	<b>40</b>
6.1	Introduction . . . . .	40
6.2	Resource Allocation Models in Cooperative Peer-to-peer Networks . . . . .	41
6.2.1	System model and problem statement . . . . .	41
6.2.2	Distributed bandwidth allocation in cooperative peer-to-peer networks . . . . .	43
6.3	Resource Allocation Models in Non-Cooperative Peer-to-peer Networks . . . . .	47

6.3.1	System model and problem statement . . . . .	49
6.3.2	Reputation-assisted utility maximization algorithms . . . . .	50
<b>7</b>	<b>Impact of Stochastic Geometry on Fading and Interference Modeling in Wireless Networks</b>	<b>53</b>
7.1	Introduction . . . . .	53
7.2	System Model and Assumptions . . . . .	54
7.2.1	Spatial gain matrix . . . . .	54
7.2.2	The MIMO Wishart-Poisson model . . . . .	55
7.2.3	Shannon Transform . . . . .	56
7.3	Scaling laws analysis: SIMO upper bound . . . . .	56
7.4	Cut-set bound . . . . .	57
7.4.1	High and low-power mutual information analysis . . . . .	58
7.4.2	Upper bounding the information flow . . . . .	58
7.4.3	On specific spatial correlation models . . . . .	59
7.5	Planned developments . . . . .	61
7.5.1	Short-Range Interference Mitigation . . . . .	61
<b>8</b>	<b>Status of JRAs</b>	<b>64</b>
8.1	JRA 1: Distributed implementations of backpressure protocols in wireless networks . . .	64
8.2	JRA 2: On the Interplay between MAC Protocols and Data Fusion in Wireless Sensor Networks . . . . .	65
8.3	JRA 3: Network entity behavioral modeling as a dynamic game . . . . .	65
8.4	JRA 4: Connectivity and MAC issues and the impact of different node spatial distributions	66
8.5	JRA 5: Scaling laws in wireless networks . . . . .	66
8.6	JRA 6: Cooperative multi-casting algorithms in wireless networks . . . . .	67
<b>9</b>	<b>Conclusions</b>	<b>68</b>

## 1 INTRODUCTION

This deliverable reports on the findings of the NEWCOM++ consortium in Work Package WP10 in the area of Network Theory and presents the recent research achievements pertaining to fundamental performance limits of networks and ways to achieve them. These limits are explored under the premise of autonomous networking where nodes need to be in position to ensure proper network operation. The objectives of WPR.10 are summarized as follows:

- Determine and characterize the fundamental performance limits of wireless networks in terms of throughput, delay and energy efficiency, and to identify fundamental tradeoffs among these parameters. Specifically, it is important to address fundamental theoretical aspects which are essential for wireless networks, including scaling laws and asymptotic behavior of wireless systems when users and nodes dramatically increase, theoretical bounds to such metrics as capacity and network lifetime.
- Develop a network information theory for understanding the theoretical foundations necessary for quantifying fundamental performance limits of wireless networks in capacity, throughput, and delay and devise techniques to closely approximate and even achieve them.
- Understand fundamental tradeoffs and interdependencies in wireless networks, including the interplay between capacity, energy consumption, stability and delay. To this end, information theory will be combined with non-classical constraints such as finite battery life, traffic characteristics, topology and mobility.
- Devise distributed optimization and game-theoretic methods for distributed self-regulating wireless network paradigms, ranging from wireless sensory ones to wireless overlays and autonomous computing. The focus should be on decentralization of network operations and its impact of wireless networks fundamental performance limits.

This report aims at addressing topics that fall within context of the objectives above. A first topic we study is that of modeling selfishness and cooperation in a network of autonomous nodes through a utility vs. cost approach. Such a model aims at understanding fundamental insights and design algorithms that guarantee cooperation and discourage selfishness. We focus on scenarios where there is a need for support of traffic with various QoS requirements. In this setting, it is node contention that arises for obtaining channel access when nodes use the Carrier Sense multiple access protocol. We model the interaction among nodes as a noncooperative game. We present a game-theoretic model with prioritized data transmission in networks where nodes are considered as potential cheaters which should be punished through a deliberate jamming mechanism when misbehaving and trying to monopolize wireless resources. Accordingly, we describe the distributed algorithm to be performed by network nodes and assess the validity of both the model and the implementation algorithm through simulations.

Next, we present a mathematical approach to evaluate the *area throughput* and energy consumption of a multi-sink Wireless Sensor Network (WSNs). Massively dense sensor networks are an important class of networks where the study of performance limits will have direct impact on the network operational objectives. The WSN is organized into clusters, with one sink per cluster collecting data from sensors. A small variation of the Thomas point process is used to model sensors and sink positions in the target area. We denote as area throughput the amount of samples per second successfully transmitted to sinks. Both area throughput and energy consumption are fundamentally related to connectivity and access control issues. The aim of this chapter is to devise a mathematical model that takes access control and connectivity issues into account under a unified framework. We study the behavior of these two performance metrics when varying the target rate, defined as the maximum number of samples the network was deployed to deliver. Results show that a tradeoff between area throughput and the energy consumption must be found. Finally, the impact of different sensor and sink distributions on area throughput is evaluated.

We then consider wireless sensor networks endowed with the task of estimating an unknown parameter we study opportunistic power allocation and control for energy conservation and network lifetime increase. We focus on the design of Opportunistic Power Allocation (OPA) schemes suitable for decentralized parameter estimation in WSNs. We focus on schemes that maximize network lifetime, minimize

the required transmit power and minimize the measurement distortion. In the proposed schemes, we adopt the amplify-and-forward technique for the communication of the sensor observations to a specific fusion center through a set of orthogonal channels. The various power control schemes have one feature in common: only sensors experiencing certain local conditions (i.e. have a metric above a global threshold) are allowed to participate in the estimation process. This strategy is aimed at retaining as much performance as possible of the corresponding *optimal* power allocation scheme while keeping network signalling and energy consumption under control.

Chief among the network control mechanisms that shape performance limits is resource allocation and in particular scheduling. We study message passing algorithms for performing the scheduling operation in a decentralized fashion. We discuss the decentralized formation of independent node sets and asynchronous operation. Message passing algorithms are part of a current Joint Research Activity that aims at applying the rationale of message passing for designing maximum throughput algorithms in IEEE 802.11 CSMA/CA wireless networks.

In the sequel, we discuss distributed resource allocation schemes for wireless peer-to-peer networks. The increasing popularity of these networks and machinery that governs node interactions makes their study very challenging. First, we begin our study for such a network with the assumption that nodes are cooperating. In this case the overall network operation can be modeled as an optimization problem which, however, is amenable to distributed solution by peers that constitute the network. In the sequel, we relax this assumption and define a respective model that captures peers' selfish behavior. We propose and evaluate a reputation based mechanism which is proved to reveal hidden peers' intentions for cooperation.

Finally, in the last chapter, we study the impact of stochastic geometry of node location on fading and interference modeling in wireless networks. In the analysis of large random wireless ad hoc networks, the underlying node distribution is almost exclusively assumed to be the homogeneous Poisson point process. Despite the nice analytical properties of this model, the spatial randomness has been mainly exploited for connectivity and interference level analysis, but has not yet been taken into account explicitly in the scaling laws evaluation. We take a first step towards finding an upper bound on aggregate throughput when the additional randomness due to the spatial node distribution is taken into account, together with the presence of power attenuation and random phase changes. This could be seen as a first attempt to connect some overly optimistic results based on stochastic channel model to more realistic analysis, relying on electromagnetic propagation arguments.

## 1.1 Glossary

**Transport capacity** The amount of bits transported per unit of time and unit of distance in the network

**Network scaling law** A functional relationship between two defining parameters in networks. For instance, a relationship that determines transport capacity  $T(n)$  as function of the number of network nodes is a transport capacity scaling law.

**Connectivity** The concept according to which there exists a path between every pair of distinct network node.

**PPP (Poisson point process)** A static random process that describes the random occurrence of single events in time or space.

**Back-pressure policy** A routing, scheduling and resource allocation policy that is based on the simple principle of performing resource allocation decisions based on queue backlog differentials. It is named after the corresponding natural property of fluid flows. The back-pressure policy is provably has the largest capacity region, namely it can support the largest amount of load such that queue backlogs remain bounded.

**Protocol misbehavior** The intentional deviation from legitimate protocol operation, initiated due to

the selfish inclination of a node to be better off either by obtaining higher share of resources in the network than the nominal one or by preserving costly resources against a protocol rules.

**Distortion** The error incurred while estimating an unknown parameter or process through some estimation scheme.

**Nash Equilibrium** When defined in a utility maximization context, it is an operating point, or strategy vector, at which the utility of each node cannot be increased if this node unilaterally changes its strategy. When defined in a cost minimization context, it is an operating point, or strategy vector, at which the cost of each node cannot be decreased if this node unilaterally changes its strategy.

**Pareto Equilibrium** It is an operating point which has the following property: there does not exist a way to change from one allocation to another, which can make at least one individual better off, without making any other individual worse off.

**Nash Bargaining Solution** The Nash bargaining game is a two-player game, where two players demand a portion of some good. If the two proposals sum to no more than the total good, then both players get their demand. Otherwise, both get nothing. A Nash bargaining solution is a (Pareto efficient) solution to a Nash bargaining game.

**Message Passing Algorithms** Class of algorithms that are based on iterative passing of certain messages among nodes, such that nodes solve a hard combinatorial optimization problem without the need for central administration.

**Independent Set** A set of nodes in a graph, no pair of which are connected through an edge.

**Spatial Correlation** The term that is used to describe the phenomenon that random points in space exhibit similarity in certain properties.

## 1.2 Acronyms

<b>SINR</b>	Signal to Interference and Noise Ratio
<b>SNR</b>	Signal to Noise Ratio
<b>Bps</b>	Bits per second
<b>MIMO</b>	Multiple Input Multiple Output
<b>SIMO</b>	Single Input Multiple Output
<b>MISO</b>	Multiple Input Single Output
<b>PPP</b>	Poisson Point Process
<b>WSN</b>	Wireless Sensor Network
<b>FDMA</b>	Frequency Division Multiple Access
<b>NUM</b>	Network Utility Maximization
<b>KKT</b>	Karush Kuhn Tucker
<b>MAC</b>	Medium Access Control
<b>QoS</b>	Quality of Service
<b>FC</b>	Fusion Center
<b>CSI</b>	Channel State Information
<b>CRLB</b>	Cramer Rao Lower Bound
<b>BLUE</b>	Best Linear Unbiased Estimator
<b>REI</b>	Residual Energy Information
<b>CDF</b>	Cumulative Density Function
<b>PAN</b>	Personal Area Network
<b>JRA</b>	Joint Research Activity
<b>LP</b>	Linear Programming
<b>ILP</b>	Integer Linear Programming
<b>CSMA</b>	Carrier Sense Multiple Access
<b>CA</b>	Collision Avoidance
<b>OPA</b>	Opportunistic Power Allocation
<b>MWIS</b>	Maximum Weight Independent Set
<b>DCF</b>	Distributed Coordination Function
<b>DIFS</b>	DCF Interframe Space
<b>WF</b>	Water Filling
<b>AWGN</b>	Additive White Gaussian Noise
<b>UPA</b>	Uniform Power Allocation
<b>LT</b>	Lifetime
<b>NP</b>	Non-polynomial
<b>TCP</b>	Transport Control Protocol
<b>BS</b>	Base Station
<b>ACK</b>	Acknowledgment
<b>ML</b>	Maximum Likelihood
<b>AP</b>	Access Point
<b>BPP</b>	Binomial Point Process
<b>TPP</b>	Thomas Point Process
<b>OPNET</b>	Optimized Network Evaluation Tool
<b>IEEE</b>	Institute of Electrical and Electronic Engineers

## 2 COOPERATION AND SELFISHNESS IN WIRELESS NETWORKS

### 2.1 Introduction

In several wireless scenarios, cooperation between nodes is crucial for efficient network operation. Indeed, cooperation is necessary to ensure the correct functionalities of contention based MAC protocols, routing in ad-hoc networks, and spectrum sharing, to name a few. Unfortunately, *selfish* behaviors may emerge in several cases which cannot be dealt with by traditional security strategies. In fact, security traditionally copes with *malicious* behaviors, i.e., behaviors aimed at harming communication. Differently, a behavior is "**selfish** if it aims at obtaining an advantage that can be quantitatively expressed in the units (bit rate, Loules or coverage) of wireless networking or in a related incentive system (e.g. micro-payments). Any other misbehavior is considered to be **malicious** [1]."

The objective of this chapter is to lay a theoretical framework for the characterization and study of *selfishness* and *cooperation* in wireless sensor networks. The final framework will be hopefully as general as possible in the characterization of the most appropriate utility functions and in the identification of the conditions that should be met in such a way that the network operates efficiently. However, the framework will be utilized to study specific scenarios such as MAC protocols and forwarding in ad hoc networks.

Indeed, in the first phase of the project, attention has been focused on the study of selfishness and the design of strategies that enforce cooperation between nodes, in the case of CSMA-like medium access control which support nodes with different level of priorities [2]. Details of this activity is reported in the following of this chapter.

#### 2.1.1 Background

The considered scenario can be modeled using a game theoretic approach. Game theory, although originally conceived for economic applications, has been recently used to model wireless network scenarios. As an example, in [3] the authors use the game theory to model a slotted ALOHA scenario where two power-constrained nodes can jam each other. There, considerations on optimal access and jamming strategies are drawn. In [4], similarly to [3], stability in multi-packet Aloha networks is studied and modeled through a game-theoretic approach. Another example of a game-theoretic framework for dealing with the MAC layer misbehavior is provided in [5]. Using a dynamic game model, the authors derive the strategy that each node should follow in terms of controlling channel access probability by adjustment of contention window, so that the network reaches its equilibrium. However, QoS support is not addressed in [5].

Starting from the work in [5], we have proposed to model the prioritized transmission of traffic in wireless CSMA/CA networks through a game-theoretic approach. We have considered a simple CSMA/CA network where different types of user traffic can be supported and use a redefinition of the penalization mechanism to be used to let nodes well behave reaching an efficient utilization of the wireless medium. The penalization mechanism has been defined to let the system work around a Nash equilibrium that is also Pareto optimal and allow for an efficient utilization of the wireless medium. Then, for the sake of comparison, we have compared the analytical results to those obtained using the OPNET Modeler in order to assess the validity of the algorithm used to implement the mathematical model.

#### 2.1.2 System Model

Let us consider a network composed of  $N$  wireless nodes employing a CSMA/CA MAC protocol. Nodes are assumed to use an IEEE 802.11 DCF-like access mechanism for contending over the wireless medium. Furthermore, we assume that they are in the same collision domain so that the hidden terminal problem can be neglected<sup>1</sup>.

<sup>1</sup>This is a common simplifying assumption used in the literature [5] and is justified by considering as contending nodes, time by time, only those nodes that are in proximity and can hear each other.

Also each node is assumed to transmit traffic labeled as belonging to a certain priority class during all network lifetime and this class does not change during network functioning, unless a refresh procedure is invoked. We assume that nodes do not lie about their traffic priority class given that schemes exist that allow authentication of the source of a certain packet and its priority [6]. Each node is assumed to be selfish, i.e. it tries to monopolize the wireless resource on its turn. This means that each node can be potentially seen as a *cheater* who tunes its contention window so as to maximize its profit, i.e. its use of the wireless resource. This basically means that cheater nodes set their window size to lower values so as to reduce contention and achieve higher wireless resource utilization. Such a scenario can be modeled as a *game*, where *players* can be identified with nodes and try to maximize their *utility* identified with throughput.

Recently, there has been some effort on modeling these games related to medium access, e.g. in [5], but no consideration of QoS requirements was introduced. We advocate that the condition where nodes can have different requirements in terms of traffic and thus priority is realistic and interesting. Due to space constraints in the rest of this paper we will assume knowledge of some fundamentals and notation on game theory. A more detailed tutorial on game theory can be found in [7].

We assume as a starting point the dynamic game model introduced in [5] where a set of cheaters,  $C$  is considered. In our work, instead, we assume that all nodes are potential cheaters and thus are able to tune their contention window size  $W_i$  so as to maximize their utility,  $U_i$ , identified with their throughput,  $r_i$ . The contention window size is assumed to take values in the interval  $[W_m, W_M]$ . Cheaters emit traffic belonging to  $Z$  different traffic priority classes. Cheaters are assumed to be rational, i.e. each cheater makes rational reasoning and tries to maximize his own benefit. To this end, cheater nodes are assumed *not* to follow the CSMA/CA exponential back-off mechanism and thus try to tune their contention window size on their advantage.

As a preliminary step, in order to characterize the game, we must define a generic node strategy which can be identified with the values assumed by his contention window size at the observation time instants,  $T_i$ , i.e.  $S_i = \{W_i(T_1), W_i(T_2), \dots, W_i(T_y)\}$ , where  $T_y$  is the time when the game stops. In [5], the utility, i.e. the node throughput is derived from the formula proposed in [8]. According to this model, the access probability of a cheater at a given time instant  $\tau_i^c$ , can be related to its contention window size  $W_i$  as shown below:

$$\tau_i^c = \frac{2}{1 + W_i} \quad (1)$$

Then, the throughput of the cheater, as defined in [5], is:

$$r_i = \frac{\tau_i^c c_i^1}{\tau_i^c c_i^2 + c_i^3} \quad (2)$$

where:

- $\alpha_{-i} = \prod_{j \neq i} (1 - \tau_j^c) \prod_k (1 - \tau_k^l)$
- $s_{-i} = \sum_{j \neq i} \tau_j^c \prod_{k, d \neq i, j} (1 - \tau_k^c) (1 - \tau_d^l)$
- $c_i^1 = \alpha_{-i} \bar{L}$
- $c_i^2 = \alpha_{-i} (T_s - ST) - s_{-i} (T_s - T_c)$
- $c_i^3 = (1 - \alpha_{-i} - s_{-i}) T_c + s_{-i} T_s + \alpha_{-i} ST$
- $\tau_i^l$  is the access probability of the nodes which do not act as cheaters
- $\bar{L}$  is the average packet size
- $ST$  is the slot time considered in the standard
- $T_s$  is the average time needed to transmit a correct frame
- $T_c$  is the average time lost in a collision

According to the standard, time  $T_s$  and  $T_c$  are defined as  $T_s = T_{PHYh} + T_{MAC} + \bar{L} + SIFS + \delta + T_{ACK} + DIFS + \delta$  and  $T_c = T_{PHYh} + T_{MAC} + \bar{L} + DIFS + \delta$ , being  $\delta$  the propagation delay and the other time intervals defined by the standard. Using the throughput computed in [8], we represent the model in terms

of the strategy of a player, i.e., the set of contention window and payoff values. The strategic form for an  $N$ -players game is the  $N$ -tuple  $(\Sigma_1, \dots, \Sigma_N, f_1, \dots, f_N)$ , where  $\Sigma_i$  is the strategy of player  $i$ , i.e. its contention window size values at the different time instants and  $f_i$  is its payoff function.

It has been demonstrated in [5] that a game like the one described above has  $W_M^N - (W_M - 1)^N$  Nash equilibrium points, all characterized by having at least one node with a unit contention window. When there is only one cheater having a unit contention window, it gets all the throughput and other nodes get zero pay-off; when more than one cheaters have a unit contention window, the so called *tragedy of commons* is met. So it is necessary to figure out if there is a way to let the system work in appropriate fair conditions. To this purpose, exploiting the results obtained in [5], a Nash bargaining framework can be discussed showing that a unique Pareto optimal solution to the contention window optimization problem exists, different from the unit contention window size. The problem now becomes that of letting the system work and converge towards this equilibrium point. This can be obtained by setting up a penalization mechanism. The penalization mechanism, implemented at all nodes, guarantees that misbehaving nodes, i.e. nodes who would like to set their contention window to a lower value, are punished by other competing nodes so as to let the system work around a fairness equilibrium point. To this end, a dynamic game can be proposed where nodes modify their behavior and act based on other nodes moves. Accordingly, the pay-off function of node  $i$  can be redefined by considering a penalty as:

$$f_i = U_i - P_i = r_i - P_i \quad (3)$$

In the above formula,  $P_i$  represents the penalty suffered by node  $i$  as a consequence of what was imposed by other nodes. In general, the penalty that player  $j$  inflicts to player  $i$  is:

$$P_i = \begin{cases} r_i - r_j & \text{if } \tau_i > \tau_j \\ 0 & \text{otherwise} \end{cases} \quad (4)$$

The above penalization-aware definition of the utility function proposed in [5], however, does not take into account the possibility to support traffic with different QoS requirements. In this work, we propose to redefine the penalization mechanism to take into account this aspect. The penalization mechanism is defined to produce a Nash equilibrium that allows an efficient utilization of the wireless medium, so it is Pareto optimal, and the throughput of a player depends on its priority.

### 2.1.3 Penalty Definition

In our scenario we consider  $Z$  different priority classes. We would like to relate the difference between the two generic users' throughput to the priority classes. To this end, we call  $p_{diff}(N, Ch_u)$  the percentage of throughput that two players with contiguous priority classes diverge. Observe that  $p_{diff}$  in general depends on the number  $N$  of nodes in the domain or the channel utilization,  $Ch_u$ . However, for sake of simplicity, in the following we will assume that  $p_{diff}$  is constant. More specifically, if we assume that nodes  $i$  and  $j$  emit traffic belonging to different traffic priority classes,  $a$  and  $b$  respectively, where  $a = b + 1$ , the penalization mechanism should guarantee that  $r_i > r_j$  and in particular,  $r_i = r_j + p_{diff} \cdot r_j$ . So, we can define a new parameter denoted as *expected throughput* and given as follows:

$$r_{i,j}^{exp} = \begin{cases} [1 + p_{diff}]^{(pr_j - pr_i)} \cdot r_i & \text{if } pr_i < pr_j \\ \frac{1}{[1 + p_{diff}]^{(pr_i - pr_j)}} \cdot r_i & \text{otherwise} \end{cases} \quad (5)$$

The above formula represents the throughput that node  $i$  expects from node  $j$ , where  $pr_i$  is the priority of node  $i$  and  $pr_j$  is the priority of node  $j$ . We want to redefine the payoff function in equation (3) by considering a penalty which is a fraction of the node utility, i.e.  $P_i = \xi \cdot U_i = \xi \cdot r_i$ . In this way we update penalization so as to make it dynamically adaptable to the current network conditions. As a consequence, from (3) it follows  $f_i = U_i - P_i = U_i - \xi \cdot U_i = (1 - \xi) \cdot r_i = \wp_i \cdot r_i$  where  $\wp_i$  is the overall reduction probability that is related to the penalization that all other nodes, other than  $i$  itself, inflict to  $i$ . In particular we define  $\wp_i$  as:  $\wp_i = 1 - \prod_{j=1, j \neq i}^N (1 - P_{j,i})$ .

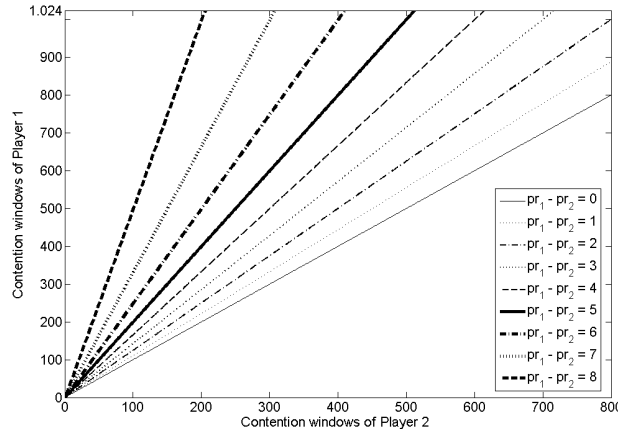


Figure 1: Nash equilibria of a two player game depending on the difference between the traffic priority classes.

$pr_1 - pr_2$	$W_1$	$W_2$	$r_1$ [Mb/s]	$r_2$ [Mb/s]	Ch. util. [%]
0	20	20	0.8149	0.8149	81.49%
2	17	21	0.9058	0.7247	81.50%
4	16	26	1.0216	0.6130	81.73 %
6	13	31	1.1746	0.4699	82.22 %
8	10	46	1.3908	0.2782	83.44 %

Table 1: Pareto optimal points obtained in case of  $N = 2$  nodes and different traffic priorities.

Accordingly, the penalization probability, i.e. the probability that node  $j$  penalizes node  $i$ ,  $P_{j,i}$ , will be related to the percentage of deviation from the expected throughput value. More specifically,  $P_{j,i}$  will be:

$$P_{j,i} = \begin{cases} 1 - \frac{r_i - r_{j,i}^{exp}}{r_i} & \text{if } r_i \geq r_{j,i}^{exp} \\ 1 & \text{otherwise} \end{cases} \quad (6)$$

This re-formulation of the penalty allows to extend the framework in [5] when considering the difference in the traffic priority classes. In fact, if  $pr_i = pr_j$  it follows that  $f_i = r_i$ . By generalizing the game for  $N$  players, we obtain that the Pareto Optimal Point is the one where players, belonging to the same traffic priority class exhibit an access priority whose value can be obtained by [8] as:

$$\tau_{fair}(N) \approx \frac{1}{N \sqrt{T_c / (2 \cdot ST)}} \quad (7)$$

By using the reformulated framework and assuming to consider only two players, where the traffic of the first one has higher priority with respect to the second one, a number of Nash equilibria can be identified. They are shown in Figure 1 when the difference in the traffic priority classes increases. This exemplary figure has been obtained assuming  $p_{diff} = 10\%$ . For sake of completeness, Table 1 shows the Pareto optimal points for each set of the Nash equilibria and different combinations of traffic priority classes difference. As expected, the throughput of player 1,  $r_1$ , belonging to the higher traffic priority class, increases when the difference in the priority values increases as well. Opposite considerations apply to player 2. Also, channel utilization increases when  $(pr_1 - pr_2)$  increases.

#### 2.1.4 Distributed Algorithm

In the previous sections we discussed the penalty function and analyzed the static game to find the Pareto Optimal Equilibria. In this section we describe the algorithm to reach the optimal point in a distributed way. The initial assumptions are:

- The number of nodes is known in advance to all players,
- All nodes can be cheaters in general,
- All nodes are in the same radio range,
- Nodes always have a frame to transmit.

The algorithm for reaching the Pareto-Optimal Equilibria performs the following tasks:

1. Define the contention window values both at the initialization phase and during network functioning,
2. Define the penalization values once estimated the nodes' throughput,
3. Calculate the pay-off value for each node.

In Figure 2, the pseudo-code of the algorithm main function is shown. After the initialization phase, the contention window value is updated exploiting the results in (7). The initial value is fair and chosen as the initial starting point in the hypothesis of fairly sharing the available bandwidth at the beginning of network activity. Then, taking into account the difference in the priority classes, the system evolves among Pareto optimal equilibria conditions. To this purpose, the values of the access probabilities will be evaluated using equation (1). Then, the value of the real and expected throughput of each cheater will be evaluated through equations (2) and (5). Consequently all nodes will be able to calculate the penalty to inflict to each cheater. This will allow to calculate the pay-off value which is needed to estimate the new contention window size.

The penalization mechanism will be implemented by jamming the traffic of the nodes that violate the expected throughput. In fact, jamming does not allow for correct reception of the traffic sent by a certain cheater to a specific destination. Consequently no confirmation ACKs will be received by the sender. A node will estimate the probability to be penalized by network nodes through consideration of the ratio between the number of data packets it sent in the last observation window and the number of ACKs being received.

Two kinds of cheater nodes can be distinguished:

- *Repentant cheaters* which tend to increase their contention window size and reduce their throughput, once jammed by other nodes
- *Recidivous cheaters* who keep on decreasing their contention window size even if jammed by other nodes

If a node is classified by others as a repentant cheater, other nodes do not penalize this node anymore since they will appreciate its trend to comply with network rules. Instead, if a node is classified as recidivous cheater, other nodes will penalize it according to the penalty estimation in equation (6).

Concerning the evaluation of the contention window size, note that each player exhibits a rational behavior so as to maximize its throughput. To this purpose, a cheater aims at not being punished or jammed by other nodes and consequently it would like to be considered by other nodes as a repentant rather than recidivous cheater. Accordingly, each cheater evaluates if it exceeds the expected throughput and, if this is the case, it decreases its contention window size of a minimal value so that other nodes judge it as a repentant player. So, at each cycle, a cheater estimates the throughput that other nodes expect from it and, if at least one node judges it as exceeding the expected throughput, it increases its contention window size so as not to be jammed.

If, instead, its throughput is not exceeding the expected value, the cheater node aims at increasing its pay-off. Accordingly, cheaters will pass through a sequence of efficient equilibrium conditions while also taking into account different traffic priority classes. Penalization represents deviation from the optimal working point. So when no nodes penalize a cheater, it can move its working point towards the Pareto optimal condition. Instead, as soon as a node starts to be penalized, it means it is deviating from the equilibrium and thus a feedback mechanism is applied to let the system work properly around the equilibrium.

**Function 1****Main**


---

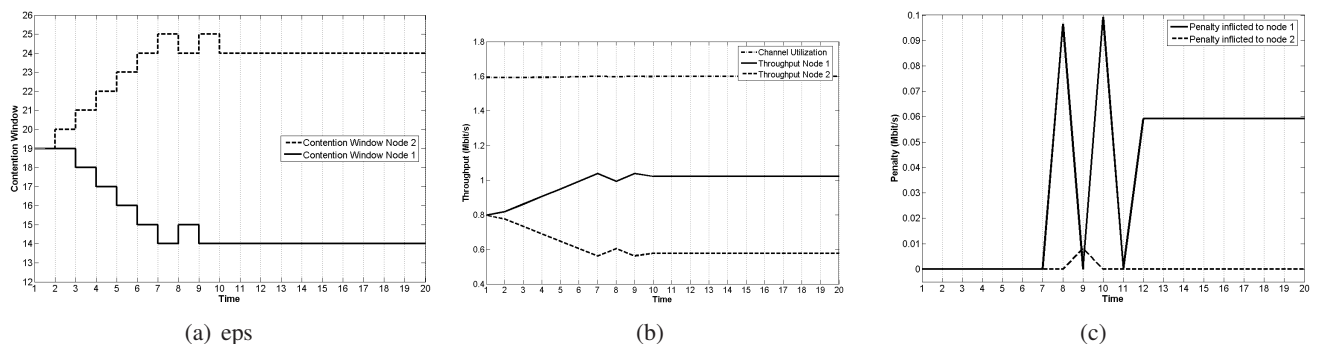
```

/* INITIALIZATION PHASE */
//Define the initial CW value being N the number of nodes
 $W_i(0) = \frac{2}{\tau_{fair}(N)} - 1$  and  $\tau_{fair}(N)$  defined in eq. (7)
//Evaluate the throughput of each node and its expected value
 $(r_i(0), r_{j,i}^{exp}(0)) = evaluate\_throughput(i)$ ;
/*Build  $P_{i,j}$  a matrix containing the penalty values that node  $i$  inflicts to all other nodes  $j$ */
 $P_{i,j}(0) = evaluate\_penalty(r_i, r_{j,i}^{exp}, pr_i)$ ;
//Evaluate the pay-off value
 $f_i(0) = evaluate\_pay\_off()$ ;
/* END OF THE INITIALIZATION PHASE */
while TRUE do
  //Define the new contention window according to the pay-off
   $W_i(t) = evaluate\_next\_cw(f_i(t-1))$ ;
  //Evaluate the new throughput value
   $(r_i(t), r_{j,i}^{exp}(t)) = evaluate\_throughput(i)$ ;
  //Update the penalization
   $P_{i,j}(t) = evaluate\_penalty(r_i, r_{j,i}^{exp}, pr_i)$ ;
  //Evaluate the new pay-off value
   $f_i(t) = evaluate\_pay\_off()$ ;
end while

```

---

Figure 2: Pseudo-code of the distributed algorithm.

Figure 3: (a) Contention window size (b) Throughput and channel utilization (c) Penalty for a scenario with  $N = 2$ ,  $pr_1 = 5$  and  $pr_2 = 1$ .

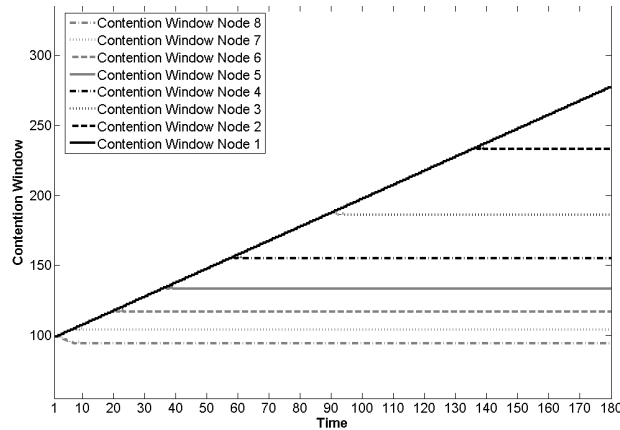


Figure 4: (a) Contention window size for a scenario with  $pr_i = i$  and  $i \in 1 \dots 8$ .

$pr_i$	1	2	3	4	5	6	7	8
$f_i$	0.08	0.09	0.09	0.09	0.1	0.12	0.16	0.29
$r_i$	0.08	0.11	0.14	0.17	0.20	0.23	0.26	0.29

Table 2: Average throughput and payoff for a scenario with  $pr_i = i$  and  $i \in 1 \dots 8$ .

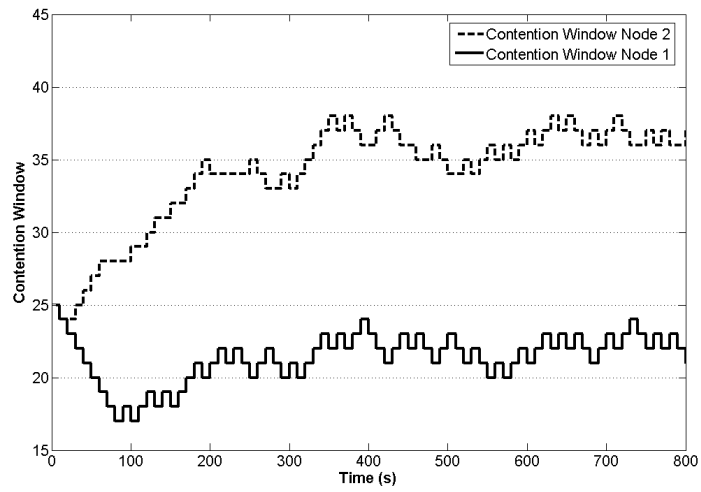
## 2.2 Performance Results

In this section we show the performance results obtained both analytically and simulatively through the OPNET Modeler. We illustrate the results obtained for a scenario where two nodes contend for the wireless channel access. These nodes have different traffic priority classes, namely node 1 traffic is labeled as class 5, i.e.  $pr_1 = 5$ , and node 2 traffic is labeled as class 1, i.e.  $pr_2 = 1$  where higher  $pr_i$  means higher traffic priority. Consequently, node 1 is expected to exhibit a lower contention window size and higher throughput and channel utilization than node 2. This is evident looking at Figures 3(a) and 3(b). Moreover, let us observe that the algorithm converges faster since after only 10 seconds the two nodes stabilize to the equilibrium point. Concerning the penalty shown in Figure 3(c), we observe that the contention window stabilizes when one of the two nodes is penalized which happens when node 1 and 2 try to decrease their contention window size.

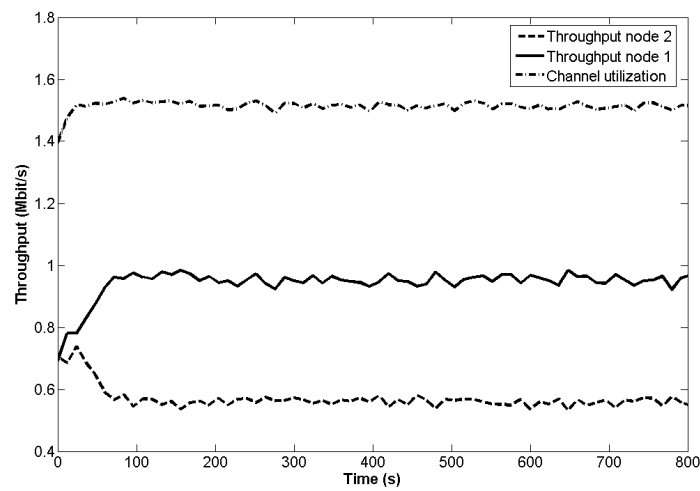
In order to investigate the dynamics of a more crowded scenario, in Figure 4 we show the contention window size in case of eight players with eight different traffic priority classes. As expected, contention windows are in decreasing order of priority. The corresponding average throughput and the pay off values are shown in Table 2 and increases with the traffic priority class. The interesting aspect here relies on the loss of performance due to penalization, especially in case of nodes 4, 5 and 6 who exhibit a throughput violating the expected values and, thus, are penalized more. Concerning simulation results, similarly to the analytical study, we addressed a scenario with two nodes having  $pr_1 = 5$  and  $pr_2 = 1$ . In Figures 5(a) and 5(b), we show the contention window size, the throughput and channel utilization obtained in this case. By comparing Figures 3 and 5, we observe similar behavior especially in terms of throughput and utilization. Finally, in Table 3 we summarize the throughput results obtained using the game-theoretic analysis and the simulation. We observe that throughput is not dissimilar in the two cases. This assesses the validity of the developed framework and the correspondence between analysis and simulations.

## 2.3 Conclusions and future work

In the first phase of the project we introduced a game-theoretic model of prioritized transmission in CSMA/CA networks. Distributed algorithms needed to let the system work properly around the estimated Pareto equilibrium points have been discussed. Analytical results have been compared to those obtained using the OPNET Modeler to assess the validity of the framework and the efficacy of the algorithm.



(a)



(b)

Figure 5: OPNET Modeler: (a) Contention window (b) Throughput and channel utilization for a scenario with  $N = 2$ ,  $pr_1 = 5$  and  $pr_2 = 1$ .

$pr_1 - pr_2$	$r_1^A$	$r_2^A$	$r_1^O$	$r_2^O$
0	0.796	0.796	0.750	0.749
2	0.885	0.708	0.836	0.668
4	1.021	0.577	0.943	0.566
6	1.161	0.446	1.077	0.453

Table 3: Two nodes game with different priorities. Comparison between: Pareto Optimal Points Analytical Results (A) and OPNET Modeler results (O).

As mentioned above, the research work is the prelude of a Joint Research Activity (JRA) between CNIT-University of Catania and NKUA/IASA. We are currently considering the case in which all nodes can have both cooperative and a selfish behavior depending on what is the most convenient choice. In particular, some preliminary results provide the hint that a certain number of cooperating nodes should be available in the system in order for the network to converge towards a state in which resources are utilized efficiently. Accordingly, network administrator could introduce in the system special nodes that have the objective of participating in the cooperation enforcement (sort of *guardian nodes*). In the future we plan to study the dynamics of the system. To this purpose we will identify the most appropriate modeling tool. Markov chains and Markov Decision Processes will be considered as a first option but other modeling tools will be considered as well.

### 3 AREA THROUGHPUT AND ENERGY CONSUMPTION FOR CLUSTERED WIRELESS SENSOR NETWORKS

#### 3.1 Introduction

Wireless Sensor Networks (WSNs) [9] have become a subject of intense study recently as they are one of the classes of networks that are expected to form the Wireless Internet. In the most common scenario considered in the literature a collection of sensor nodes (hereafter called simply *sensors*) is assumed to be deployed in a target area, each taking measurements on local environmental conditions which are then communicated to one or more sinks. Accurate estimation of the environment requires sufficient amount of measurement data sampled from the area of interest (target area). Because of this, it is of interest to study the capacity of such networks. Energy consumption is the other key performance figure for any WSN. The focus of this chapter is to study both of these metrics in a unified framework.

When the number of sensors on the target area is large, several sinks are usually distributed to gather data and sensors are often further organized in clusters. One sink per cluster forwards the queries to sensors, and collects the responses. These networks, called *clustered* WSNs in the following, are precisely the ones studied here. The aim of this chapter is to evaluate the *area throughput* and the energy consumed by the network in the above scenario. The *area throughput* is defined as the number of samples per unit of time successfully transmitted to the centralized unit, originating from the target area. Both the *area throughput* and energy consumption are analytically evaluated here, and both MAC and connectivity issues are taken into account under a joint approach for the evaluation of these target metrics.

All of the results are obtained as a function of the *target rate*, defined as the maximum number of samples the network was deployed to deliver, that is, the amount of traffic that sensors are able to offer to the infrastructure. The analytical framework developed is generic, but we also show how to apply it specifically in networks based on the widely adopted IEEE 802.15.4 MAC protocol [10]. We also explicitly consider the effect of sensors deployment. While uniform distribution of sensors after deployment is often a useful approximation, it is not always achievable or not even desirable in practice. For many deployment techniques, such as real drops, sensors tend to become placed in clusters of different sizes. The clustering of short range radios has been shown to occur also in other natural contexts, see, for example, [11]. We employ a parameterized model for describing these clusters, called the *Thomas point process* (TPP). The use of TPP allows us to characterize in detail the impact of the inhomogeneity and node densities on the metrics of interest. We shall give a detailed introduction to these models and other elements of our system model below.

The rest of the chapter is organized as follows. We first give an overview of the state of the art in Section 3.2. Section 3.3 introduces the system model and describes the considered deployment scenario. In Section 3.4 the *area throughput* is defined and analytically evaluated and energy considerations are also provided. In Section 3.5 the mathematical model of 802.15.4 used here, is briefly introduced. Finally, in Section 3.6 numerical results are presented.

#### 3.2 Related Works

Many works in the literature are related to the modeling of different MAC protocols, and also to connectivity models, but very few papers jointly consider the two issues under a mathematical approach. Some analysis of the two aspects are performed through simulations [12]. Many papers devoted their attention to connectivity issues of wireless ad-hoc and sensor networks in the past (e.g., [13]). Single-sink scenarios have attracted more attention so far. However, an example of multi-sink scenario can be found in [14]. The very typical models for nodes spatial distribution in static wireless networks (i.e. not considering distributions originated from a particular mobility pattern of nodes) are the Poisson point process (PPP) and the Binomial point process (BPP) with very few exceptions ([15] is one of them). In [16] and [17], the authors use (among others) a modified Thomas model [18] for describing real-world nodes deployments with a good accuracy. All previously cited works do not account for MAC issues, with the one exception known to us in a slightly different context, namely the work by Hoydis et al. [19].

The model proposed here is based on the following previous works. The *area throughput* concept was introduced in [20] where authors also presented a mathematical model for its evaluation limited to the case of uniformly distributed sensors and sinks. Here we extend this analysis to non-uniform deployments. Moreover, in [20] no energy consideration was provided. The mathematical model used to derive the probability of success for the transmission of a packet in an IEEE 802.15.4 (Non Beacon-Enabled mode) single-sink scenario has been introduced in [21, 22]. Finally, in [21] a mathematical model to derive the energy consumption of an IEEE 802.15.4 device transmitting packets of a fixed size, is introduced. Here this model has been extended to handle the case where packets of arbitrary size (see Section 3.5) are transmitted, and used for the evaluation of the energy consumed with respect to our reference scenario.

### 3.3 System Model

In this section, we detail the system model considered in the rest of the chapter. We assume that sensors are deployed in clusters each containing one sink and a number of cluster members. We further assume that the sinks are deployed uniformly on a plane, with overall density  $\rho$  [ $m^{-2}$ ]. For convenience in the calculations we assume an infinite plane surface on which sensors are deployed. In practise our results will be a good approximation in the finite area case provided the average transmission range of the devices is small enough. Otherwise, dealing with the edge effects would require additional work, and the shape of the deployment area should be included as a parameter in the system model. We then assume that each cluster associated to a given sink has a Poisson distributed number (with mean  $\mu$ ) of cluster members. The locations of these cluster members are taken to follow normal distribution with mean at the location of the sink, and with covariance matrix  $\text{diag}(\sigma_x^2, \sigma_y^2)$ . This is a small variation of the TPP used as a sensor location distribution model in, for example, [17].

In order to reason about the connectivity structure of the clusters a model for connectivity is needed. We use the link model employed in [20], which accounts for both distance-dependent deterministic loss and channel fluctuations. It is given in terms of the connection probability for nodes at distance  $d$  apart, which takes the form

$$C(d) = 1 - \frac{1}{2} \text{erfc} \left( \frac{L_{\text{th}} - k_0 - k_1 \ln d}{2\sigma_S} \right), \quad (8)$$

where  $\sigma_S$  is the standard deviation of the channel fluctuations Gaussian distributed,  $L_{\text{th}}$  is the maximum tolerated loss,  $k_0$  and  $k_1$  are model dependent constants.

For data gathering and communications, we assume a simple polling model, in which sinks periodically issue queries causing all the cluster members perform sensing and communicating their measurement results back to the sinks they are associated with. We also assume that for communication the sensors utilize standard IEEE 802.15.4 [10], with the sinks acting as PAN coordinators and network operating in the Non Beacon-Enabled mode. We assume that the different PANs established by the sinks use different frequency channels (spatial reuse is used in case more than 16 PANs are present). Therefore no collisions can occur between nodes belonging to different PANs. However, nodes belonging to the same cluster will compete on channel access when they try to transmit their packets to the sink. Since our focus is on gathering of data from sensors to sinks, we shall assume that any communication between the sinks does not interfere with the intra-cluster communications.

We shall conclude this section by a short discussion on the limitations and possible extensions of this system model. The assumption of IEEE 802.15.4 radio is in itself a non-controversial one. However, assuming the use of the IEEE 802.15.4 MAC layer is a choice that can obviously be relaxed. Numerous alternative MAC protocols have been developed by the sensor networking community, each with their own pros and cons. Nevertheless, due to its standardised state, we believe that the IEEE 802.15.4 MAC makes for a natural starting point. Also the network deployment model can obviously be changed. Such a change can be made in two manners: different sinks and sensors distributions could be studied and also the way sensors are associated to sinks can be modified.

### 3.4 Derivation of Network Connectivity and Energy Consumption of Sensors

According to our assumptions, network connectivity is enhanced as the number of sensors that can gain access to a sink is made as large as possible. Communication from sensor to sink is permitted if the power received by the latter is sufficient (in which case the sensor is said to be *audible* to the sink), and if the number of (tentative) communication attempts taking place simultaneously is not too large (in which case we expect the transmission to be successful)<sup>2</sup>. The first condition relates to the physical layer, while the second is a MAC issue. Now we treat the two aspect separately in the next two subsections, ending up with a unified model that yields the *area throughput* [20], which is defined and characterized precisely in the following. Energy considerations are discussed in Section 3.4.3.

#### 3.4.1 Evaluating Audibility of Sensors

Let us recall from our system model that we assume sinks uniformly distributed on the infinite plane with density  $\rho$  [ $m^{-2}$ ] and that sink each gives rise to a cluster which hence contains one sink and a number of cluster members,  $n$ , Poisson distributed with mean  $\mu$ . The p.d.f. of the positions of a sensor in a cluster is a 2D Gaussian, i.e.

$$f_{X,Y}(x,y) = \frac{1}{2\pi\sigma_x\sigma_y} e^{-\frac{x^2}{2\sigma_x^2}} e^{-\frac{y^2}{2\sigma_y^2}}, \quad (9)$$

where we assumed that the cluster center lies at the origin.

Now suppose each sensor has to reach its sink through direct single hop communication. If we employ the random connection model and denote by  $C(d)$  the probability (8) that two sensors at distance  $d$  are audible, the probability that an arbitrary sensor in a cluster is audible to the sink is (after deconditioning with respect to the position)

$$p = \frac{1}{2\pi\sigma_x\sigma_y} \int_{-\infty}^{\infty} \int_{-\infty}^{\infty} C(\sqrt{x^2+y^2}) e^{-\frac{x^2}{2\sigma_x^2}} e^{-\frac{y^2}{2\sigma_y^2}} dx dy. \quad (10)$$

Assuming independence between two audibility events, we have for a single cluster

$$\text{Prob}\{k \text{ audible sensors} | n \text{ sensors in all}\} = \binom{n}{k} p^k (1-p)^{n-k}, \quad (11)$$

yielding

$$\text{Prob}\{k \text{ audible sensors}\} = \sum_{n=k}^{\infty} \binom{n}{k} p^k (1-p)^{n-k} \frac{\mu^n}{n!} e^{-\mu}. \quad (12)$$

The expected number of sensors per cluster that are audible to the sink is now given by

$$\bar{k} = \sum_{k=0}^{\infty} k \cdot \sum_{n=k}^{\infty} \binom{n}{k} p^k (1-p)^{n-k} \frac{\mu^n}{n!} e^{-\mu}. \quad (13)$$

#### 3.4.2 MAC and Throughput Considerations

We assume that sinks periodically send queries to sensors belonging to their clusters and wait for replies. We denote by  $f_q = 1/T_q$  the frequency of the queries transmitted by the sinks. Each sensor takes upon reception of a query one sample of a given phenomenon (e.g. atmospheric pressure, or temperature) and forwards it through a direct link to the sink. Once transmission is performed, it switches to an idle state until the next query is received. We call the interval between two successive queries a *round*.

We define the *area throughput*, denoted by  $S$ , as the number of samples per second successfully transmitted to the sinks from the target area  $A$ . Its derivation follows directly from the evaluation of the

<sup>2</sup>The reverse communication (sink to sensor(s)) only requires audibility, i.e., no MAC failures occur since different sinks use different frequencies.

cluster throughput,  $S_c$ , defined as the number of samples per second successfully transmitted to a sink by the sensors belonging to its cluster.

By following the same rationale as in [20], we first consider the probability of successful data transmission by an arbitrary sensor to its cluster head, when  $n$  sensors are present in the cluster and  $k$  sensors out of  $n$  are audible to the sink (channel fluctuations are accounted for). This probability,  $P_{s|n,k}$ , can be computed as (from (10) and (11))

$$\begin{aligned} P_{s|n,k} &= p \cdot P_{\text{MAC}}(k) \cdot \text{Prob}\{k \text{ audible sensors} | n \text{ sensors in all}\} \\ &= p \cdot P_{\text{MAC}}(k) \cdot \binom{n}{k} p^k (1-p)^{n-k}, \end{aligned} \quad (14)$$

where we separated the impact of audibility and MAC on the transmission of samples (the sensor must be both audible to the sink and able to get its packet through). In particular,  $p$  is the probability that a randomly selected sensor in a cluster is audible to the sink (10), while  $P_{\text{MAC}}(k)$  (with  $k \geq 1$ ), is the probability of successful transmission when  $k-1$  interfering sensors are present. This factor accounts for MAC issues and is derived for IEEE 802.15.4 in Section 3.5.

Now for a cluster that has  $n$  sensors, and  $k$  of them are audible to the cluster head, we have for the cluster throughput

$$\begin{aligned} S_{c|n,k} &= n \cdot f_q \cdot P_{s|n,k} = n \cdot f_q \cdot p \cdot P_{\text{MAC}}(k) \\ &\quad \cdot \text{Prob}\{k \text{ audible sensors} | n \text{ sensors in all}\}. \end{aligned} \quad (15)$$

By first deconditioning (15) with respect to  $k$  we obtain

$$\begin{aligned} S_{c|n} &= n \cdot f_q \cdot p \cdot \frac{1}{M} \sum_{k=1}^n P_{\text{MAC}}(k) \\ &\quad \cdot \binom{n}{k} p^k (1-p)^{n-k} \text{ [samples/sec]}, \end{aligned} \quad (16)$$

which is the cluster throughput when  $n$  sensors are present in the cluster, with  $M = \sum_{k=1}^n \binom{n}{k} p^k (1-p)^{n-k}$  being a normalizing factor. Recalling that  $n \sim \text{Poisson}(\mu)$ , we finally obtain

$$\begin{aligned} S_c &= f_q \cdot p \cdot \frac{1}{M} \sum_{n=1}^{+\infty} n \sum_{k=1}^n P_{\text{MAC}}(k) \\ &\quad \cdot \binom{n}{k} p^k (1-p)^{n-k} \frac{\mu^n}{n!} e^{-\mu} \text{ [samples/sec]}. \end{aligned} \quad (17)$$

Now note that in any closed domain of area  $A$  there are on average  $\rho A$  clusters. For the sake of simplicity but without loss of generality we consider a square of side length  $L$ , so that  $A = L^2$ . Thus by assuming independence from cluster to cluster and neglecting border effects, i.e.,

- $\sigma_x, \sigma_y$  small enough such that each cluster having its cluster-head in  $A$  is entirely contained in  $A$  with high probability;
- $L \gg$  average transmission range;

the area throughput  $S$ , is simply given by

$$\begin{aligned} S &= \rho \cdot A \cdot S_c = \rho \cdot A \cdot f_q \cdot p \cdot \frac{1}{M} \sum_{n=1}^{+\infty} n \sum_{k=1}^n P_{\text{MAC}}(k) \\ &\quad \cdot \binom{n}{k} p^k (1-p)^{n-k} \frac{\mu^n}{n!} e^{-\mu} \text{ [samples/sec]}. \end{aligned} \quad (18)$$

Now define the target rate  $G$  as the average number of data samples per unit of time the network was deployed to deliver. It is given by

$$G = \bar{N} \cdot f_q \text{ [samples/sec]}, \quad (19)$$

where  $\bar{N}$  is the average number of sensors in the selected area. By once again neglecting border effects (i.e. assuming that the border of the area does not cut off part of a cluster), the number of selected sensors is the product of two Poisson r.v.'s, namely the number of clusters times the number of sensors per cluster. As these numbers are uncorrelated, their expectations satisfy  $\bar{N} = \rho A \cdot \mu$ , from which

$$\mu = \frac{GT_q}{\rho A}. \quad (20)$$

Finally, by substitution of (20) into (18), we obtain

$$\begin{aligned} S(G) &= \rho \cdot A \cdot f_q \cdot p \cdot \frac{1}{M} \sum_{n=1}^{+\infty} n \sum_{k=1}^n P_{\text{MAC}}(k) \\ &\quad \cdot \binom{n}{k} p^k (1-p)^{n-k} \frac{\left(\frac{GT_q}{\rho A}\right)^n}{n!} e^{-\frac{GT_q}{\rho A}} \text{ [samples/sec]}. \end{aligned} \quad (21)$$

### 3.4.3 Energy Considerations

Once a sensor receives the query coming from the sink it starts the algorithm to try to access the channel and, in case of success in accessing the channel, it transmits the packet. At the end of transmission, it switches off until the reception of the next query and in this state it does not consume energy. Therefore, a sensor consumes energy when receives the query and when it performs the MAC protocol (including states such as backoff, sensing, transmission, etc.). We denote as  $E_{\text{MAC}}(k)$  the mean energy spent by a sensor for performing the MAC protocol. This energy depends on the mean number,  $k$ , of sensors audible to a sink and hence competing for the channel. Recall that  $k \leq n$  holds, where  $n$  is the number of sensors in the cluster. Obviously, in case a sensor is isolated (not audible by the sink) it will not spend energy for that round. Therefore, the mean energy spent by a sensor in the network in a round,  $E_{\text{round}}$ , is given by

$$E_{\text{round}} = p \cdot (E_{\text{rx}} + \overline{E_{\text{MAC}}}) \text{ [J/sample]}, \quad (22)$$

where  $p$  is given by (10),  $E_{\text{rx}}$  is the energy spent to receive the query and  $\overline{E_{\text{MAC}}}$  is the mean energy spent for accessing the channel and transmitting the packet.

By following the same reasoning as before, for a cluster composed of  $n$  sensors we have

$$E_{\text{MAC}}|_n = \frac{1}{M} \sum_{k=1}^n E_{\text{MAC}}(k) \binom{n}{k} p^k (1-p)^{n-k}, \quad (23)$$

where we have averaged over the number of audible sensors (which are at most  $n$ ) and  $M = \sum_{k=1}^n \binom{n}{k} p^k (1-p)^{n-k}$ . By further deconditioning with respect to  $n$ , we obtain

$$\overline{E_{\text{MAC}}} = \frac{1}{M} \sum_{n=1}^{+\infty} \sum_{k=1}^n E_{\text{MAC}}(k) \binom{n}{k} p^k (1-p)^{n-k} \frac{\mu^n}{n!} e^{-\mu}. \quad (24)$$

$E_{\text{MAC}}(k)$  is derived in Section 3.5 for the case of IEEE 802.15.4.

## 3.5 The Model of IEEE 802.15.4

In this section we introduce the mathematical model used to derive the success probability,  $P_{\text{MAC}}(k)$ , together with the MAC energy consumption model when an IEEE 802.15.4 single-sink scenario is considered. The Non Beacon-Enabled mode of the IEEE 802.15.4 is assumed throughout [10]. The model used here has been initially developed in [21, 22]. For details on the protocol we refer to the standard as well. Here we simply underline that each time a sensor finds the channel busy it moves to a new backoff

stage, trying again to access the channel. Since there exist  $NB_{max} + 1$  (where  $NB_{max} = 4$ ) possible backoff stages, a maximum number of times a sensor can try to access the channel, is imposed. According to this, there will be a maximum delay affecting packet transmission.

We assume that nodes transmit packets of size  $10 \cdot D$  Bytes, with  $D$  being a constant integer and that the query has size 10 Bytes. Since a bit rate,  $R_b$ , of 250 kbit/sec is used, the time needed to transmit a packet is  $D \cdot T$ , where  $T = 320 \mu\text{sec}$ , and the query is transmitted in  $T$ . In this case, the maximum delay a packet may experience in reaching the sink will be equal to  $(121 + D) \cdot T$  [22]. Therefore, to ensure that all nodes have finished the CSMA/CA algorithm before the arrival of the next query, we set  $T_q = (121 + D) \cdot T$ . The probability,  $P_{MAC}(k)$ , that a sensor successfully transmits its packet to the sink when  $(k - 1)$  interfering sensors are present is derived in [22]. Regarding energy consumption, in [21] the mean energy spent by a sensor when  $(k - 1)$  interfering sensors are present,  $E_{MAC}(k)$ , is derived, but only in the case  $D = 1$ . Here the extension of the model to the case  $D > 1$  is provided.

According to the 802.15.4 CSMA/CA protocol, once the sensor receives the query, it starts the backoff algorithm, at the end of which it senses the channel. If the channel is found free the transmission occurs. Therefore, after reception of query, a sensor consumes energy when: (a) it performs backoff; (b) it senses the channel and (c) it transmits the packet. We let  $P_s = 82.5$  mW be the power spent in receiving and sensing states;  $P_{BO} = 50$  mW the power spent in backoff state and  $P_t = 75.8$  mW the power spent in transmission (see Freescale IEEE 802.15.4 devices).

In the model time axis is divided into a finite number of slots of duration  $T$  and the probabilities of being in the different states depend on the slot considered. We denote by  $P\{T^j\}$  the probability that a sensor finishes the transmission of a packet in slot  $j$ , and by  $P\{S_k^j\}$  the probability of being in sensing in the  $k$ th backoff stage and at the  $j$ th slot. The mean energy spent by a sensor in a round is now

$$E_{MAC}(k) = \sum_{j=0}^{121+D} E_t^j(k) + E_s^j(k) + E_{BO}^j(k), \quad (25)$$

where  $E_t^j$ ,  $E_s^j$ , and  $E_{BO}^j$  are the different energy contributions spent in transmission, sensing and backoff, respectively, for a sensor ending its transmission in slot  $j$ .

Since no retransmission is performed, each sensor will transmit only one packet per round. Therefore,

$$E_t^j = P_t \cdot \frac{D \cdot N_{bit}}{R_b} \cdot P\{T^j\}, \quad (26)$$

where  $N_{bit} = 10$  Bytes is the number of bits transmitted in  $T$ . The energy spent in the sensing state depends on how many slots are used by the sensor for sensing the channel. A sensor transmitting in slot  $j$  could have sensed the channel for one slot, in case it has found the channel free at the end of the first backoff stage, for two slots in case it has found the channel free at the end of the second backoff stage, etc. This energy is given by

$$E_s^j = P_s \cdot \frac{N_{bit}}{R_b} \cdot (1 - p_b^{j-D}) \sum_{k=0}^{NB_{max}} (k + 1) \cdot P\{S_k^{j-D}\}, \quad (27)$$

where  $p_b^j$  is the probability to find the channel busy in slot  $j$ , and  $(1 - p_b^{j-D}) \cdot P\{S_k^{j-D}\}$  is the probability that a sensor at the end of the  $k$ -th backoff stage, finds the channel free and ends transmitting in slot  $j$ . Finally, the energy spent in the backoff state depends on how many slots are occupied by the sensor for the backoff procedure. This number depends, in turn, on the number backoff stages performed. Therefore, we have

$$E_{BO}^j = P_{BO} \cdot \frac{N_{bit}}{R_b} \cdot (1 - p_b^{j-D}) \sum_{k=0}^{NB_{max}} (j - k - D) \cdot P\{S_k^{j-D}\}, \quad (28)$$

where  $(j - k - D)$  is the number of slots during which a sensor that has finished the  $k$ -th backoff stage, has performed backoff. This value is the same no matter what values of backoff counter are extracted in each backoff stage.

### 3.6 Numerical Results

In this section, the behavior of the *area throughput* and of the energy consumption as functions of the *target rate*,  $G$ , for different packet sizes, clusters shaping factors and sink densities, are shown. In addition to illustrating results from the analytical calculations, we confirm these by showing results obtained from a simulator environment. Results are obtained by setting  $A = 1 \text{ km}^2$ ,  $k_0 = 40 \text{ dB}$ ,  $k_1 = 13.03$ ,  $L_{\text{th}} = 95 \text{ dB}$  and  $\sigma_s = 4 \text{ dB}$ . Moreover, in the following, we will assume  $\sigma_x = \sigma_y = \sigma$ . A square area,  $A$ , where sinks and sensors are distributed according to the small variation of the TPP described in Section 3.3, is considered as target area.

In Figure 6,  $S$  as a function of  $G$  for different  $D$ ,  $\sigma$  and sinks density,  $\rho$ , is given. Both analytical results (lines) and simulation results (markers) are shown. In the simulator clusters are formed in the following way: sensors choose the nearest, measured in Euclidean distance, sink to transmit to. Instead, the model forces a sensor to connect to the sink with respect to which it has been deployed according to the TPP (see Sec. 3.3). As we can see a good agreement between results is obtained. The differences are due to border effects and the different cluster heads selection strategies. Of course, we expect that by increasing  $\rho$  and  $\sigma$  results will differ owing to the overlapping of clusters. As we can see, once we fix  $\rho$  and  $D$ , when the *target rate* is low, by decreasing  $\sigma$ ,  $S$  gets larger; conversely, for high  $G$ , larger shaping factors improve performance due to fewer packet collisions. By increasing  $D$  and  $\rho$ , the intersections between curves related to  $\sigma = 10 \text{ [m]}$  and  $\sigma = 40 \text{ [m]}$  are obtained for lower values of  $G$ . In fact, once we fix  $\rho$ , an increase of  $\sigma$  brings to have a larger number of isolated nodes, but also to a smaller average number of sensors trying to connect to the same sink (i.e., fewer MAC losses). Therefore, for low  $G$ , connectivity is the main cause of losses and small  $\sigma$  are advantageous; conversely, for high *target rate*, it is better to fix large  $\sigma$ , to decrease MAC losses. Finally, we note that  $S$  shows a maximum:  $S$  increases with  $G$  till MAC losses become significant. The maxima are reached for larger values of  $G$ , when decreasing  $D$  and  $\rho$ .

In Figure 7 the energy per second per sample consumed (on average) by a single sensor in the network,  $E = E_{\text{round}}/T_q \text{ [mJ/sec/sample]}$  is shown as a function of  $G$  for different values of  $D$  and  $\sigma$ . The Figure was obtained by setting  $\rho = 10^{-5} \text{ [m}^{-2}\text{]}$ . As  $\sigma$  decreases,  $E$  gets larger since it is more likely that the sensor is audible to the sink and hence that it consumes energy at all. Moreover, for low *target rate*, by increasing  $D$ ,  $E$  gets larger as well, since a greater amount of energy is spent for transmitting larger packets. Conversely, for high  $G$ , the larger  $D$  is, the lower will be the probability that a node succeeds in accessing the channel, decreasing the energy spent by the node. By comparing Figures 6 and 7 we can deduce that a tradeoff between energy consumption and *area throughput* must be found.

In Figure 8 we show the behavior of  $\eta = S/(T_q E_{\text{round}} G) \text{ [samples/sec/mJ]}$ , that is the number of samples per second received (on average) by the sinks, per mJ of energy spent. As expected,  $\eta$  increases by increasing  $\rho$ , since a greater number of sinks help reducing the size of clusters (thus reducing collisions and improving efficiency), and by decreasing  $D$ , since, once again, MAC losses decrease. Finally, in Figure 9 we show  $S(G)$  for different sensors and sinks distributions and demonstrate the impact of the cluster formation mechanism based on Monte Carlo simulations. The results clearly show the limitations on the area throughput imposed by fixed sink deployments, and the relatively good performance obtained by simple randomized cluster head selection. The feasibility of the latter approach is, however, clearly dependent on the application scenario considered.

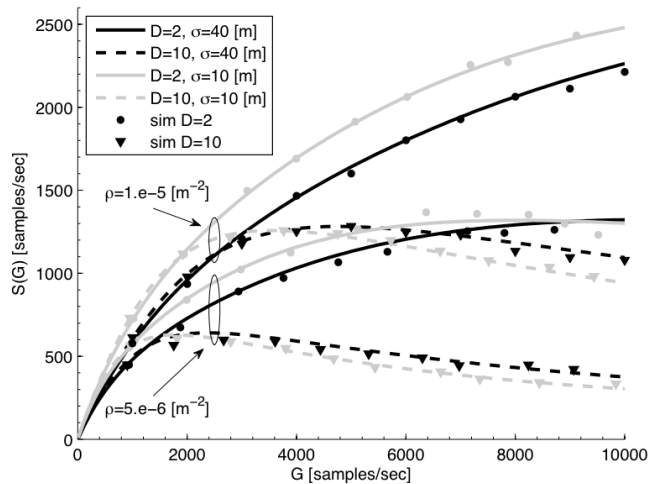


Figure 6: Area throughput  $S$  as a function of  $G$  for different values of  $D$ ,  $\rho$  and  $\sigma$ .

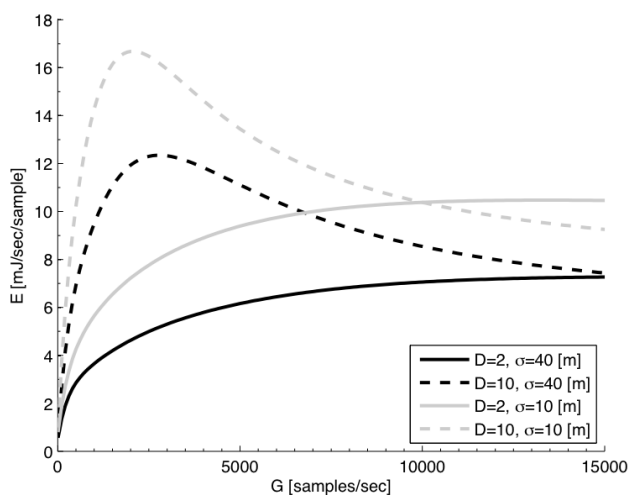


Figure 7:  $E_{\text{round}}/T_q$  as a function of  $G$ , by varying  $D$  and  $\sigma$ .

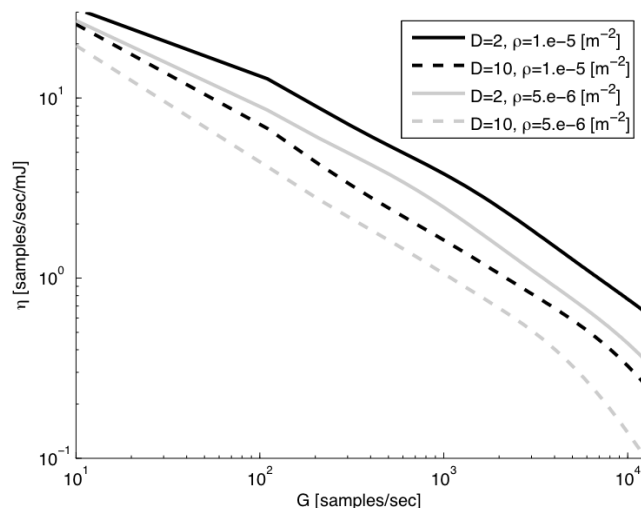


Figure 8:  $\eta$  as a function of  $G$ , by varying  $D$  an  $\rho$ .

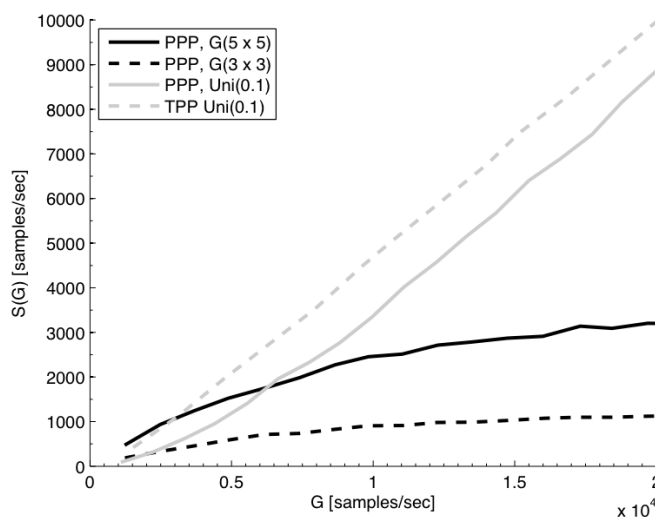


Figure 9: The area throughput for different node location distributions (indicated in the legend) and cluster formation techniques ( $G(n \times m)$  denotes cluster heads forming an  $n \times m$  grid, and  $Uni(p)$  denotes uniformly random selection of cluster heads from the node population with probability  $p$ ).

## 4 OPPORTUNISTIC POWER ALLOCATION SCHEMES FOR WIRELESS SENSOR NETWORKS WITH ONE-BIT OF FEEDBACK

### 4.1 Introduction

Recent advances in hardware have enabled the design of small and inexpensive devices equipped with some limited sensing and communication capabilities called sensors. Typically, these sensors are deployed in a field to form a Wireless Sensor Network (WSN) in order to sense or detect a given phenomenon. Some applications of interest include environmental monitoring, robotic control or guidance in automatic manufacturing environments, etc.

In WSN scenarios, where sensor nodes are equipped with finite batteries which turn out to be expensive or impossible to replace, energy efficiency is a key aspect. This is in stark contrast with wireless data networks where, in general, energy consumption is not an issue but data rates. This fact has spurred lots of interest in decentralized and distributed signal processing techniques that, while exhibiting energy-efficient and low-complexity features, allow for the maximization of some goal function such as the estimation accuracy, probability of detection, etc. In the context of this work, by *decentralized* estimation problem we mean a set up where the parameter of interest is measured in remote nodes (the sensors) and, then, such observations are conveyed to a Fusion Center (FC) for further processing.

In [23] the authors address the problem of decentralized estimation, where each sensor is only allowed to send binary (i.e. one-bit) observations to the FC. Interestingly, this work introduces a class of ML (Maximum Likelihood) estimator that, in combination with such one-bit observations, attains a variance which is very close to the CRLB (Cramer-Rao Lower Bound) with *analog* information. In addition, [24] proposes a simple probabilistic quantization scheme to be used in combination with a low-complexity Best Linear Unbiased Estimator (BLUE).

In a multi-terminal setting, the source-channel coding separation theorem does not lead to optimal solutions. Instead, the analog re-transmission of the sensor observations (i.e. amplify-and-forward approach) scales optimally in terms of distortion [25]. Motivated by these findings (although in a slightly different setting), the authors in [26] derive the optimal power allocation for two different problems of interest: (i) the minimization of distortion subject to a sum-power constraint, and (ii) the minimization of transmit power subject to a maximum distortion target. In both cases, the optimal power allocation is given by a kind of water-filling solution (referred to in the sequel as WF-D and WF-P) in which sensors with poor channel gains or noisy observations should remain inactive to save power. This finding builds a bridge between opportunistic communications (originally addressed in a wireless *data* network context for the multiple-access [27] and broadcast [28] channels) and the problem of decentralized parameter estimation with wireless *sensor* networks.

The main drawbacks of [26] are (i) the need for *global* (namely, the terminal-to-BS channel gains for *all* the terminals in the network) and *perfect* CSI at the Base Station; and (ii) the computational complexity that water-filling solutions entail. Concerning signalling requirements, they can be alleviated by resorting to thresholding rules, e.g. [29], by which only terminals with channel gains above a predefined threshold are allowed to feed back information to the BS. By doing so, the signaling load decreases with of a very moderate performance loss [29]. Going one step beyond, [30] proved that, for an asymptotically high number of terminals, just one bit of feedback (instead of *analog*) per terminal suffices to capture the optimal capacity growth-rate. As for the computational burden that water-filling solutions entail, it is addressed in [31] by assuming that power is evenly allocated over a subset of terminals. This results into a simplified water-filling scheme from which the subset of active users can be easily determined.

However, not only energy efficiency but also network lifetime is of interest in WSNs. The definition of the network lifetime (LT), namely, the amount of time for which the network is operational, is clearly application-dependent. However, for simplicity and mathematical tractability, one typically defines network LT as the time elapsed until one sensor runs out of energy. In recent works [32], the authors show how a sensible use at the scheduler of Residual Energy Information (REI) in combination with CSI information is key to extend network LT. In this chapter, we propose and analyze a class of Opportunis-

tic Power Allocation (OPA) schemes suitable for decentralized parameter estimation with WSNs. We adopt the amplify-and-forward technique proposed in [33] [26] and convey sensor observations to the FC through a set of orthogonal channels. Inspired by [29] [34] and further extending the work in [35] and [36], all the OPA schemes proposed here have one feature in common: only sensors experiencing certain local conditions (i.e. above a global threshold) are allowed to participate in the estimation process. This strategy is aimed at retaining as much performance as possible of the corresponding *optimal* power allocation scheme while keeping the network signalling and the energy consumption that it entails under control. More precisely, the proposed opportunistic schemes merely require (i) the sensor-to-FC channel gains of the subset of active nodes and *statistical* CSI at the FC (in [26, 31] the channel gains of *all* sensor nodes are needed), (ii) *one* bit of feedback per sensor (instead of analog signaling as in [29] or [26]); and (iii) *local* CSI and, possibly REI, at each sensor node. In particular, we derive opportunistic power allocation schemes for the following optimization problems:

1. Minimization of distortion (OPA-D)
2. Minimization of transmit power (OPA-P)
3. Enhancement of network lifetime (OPA-LT)

We also address the case in which the local channel state information available in the sensor nodes is subject to impairments (e.g. noisy or delayed channel estimates). For brevity, we focus on deriving an improved version of the OPA-D scheme, to be referred to as OPA-DR, which is *robust* to imperfect CSI estimates. However, the extensions to the OPA-D and OPA-LT schemes are relatively straightforward, as well. For all the above-mentioned cases, we obtain closed-form expressions of the global reporting threshold, and we derive the associated power allocation rule on the basis of *local* CSI only.

## 4.2 Signal Model

Consider a WSN composed of one Fusion Center (FC) and a large population of  $N_o$  energy-constrained sensors which have been deployed to estimate an unknown scalar, slowly-varying and spatially-homogeneous parameter  $\theta$ .

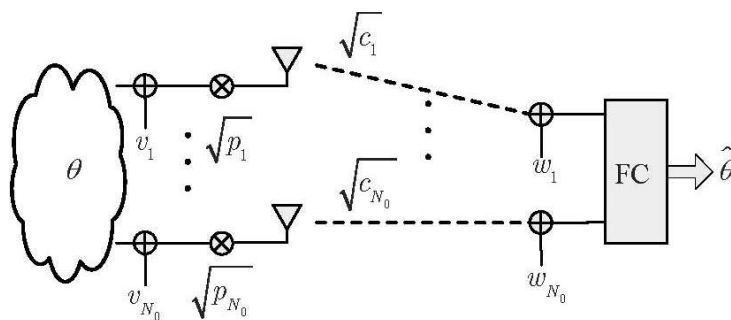


Figure 10: System Model.

According to Figure 10, the observation at sensor  $i$  can be expressed as

$$x_i = \theta + v_i \quad ; \quad i = 1, \dots, N_o. \quad (29)$$

where  $v_i$  denotes AWGN noise of variance  $\sigma_v^2$  (i.e.  $v_i \sim \mathcal{CN}(0, \sigma_v^2)$ ). Motivated by the results in [25], we adopt an amplify-and-forward re-transmission strategy. Consequently, the observation in each sensor is scaled by a factor  $\sqrt{p_i}$  before transmission. Hence, the received signal at the FC (see Fig. 10) can be modeled as:

$$y_i = \sqrt{p_i} \sqrt{c_i} (\theta + v_i) + w_i = \sqrt{p_i} c_i \theta + \sqrt{p_i} c_i v_i + w_i \quad ; \quad i = 1, \dots, N_o, \quad (30)$$

where  $w_i$  stands for i.i.d. AWGN noise (i.e.  $w \sim \mathcal{CN}(0, \sigma_w^2)$ ) and  $c_i$  denotes the channel *power* gain. For non-frequency selective block Rayleigh fading channels,  $c_i$  turns out to be an exponentially-distributed

random variable of mean  $\mu_c$ , that is,  $f_c(x) = \frac{1}{\mu_c} e^{-\frac{x}{\mu_c}}$ . Besides, the channel gains are assumed to be i.i.d. over sensors. In each time-slot, a subset of  $N \leq N_o$  *active* sensors transmit their observations to the FC over a set of orthogonal channels (e.g. FDMA) and, consequently, the  $N \times 1$  received signal vector  $\mathbf{y}$  reads

$$\mathbf{y} = \mathbf{h}\boldsymbol{\theta} + \mathbf{z}, \quad (31)$$

with  $\mathbf{h} = [\sqrt{p_1 c_1}, \dots, \sqrt{p_{NcN}}]^T$  and with  $\mathbf{z}$  standing for AWGN with (diagonal) covariance matrix  $\mathbf{C}$  given by  $\text{diag}[\mathbf{C}] = [p_1 c_1 \sigma_v^2 + \sigma_w^2, \dots, p_{NcN} \sigma_v^2 + \sigma_w^2]^T$ . In an attempt to make our estimator simple and universal (i.e. independent of any particular noise distribution), we adopt the Best Linear Unbiased Estimator (BLUE) [37, Ch. 6] in order to obtain an estimate at the FC which is given by

$$\hat{\boldsymbol{\theta}} = (\mathbf{h}^T \mathbf{C}^{-1} \mathbf{h})^{-1} \mathbf{h}^T \mathbf{C}^{-1} \mathbf{y}. \quad (32)$$

This estimator is known to be efficient for the linear signal model described above and, hence, we can take the variance as a distortion measure  $D$ :

$$D = \text{Var}(\hat{\boldsymbol{\theta}}) = \left( \sum_{i=1}^N \frac{p_i c_i}{p_i c_i \sigma_v^2 + \sigma_w^2} \right)^{-1}. \quad (33)$$

where it becomes apparent that the actual distortion depends on the power allocation strategy *and* the number of active sensors  $N$ .

From [26], the power allocation rule that minimizes the distortion for a given sum-power constraint, i.e.

$$\begin{aligned} \min_{p_1, \dots, p_{N_o}} \quad & \left( \sum_{i=1}^{N_o} \frac{p_i c_i}{p_i c_i \sigma_v^2 + \sigma_w^2} \right)^{-1} \\ \text{s.t.} \quad & (\sigma_v^2 + U^2) \sum_{i=1}^{N_o} p_i \leq P_T' \end{aligned} \quad (34)$$

where  $P_T'$  stands for total transmit power and  $\{-U \dots U\}$  denotes the dynamic range of the sensors<sup>3</sup>, is given by the following waterfilling-like (WF) solution:

$$p_i^* = \frac{\sigma_w^2}{\sigma_v^2 c_i} \left[ \frac{\sqrt{c_i}}{\sqrt{\lambda_0} \sigma_w} - 1 \right]^+ \quad ; \quad i = 1, \dots, N_o. \quad (35)$$

In this last expression, the operator  $[x]^+$  is defined as  $[x]^+ = \max\{x, 0\}$  and  $\lambda_0$  denotes the optimal water-level which is computed at the FC from  $c_i; i = 1 \dots N_o$  in order to meet the sum-power constraint. Clearly, only sensors with strong channels to the FC will be allocated some power ( $p_i > 0$ ) and, thus, will become part of the subset of  $N$  active nodes. However, the price to be paid for the optimality of such solution is two-fold: (i) the need for *global* CSI at the FC (the whole set of channel gains); and (ii) the need for the FC to inform the sensor nodes, on a *frame-by-frame* basis, about the optimal water-level. This unavoidably entails an extensive signalling between the FC and the sensor nodes and, ultimately, an increased energy consumption (which is barely desirable in WSNs).

When no CSI is available at the FC or in the absence of signalling channels between the FC and the sensors, one can alternatively resort to a Uniform Power Allocation (UPA) rule. In this case, *all* the sensors remain active (regardless of their channel condition) and evenly allocate transmit power according to  $p_i = P_T/N_o; i = 1, \dots, N_o$ . Reasonably, a substantial performance gap can be expected between the WF (optimal) and UPA strategies in many scenarios.

<sup>3</sup>For the ease of notation, in the sequel we re-define  $P_T = P_T' / (\sigma_n^2 + U^2)$ .

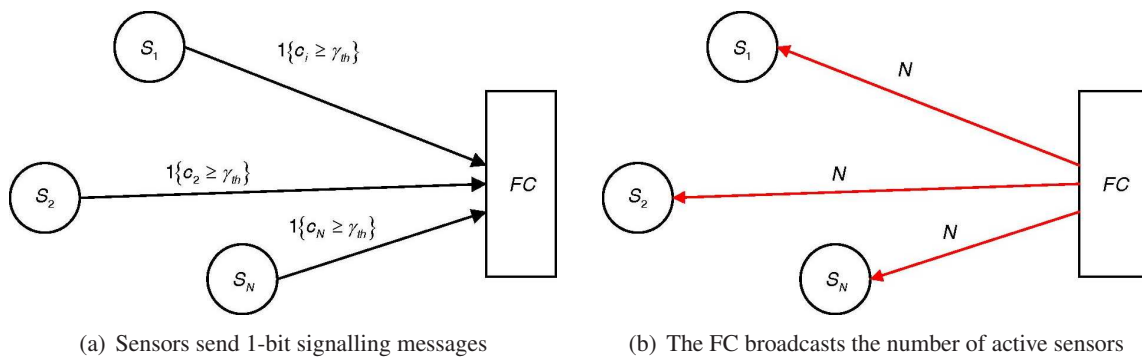


Figure 11: Identification of the subset of active sensors.

### 4.3 Opportunistic Power Allocation: Protocol Description

In an attempt to keep signalling as low as possible while retaining part of the optimality of water-filling solution, we propose a novel power allocation rule. This scheme, which in the sequel will be referred to as Opportunistic Power Allocation (OPA), is characterized by the following algorithm and communication protocol:

1. **Initialization:** Compute and broadcast the reporting threshold  $\gamma_{th}$ . This threshold ultimately depends on the design criterion: minimization of the transmit power, maximization of the overall distortion, or the enhancement of network lifetime.
2. **Identification of the set of active sensors:** Each sensor node notifies the FC whether it will participate in the estimation process or not. Only sensors above the threshold will participate. The *number* of active sensors in each time slot,  $N = N[s]$ , is then broadcasted by the FC.
3. **Power Allocation and Transmission:** The  $N$  active sensor nodes adjust their transmit power accordingly and send their observations to the FC<sup>4</sup>.
4. **Go to Step 2**

Prior to further formalizing the algorithms, we will briefly summarize the signalling and CSI requirements associated with this protocol, namely,

- At the Fusion Center: As will be shown in subsequent sections, only *statistical* CSI (and, in some cases, REI) is needed in order to compute the closed-form expressions of the reporting threshold in Step #1. The channel gains of the *subset of active nodes* are also necessary to estimate the underlying parameter  $\theta$  according to (32), whereas in [26] all the channel gains must be known to the FC.
- At the sensor nodes: Each sensor must be aware of its *own* channel gain<sup>5</sup> (i.e. *local* Channel State Information) and, possibly, REI in order to (i) determine whether it belongs to the subset of active nodes (Step #2); and (ii) adjust its transmit power accordingly (Step #3). Besides, the number of active sensors in each time slot must also be broadcasted by the FC.

Finally, one signalling bit is needed for each sensor to indicate to the FC whether it belongs or not to the subset of active nodes in the current time-slot (Step #2).

<sup>4</sup>The task of scheduling active sensors on orthogonal channels is delegated to the MAC layer and, therefore, is out of the scope of this work.

<sup>5</sup>To that extent, a training sequence could be sent by the FC at the beginning of each time slot. However, most of the energy consumption here is restricted to the transmitter (the FC) rather than the receiver (the energy-constrained sensor node).

#### 4.4 OPA for the minimization of distortion (OPA-D)

Here, we attempt to find a threshold  $\gamma_{\text{th}}$  that minimizes the expected distortion (w.r.t. the channel realizations and the number of active sensors) subject to a sum-power constraint:

$$\begin{aligned} \gamma_{\text{th}}^* &= \arg \min_{\gamma_{\text{th}}} \left\{ \mathbb{E}_{\{c_i\}_{i=1}^N; N; \gamma_{\text{th}}} \left[ \left( \sum_{i=1}^N \frac{p_i c_i}{p_i c_i \sigma_v^2 + \sigma_w^2} \right)^{-1} \right] \right\} \\ \text{s.t.} \quad & \sum_{i=1}^{N_o} p_i \leq P_{\text{T}}. \end{aligned} \quad (36)$$

We propose to uniformly allocate the available transmit power among the set of *active* sensors only, namely

$$p_i = \begin{cases} \frac{P_{\text{T}}}{N} & \text{if } c_i > \gamma_{\text{th}} \quad ; \quad i = 1, \dots, N_o \\ 0 & \text{otherwise.} \end{cases} \quad (37)$$

since, in this way, we avoid wasting resources in sensors experiencing non-favorable channel conditions (e.g. as occurs in UPA schemes, where *all* sensors do transmit with identical power levels).

In these conditions, the optimal threshold  $\gamma_{\text{th}}^*$  can be found by solving the following optimization problem:

$$\gamma_{\text{th}}^* = \arg \min_{\gamma_{\text{th}}} \left\{ \mathbb{E}_{N; \gamma_{\text{th}}} \left[ \mathbb{E}_{\{c_i\}_{i=1}^N | N; \gamma_{\text{th}}} \left[ \left( \sum_{i=1}^N \frac{\frac{P_{\text{T}}}{N} c_i}{\frac{P_{\text{T}}}{N} c_i \sigma_v^2 + \sigma_w^2} \right)^{-1} \right] \right] \right\}. \quad (38)$$

Unfortunately, this last expression is barely tractable. However, we can derive an approximate and tight threshold  $\check{\gamma}_{\text{th}}^*$  (see [35] for the derivation) which reads

$$\check{\gamma}_{\text{th}}^* = \left[ 2\mu_c W_0 \left( \frac{1}{2} \sqrt{\frac{N_o \sigma_w^2 e}{P_{\text{T}} \sigma_v^2 \mu_c}} \right) - \mu_c \right]^+ \quad (39)$$

where  $W_0(x)$  stands for the positive real branch of the Lambert function which is defined as  $x = W_0(x) e^{W_0(x)}$ .

In order to give some insight into the behavior of such approximate threshold of (39), we depict in Fig. (12) the corresponding individual probability of activation, i.e.,  $p = e^{-\frac{\gamma_{\text{th}}}{\mu_c}}$ . First, one can observe that for an increasing transmit power, the probability of activation grows, as well. In other words, since power is not a scarce resource anymore, a higher number of sensors are allowed to participate in the estimation process (even if their contribution might be somewhat marginal due to less favorable channel conditions). Second, the growth rate of the individual probability of activation clearly depends on the quality of the sensor observations. For observations with poor quality (e.g.  $\sigma_v^2 = 0.1$ ), the system tends to activate more sensors in order to average out the observation noise. Conversely, in scenarios with higher observation qualities (e.g.  $\sigma_v^2 = 0.0001$ ), to select the sensors with strongest channel gains is more beneficial.

In Figure 13, we depict the average distortion attained by the OPA-D scheme as a function of the network size ( $N_o$ ) for a given sum-power constraint. First of all, one observes that the proposed opportunistic power allocation scheme performs remarkably better than its uniform power allocation counterpart: in OPA-D curves the overall distortion is 150 – 280% lower than in UPA. As expected, saving the available power for those sensors which experience better channel conditions definitely pays-off. More importantly, the performance of OPA-D is virtually identical to that of the WF-D (i.e. optimal) power allocation scheme. To insist, the WF-D scheme requires full and instantaneous CSI from *all* the sensors in the network, whereas in OPA-D this is only needed for the subset of active nodes, along with some *statistical* CSI. Besides, OPA-D effectively exploits multi-user diversity (so does WF) whereas UPA quickly saturates, as already pointed out in [26]. Finally, the performance loss resulting from the use of the approximate optimal threshold  $\check{\gamma}_{\text{th}}^*$  computed with the closed-form expression (39) instead of the actual one (which can only be computed numerically) is negligible for the whole range of values of  $N_o$ .

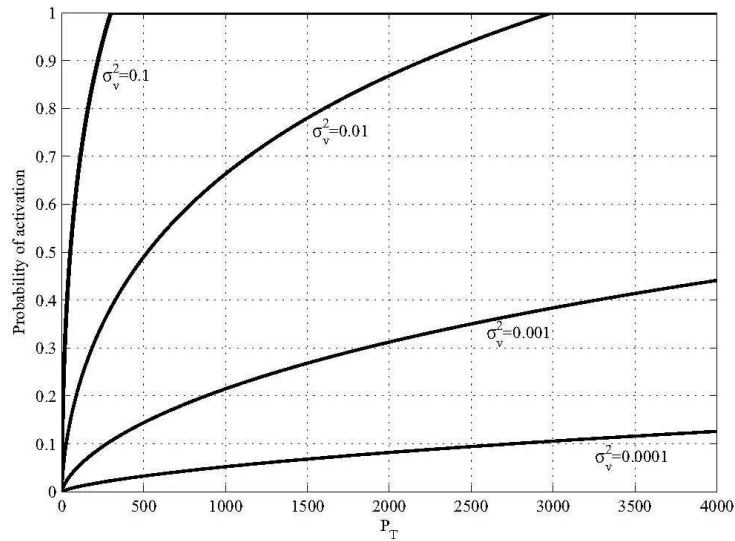


Figure 12: Probability of activation vs. total transmit power for different values of the observation noise  $\sigma_v^2$  ( $N_o = 300$ ,  $\sigma_w^2 = 0.1$ ).

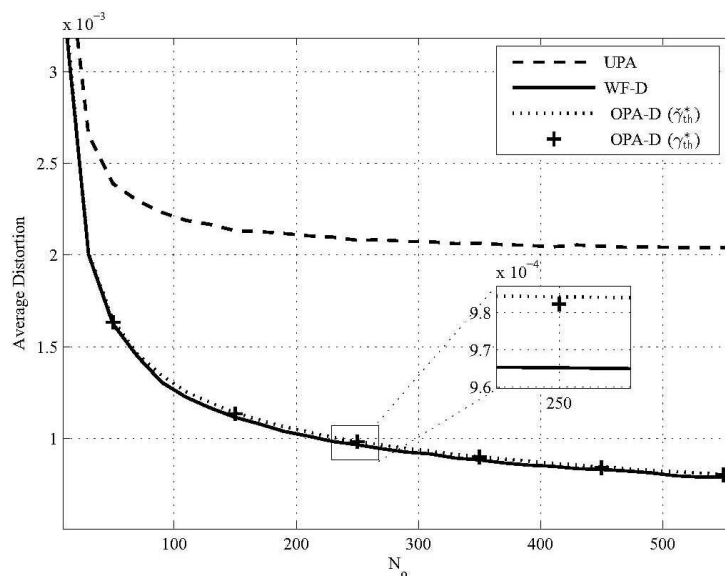


Figure 13: Average distortion vs. network size ( $P_T = 50$ ,  $\sigma_v^2 = 0.01$ ,  $\sigma_w^2 = 0.1$ ). The performance of OPA-D was evaluated with the approximate threshold  $\tilde{\gamma}_{th}$  in (39), whereas markers on that curve (+) show results with the true optimal threshold  $\gamma_{th}^*$  that was computed numerically.

#### 4.4.1 Imperfect Channel State Information

Here, we consider the realistic case in which only imperfect (e.g. noisy, delayed) CSI estimates are available at the sensors and, under this assumption, we derive the corresponding reporting threshold. Let  $h_i$  and  $\hat{h}_i$  denote the actual channel response and its estimate, and  $c_i$  and  $\hat{c}_i$  denote their respective squared magnitudes. We can model the channel estimate as:

$$\hat{h}_i = h_i + e_i \quad ; \quad i = 1, \dots, N_o \quad (40)$$

where  $e_i$  is the estimation error which is i.i.d. over the sensors and independent of  $h_i$ . Furthermore,  $e_i$  is modeled as a complex circular Gaussian random variable of variance  $\sigma_e^2$ . With these assumptions,  $h_i$  and  $\hat{h}_i$  turn out to be related through a Gaussian model, that is, the conditional random variable  $h_i | \hat{h}_i$  follows

a Gaussian distribution  $h_i|\hat{h}_i \sim \mathcal{CN}(\eta_i\hat{h}_i, \sigma_i^2)$ , with

$$\eta_i = \frac{\mu_c}{\mu_c + \sigma_e^2} \quad \sigma_i^2 = \frac{\mu_c \sigma_e^2}{\mu_c + \sigma_e^2} \quad (41)$$

Again, we obtain a similar optimization problem as in the previous section (see [38] for further details). With some algebra, the approximate threshold  $\check{\gamma}_{\text{th}}^*$  with *imperfect* CSI can be expressed in closed-form as follows:

$$\check{\gamma}_{\text{th}}^* = \left[ (\mu_c + \sigma_e^2) \left( 2W_0 \left( \frac{1}{2\mu_c} \sqrt{\frac{N_o \sigma_w^2 (\mu_c + \sigma_e^2) e^{\frac{\mu_c + \sigma_e^2}{\mu_c}}}{P_T \sigma_n^2}} \right) - \frac{\mu_c + \sigma_e^2}{\mu_c} \right) \right]^+ \quad (42)$$

In the sequel, the opportunistic power allocation scheme which operates with such reporting threshold will be referred to as Robust OPA-D (or OPA-DR). As expected, with perfect CSI (i.e.  $\sigma_e^2 \rightarrow 0$ ) the above threshold converges to that of OPA-D which is given by equation (39). Conversely, in scenarios with very poor CSI qualities ( $\sigma_e^2 \rightarrow \infty$ ) the system mimics the behavior of a UPA scheme, namely  $\check{\gamma}_{\text{th}}^* \rightarrow 0$ . Indeed, when no reliable selection of sensors can be carried out because of very poor CSI information on sensor-to-FC channel conditions, the best thing to do is to let all sensors participate in the estimation process. In Fig. 14, we plot the average distortion attained by the OPA-DR scheme as a function of the network size, and for different levels of CSI uncertainty  $\Delta_e = 10 \log(\mu_c/\sigma_e^2)$ . Interestingly, for all the OPA-DR curves, the rate at which the distortion decreases mostly mimics that of the OPA-D (with perfect CSI) and WF schemes. Hence, OPA-DR is capable of exploiting multi-user diversity in the same way as such schemes do even for high values of  $\Delta_e$  (e.g.  $\Delta_e = 0\text{dB}$ ).

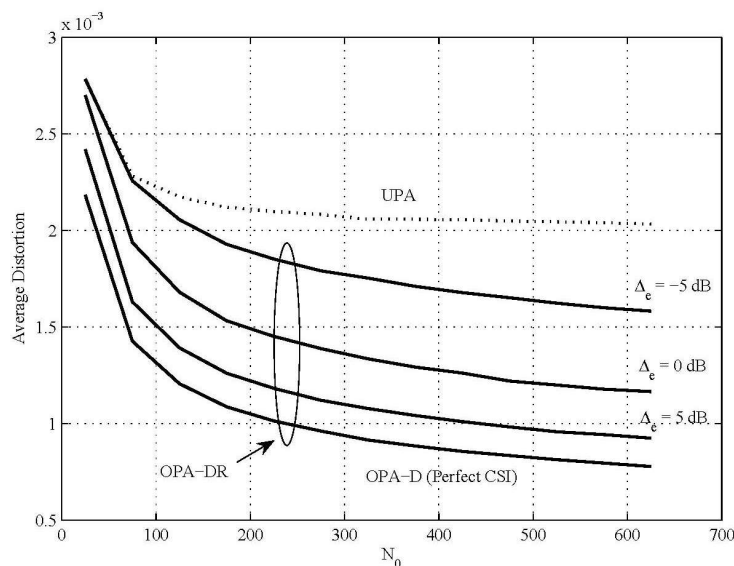


Figure 14: Average distortion of the robust OPA scheme vs. network size for different values of CSI uncertainty  $\Delta_e$  ( $P_T = 50$ ,  $\sigma_v^2 = 0.01$ ,  $\sigma_w^2 = 0.1$ , approximate threshold).

Complementarily, in Figure 15 we depict the average distortion vs. the level of CSI uncertainty ( $\Delta_e$ ). For  $\Delta_e = 15\text{dB}$  the performance is virtually identical to the case of perfect CSI, and, more importantly, with  $\Delta_e = 0\text{dB}$  it is still neatly better than that of UPA. Indeed, the OPA-DR curve only approaches the UPA bound (this meaning that no actual sensor selection is carried out) when the channel estimates are of extremely poor quality ( $\Delta_e = -15\text{dB}$ ).

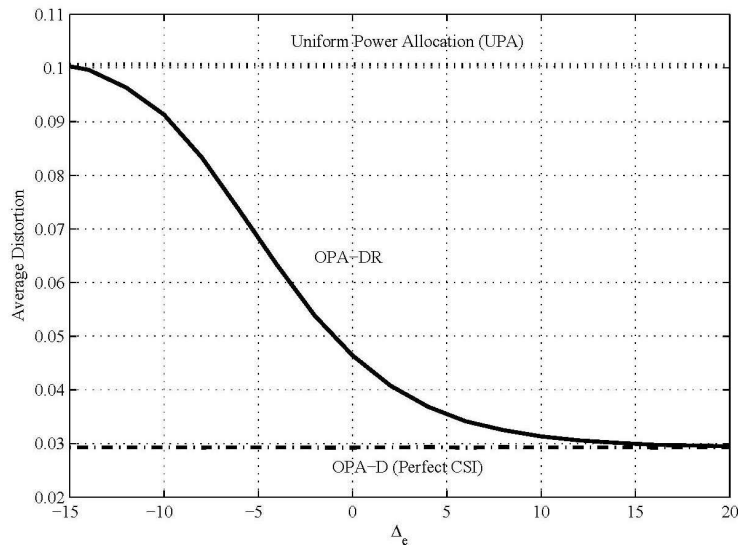


Figure 15: Average distortion vs. CSI uncertainty. The solid curve depicts the performance exhibited by the OPA-DR scheme ( $\sigma_v^2 = 0.01$ ,  $\sigma_w^2 = 0.1$ ,  $N_0 = 500$ ,  $P = 1$ , approximate threshold).

#### 4.5 OPA for the minimization of transmit power (OPA-P)

Energy efficiency is of paramount importance in wireless sensor networks. Hence, we change our design criterion and now we attempt to find a reporting threshold which minimizes the total transmit *power* subject to a given distortion constraint:

$$\gamma_{\text{th}}^* = \arg \min_{\gamma_{\text{th}}} \mathbb{E}_{\{c_i\}_{i=1}^N, N; \gamma_{\text{th}}} \left[ \sum_{i=1}^N p_i \right] \quad (43)$$

$$\text{s.t. } D = D_{\text{T}}, \quad (44)$$

where  $D$  and  $D_{\text{T}}$  stand for the actual and target distortion, respectively. From (33) the overall distortion  $D$  can be readily expressed in terms of the individual contributions  $D_i$  of each active sensor node, namely

$$D = \left( \sum_{i=1}^N \frac{1}{D_i} \right)^{-1}. \quad (45)$$

Since only *local* CSI can be assumed to be available at the sensor nodes, we further impose their individual contributions to the overall distortion to be identical. To guarantee that the constraint in (44) is met, we let  $D_i = ND_{\text{T}}$  and force each sensor to adjust *locally* its transmit power accordingly. From (33), we have

$$p_i = \begin{cases} \frac{\frac{1}{ND_{\text{T}}} \sigma_w^2}{c_i \left(1 - \frac{1}{ND_{\text{T}}} \sigma_v^2\right)} & c_i > \gamma_{\text{th}} \\ 0 & \text{otherwise.} \end{cases} \quad (46)$$

for  $i = 1, \dots, N_0$ . The optimization problem can now be re-written as

$$\gamma_{\text{th}}^* = \arg \min_{\gamma_{\text{th}}} \mathbb{E}_{\{c_i\}_{i=1}^N, N; \gamma_{\text{th}}} \left[ \sum_{i=1}^N \frac{\frac{1}{ND_{\text{T}}} \sigma_w^2}{c_i \left(1 - \frac{1}{ND_{\text{T}}} \sigma_v^2\right)} \right] \quad (47)$$

Again, the expression above is barely tractable. However, as in the previous cases, we can derive an approximate value of the optimal threshold  $\check{\gamma}_{\text{th}}^*$  (see [35]), that is,

$$\check{\gamma}_{\text{th}}^* = \left[ \mu_c W_0 \left( \frac{D_{\text{T}} N_0 e^2}{\sigma_v^2} \right) - 2\mu_c \right]^+. \quad (48)$$

#### 4.6 OPA for the Enhancement of Network Lifetime (OPA-LT)

As far as this section is concerned, we define network lifetime (LT) as the time elapsed until the first sensor runs out of energy [39]. When this occurs, the remaining  $N - 1$  active sensors scheduled in a timeslot are not capable of attaining the prescribed distortion level. Such *estimation outage* occurs because power was allocated under the assumption of having  $N$  active sensors (see Eq. 46) whereas only  $N - 1$  sensors actually conveyed their observations to the FC.

Clearly, any sensor scheduling scheme aimed at increasing network LT should take into account not only channel propagation conditions (as done in previous sections) but also information on the residual energy in the nodes (REI). In the spirit of [32], we let sensor  $i$  participate in the estimation process if and only if the product of its residual energy in time-slot  $s$ ,  $\varepsilon_i[s]$ , and the channel gain is above a threshold, namely,  $\varepsilon_i[s]c_i > \gamma_{\text{th}}[s]$ . In other words, sensors experiencing favorable channel conditions *and* sufficient residual energy are scheduled with probability

$$\Pr(\varepsilon_i[s]c_i > \gamma_{\text{th}}[s]) = e^{-\frac{\gamma_{\text{th}}[s]}{\mu_c \varepsilon_i[s]}}. \quad (49)$$

This selection strategy is known to enhance the network lifetime while, as we will see later on, it keeps the transmit power reasonably low [32]. However, it introduces individual thresholds for *each* sensor (instead of a single reporting threshold, as in OPA-P and OPA-D) which have to be re-computed during network lifetime and not only in the initialization phase. Note also that the energy vector  $\boldsymbol{\varepsilon}[s] = [\varepsilon_1[s], \dots, \varepsilon_{N_o}[s]]$  is a non-stationary stochastic process the individual entries of which are locally updated as follows,

$$\varepsilon_i[s+1] = \varepsilon_i[s] - p_i[s]T_s \quad \text{with } \varepsilon_i[0] = \varepsilon_o, \quad (50)$$

where  $p_i[s]$  denotes the transmit power in slot  $s$ ,  $T_s$  is the duration of the time slot and  $\varepsilon_o$  stands for the initial energy level. As for the power allocation rule, we again force each active sensor to evenly contribute to the overall distortion, that is, each sensor adjusts locally its transmit power according to (46).

In this context, the optimal threshold  $\gamma_{\text{th}}^*[s]$  is the one which minimizes the total transmit power under this REI-based selection rule, namely

$$\gamma_{\text{th}}^*[s] = \arg \min_{\gamma_{\text{th}}[s]} \left\{ \mathbb{E}_{\{c_i\}_{i=1}^N, N; \gamma_{\text{th}}[s], \boldsymbol{\varepsilon}[s]} \left[ \sum_{i=1}^N \frac{\frac{1}{ND_T} \sigma_w^2}{c_i \left(1 - \frac{1}{ND_T} \sigma_v^2\right)} \right] \right\}. \quad (51)$$

This problem is barely tractable and, again, we can compute an approximate value of the optimal threshold (see [36]), namely

$$\check{\gamma}_{\text{th}}^*[s] = \mu_c H(\boldsymbol{\varepsilon}[s])_{1:N'_o} \left[ W_0 \left( \frac{D_T N_o e^{\frac{H(\boldsymbol{\varepsilon}[s])_{1:N'_o} + H(\boldsymbol{\varepsilon}[s])_{1:N_o}}{H(\boldsymbol{\varepsilon}[s])_{1:N'_o}}}}{\sigma_v^2} \right) - \frac{H(\boldsymbol{\varepsilon}[s])_{1:N_o} + H(\boldsymbol{\varepsilon}[s])_{1:N'_o}}{H(\boldsymbol{\varepsilon}[s])_{1:N'_o}} \right]^+. \quad (52)$$

where  $N'$  has to be computed numerically at the FC (see [36] for a detailed information). From the equation above, one notices that, in timeslot  $s$ , the threshold  $\gamma_{\text{th}}^*[s]$  depends on the residual energy vector  $\boldsymbol{\varepsilon}[s]$  and thus, the FC needs REI for its computation. However, there is no need for sensors to send updates of their REI. Instead,  $\boldsymbol{\varepsilon}[s]$  can be locally updated at the FC as in (50), since both the individual sensors to send data and their channel gains  $c_i$  are known to the fusion center. Finally, in the case of identical residual energies,  $\varepsilon_i[s] = \varepsilon[s]$ ;  $i = 1, \dots, N_o$  one can realize that actual sensor selection rule is identical to that of the OPA-P case which simply disregards REI information.

In Figure 16, we compare the average transmit power as a function of the network size for a given distortion target,  $D_T$  and the different power allocation schemes. First, we observe that the performance of OPA-P is close to that of the WF-P (i.e. optimal) power allocation scheme. Note, however, that

such a marginal gain of WF-P entails a much larger amount of FC-sensor signalling and exchange of information. Besides, the increase in the transmit power associated with the use of OPA-LT can be regarded as very moderate (8 – 10%); this is despite of the fact that the sensor(s) experiencing the best channel conditions might not be scheduled in some situations, for instance, when some other sensor is running out of batteries. It is worth noting that, in the OPA-LT case, it is not possible (within a reasonable time frame) to numerically compute the true optimal thresholds as in the OPA-P case. Still, such curve would necessarily lie in between those of OPA-LT (upper bound, given by the approximate threshold) and OPA-P (lower bound, given by a threshold which actually disregards REI) which, as commented above, are very close to each other.

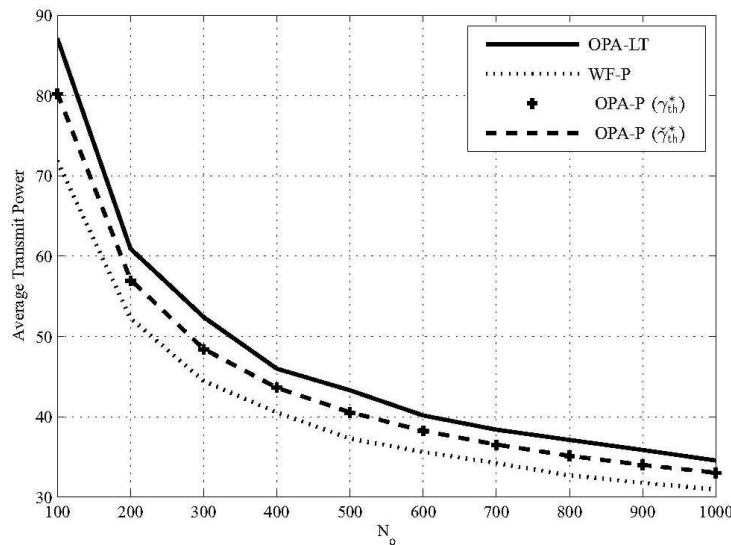


Figure 16: Average transmit power vs. network size ( $D_T = 0.001$ ,  $\sigma_v^2 = 0.01$ ,  $\sigma_w^2 = 0.1$ ). The performance of OPA-P (dotted curve) was evaluated with the approximate threshold  $\tilde{\gamma}_{th}^*$  in (48), whereas markers on that curve (+) show results with the true optimal threshold  $\gamma_{th}^*$  that was computed numerically.

In Figure 17, we depict the average network lifetime vs. the network size for a given distortion target. First, one realizes that WF-P and OPA-P yield comparable network lifetimes. More importantly, OPA-LT almost doubles the LT obtained with the other two solutions thanks to a sensible use of REI information. However, as long as the scheduling rule and the reporting threshold do not minimize the energy consumption at each time-slot anymore, the average transmit power of OPA-LT, is slightly higher now (see Fig. 16).

#### 4.7 Summary

In this section, we have proposed and analyzed a class of Opportunistic Power Allocation (OPA) schemes suitable for decentralized parameter estimation in amplify-and-forward WSNs. In these schemes, only sensors experiencing favorable conditions (i.e. above a threshold) participate in the estimation process by adjusting their transmit power on the basis of local CSI (and, in some cases, REI) information only. We have addressed a number of classical problems of interest such as the minimization of estimation distortion, the minimization of transmit power or the enhancement of network lifetime. To that extent, we have particularized the general OPA framework to each problem of interest (OPA-D, OPA-P and OPA-LT, respectively) which entails the derivation of an approximate but tight closed-form expression of the threshold along with the corresponding power allocation rule. Furthermore, we have also addressed the case with imperfect CSI to derive an improved version of the OPA-D scheme (OPA-DR) which is *robust* to such imperfections. Computer simulation results reveal that with OPA-D the overall distortion is 150 – 280% lower than that of UPA and virtually identical to that of the optimal waterfilling (WF-D)

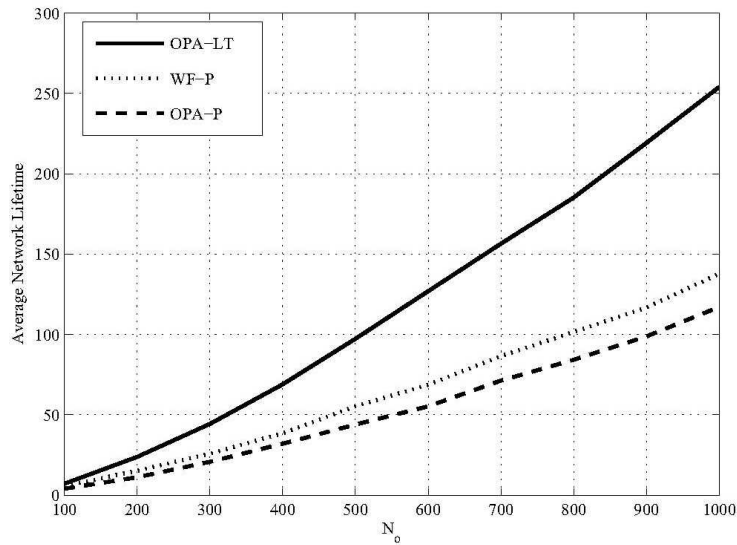


Figure 17: Average network lifetime vs. network size ( $D_T = 0.001$ ,  $\sigma_v^2 = 0.01$ ,  $\sigma_w^2 = 0.1$ ,  $\epsilon_0 = 10$ ).

scheme. To stress, the signaling and CSI requirements for all OPA schemes are far more relaxed than those of WF approaches. We have also observed that the robust version performs close to systems operating with perfect CSI even with moderate values of CSI uncertainty ( $\Delta_e = 0\text{dB}$ ). From the comparison of OPA-LT with OPA-P, we have concluded that OPA-LT leads to a two-fold extension of the network lifetime (due to a more balanced energy consumption over sensors) at the expense of a slight increase in the transmit power (8 – 10%).

## 5 MESSAGE PASSING PARADIGM IN WIRELESS NETWORKS

### 5.1 Introduction

Network protocols are based on packets exchanged by nodes in a distributed environment. Network algorithms are natural candidates to be implemented through the “message-passing” paradigm, based on exchanges of messages carried by packets. This paradigm is natural to define for uncoordinated systems with heterogeneous nodes, with different clocks, processing power, etc.

In this overview, we will focus on this paradigm applied specifically to wireless networks. In a wireless network, performances depend on the interference among neighboring nodes. In essence, a transmission is successful if the neighboring nodes are silent, otherwise collision occur. A scheduling algorithm should choose whether a node should transmit or not, trying to avoid collision. The scheduling problem can be modelled as the independent set problem taking into account the graph of the interfering nodes: when two nodes can collide with each other, in the interference graph these are connected by an edge, and any transmission configuration without collision corresponds to a set of nodes without common edges; this corresponds exactly to an independent set in the interference graph. Following the results from the cornerstone [40], it is possible to define the scheduling algorithm that is optimal, in the sense that it maximizes the throughput. This optimal algorithm is the maximum weight independent set (MWIS) problem, which is NP-hard problem. Hence, we will describe an approximated distributed algorithms to solve the problem based on message passing.

We consider a single-hop network, in which nodes communicate only to neighboring nodes. Aim of the scheduling policy is to maximize the traffic connecting neighboring nodes; this is generally considered beneficial to improve the performance of a multi-hop network, even if it is possible to devise specific counterexamples in which this is not true.

### 5.2 System Model

We consider a network of  $N$  fixed wireless nodes, and we assume to know the *interference graph*  $G = (V, E)$ , in which each node corresponds to a vertex in  $V$  and an edge connects node  $i$  to node  $j$  if they cannot transmit at the same time due reciprocal interference. Now, at any time, a set of transmissions is successful if the corresponding nodes have no edges in common. This corresponds to the classical notion of independent set in  $G$ . Let  $x_i \in \{0, 1\}$  be a binary variable which is set to 1 iff node  $i$  is transmitting at the current time; let  $X = (x_1, \dots, x_N) \in \{0, 1\}^N$  the transmission vector. Let  $N(i)$  be the set of nodes adjacent to  $i$ :  $N(i) = \{j \in V \setminus i : (i, j) \in E\}$ . At any time, to avoid collisions, the constraints of an independent set must be satisfied:

$$x_i + x_j \leq 1 \quad \forall (i, j) \in E \quad (53)$$

Let  $\Omega_G \subseteq \{0, 1\}^N$  be the set of all possible transmission vectors corresponding to an independent set on  $G$  and satisfying (53).

Now consider a queueing network in which packets are generated by the nodes and queueing occurs at the node when packets cannot be transmitted to avoid collisions. We assume that the packet size is fixed and the time is slotted, with the timeslot equal to the packet duration. At each timeslot, a scheduling decision should be taken to select the packets to transmit, or equivalently, the transmission vector  $X$ , subject to the constraints of (53).

We assume that the traffic is stationary and the packet arrivals are described by a Bernoulli i.i.d. process. In this case, it is well known that the max-pressure policy [40] achieves the maximum throughput. Since all communications are single-hop, the back-pressure policy degenerates into computing the MWIS, i.e., the optimal transmission vector  $X^*$  should be computed by solving the following integer linear program (ILP) problem:

$$X^* = \arg \max_{X \in \Omega_G} \sum_{i \in V} w_i x_i \quad (54)$$

subject to (53) where  $w_i$  is some weight associated to node  $i$ .

Let  $\lambda_{ij}$  be the average arrival rate of packet at node  $i$ . Since the traffic is single-hop, packets generated by node  $i$  are directed to one of the adjacent nodes:  $\lambda_{ij} = 0$  if  $(i, j) \notin E$ . Let  $\hat{\lambda}_i$  be the arrival rate at node  $i$ :  $\hat{\lambda}_i = \sum_{j \in N(i)} \lambda_{ij}$ . Now  $w_i$  is simply the queue size at node  $i$  and (54) corresponds the MWIS problem with weights equal to the queue sizes.

Finding the capacity region of the wireless network according to the model so far considered is NP-hard as described in [44] for the single-hop case and in [45] for the multi-hop case. An upper bound (generally not tight) on the capacity of the network can be obtained by evaluating the cliques in the interference graph [42]. A clique in  $G$  is a set of nodes that are mutually connected with each other. Intuitively, if a node belongs to a clique of size  $k$  nodes, then it will be able to transmit once every  $k$  timeslots. Hence, an upper bound on the maximum throughput sustainable by the node will be  $1/k$ .

We say that traffic  $\Lambda = \{\hat{\lambda}_i\}_{i \in V}$  is said to be admissible if

$$\hat{\lambda}_i < \frac{1}{c_i} \quad \forall i \in V$$

being  $c_i$  the size of the maximal clique containing node  $i$ ; for a isolated node,  $c_i$ . Note that if  $\Lambda$  is admissible, it does not mean that it exists a scheduling policy able to achieve a capacity region corresponding to  $\Lambda$ .

### 5.3 Message passing for MWIS

We consider the basic ‘‘min-sum’’ algorithm proposed in [41]. During each timeslot, the algorithm runs two phases.

- During the first phase, denoted as ‘‘Update’’, messages with associated a value are exchanged between all the adjacent nodes. When a node receives a message, it uses its value to compute the subsequent messages to send to its adjacent nodes. The update phase iterates until (i) either the values of the messages converge, (ii) or the maximum number of iteration  $n_{\max}$  is reached.
- The subsequent phase is denoted as ‘‘Estimate’’: each node, depending on the messages just received, decides if to turn on its transmitter ( $x_i = 1$ ) or be silent ( $x_i = 0$ ) during the timeslot.

Messages, during each iterations, are denoted by  $\Lambda^n = [\lambda_{i \rightarrow j}^n]_{(i,j) \in E}$ , for each iteration  $n = 1 \dots n_{\max}$ . Pseudocode in Fig. 18 shows the basic min-sum algorithm, denoted as BP-MWIS, written for a centralized and synchronous implementation.

```

BP-MWIS (Input:  $G = (V, E), W, n_{\max}$ ; Output:  $X$ )
// initialization
 $\lambda_{i \rightarrow j}^0 = w_i + w_j \quad \forall (i, j) \in E$ 
// update
for  $n = 1 \dots n_{\max}$  // run  $n_{\max}$  iterations
   $\lambda_{i \rightarrow j}^n = \max \left\{ 0, w_i - \sum_{k \in N(i) \setminus j} \lambda_{k \rightarrow i}^{n-1} \right\} \quad \forall (i, j) \in E$ 
   $i$  sends  $\lambda_{i \rightarrow k}^n$  to any node  $k \in N(i) \quad \forall i \in V$ 
// estimation
 $x_i = \begin{cases} 1 & \text{if } \sum_{k \in N(i)} \lambda_{k \rightarrow i}^{n_{\max}} < w_i \\ 0 & \text{else} \end{cases} \quad \forall i \in V$ 
return  $X$ 

```

Figure 18: Pseudocode of the basic message-passing algorithm for MWIS

#### 5.3.1 Convergence

It was shown in [41] that fixed points for the update phase in BP-MWIS always exist and BP-MWIS may converge or not depending on the initial conditions of the messages. Furthermore, if the algorithm con-

verges, it solves the LP relaxation of a MWIS problem on the correct graph, but with (possibly incorrect) node weights. As a conclusion, it is not possible to guarantee the convergence of the BP-MWIS to the optimal solution.

Furthermore, if there exist more than one MWIS (say MWIS-1 and MWIS-2), the algorithm may not converge at all; say for example that node  $i$  belongs to MWIS-1 and not to MWIS-2, with the weights of MWIS-1 and MWIS-2 equal by construction. In such case, messages sent by node  $i$  should be compatible with both the estimations  $x_i = 1$  and  $x_i = 0$ : this implies that the message may oscillate and not converge.

In a practical implementation, we propose the following techniques to solve the convergence issues of BP-MWIS:

- add some small noise  $\eta_i$  for each weight  $w_i$  such that the MWIS is unique. This procedure can be done in a distributed way. Note that this noise should be small enough to avoid that some independent set that is not maximum becomes the maximum one. At the same time, this noise should be large enough to be compatible with the minimum numerical precision adopted in the message exchange; note that to reach higher precision it is needed higher number of bits per message and hence larger bandwidth for the exchange of the messages.
- fix the maximum number of iterations ( $n_{\max}$ ) in the update state, to guarantee the termination of the update phase in a fixed amount of time.
- keep memory of the messages value at the end of the previous timeslot, using these messages as initial condition for the new timeslot. This allows to exploit that correlation between the MWIS computed in following timeslots.

### 5.3.2 Asynchronous implementation

BPMIS is amenable to simple asynchronous distributed implementation. Indeed, each node can update its messages independently from the other nodes, and each node can estimate its transmission state by just considering the received messages.

Note that the update relations assume that all the nodes update synchronously their messages at each iteration. This assumption is not necessary, since each node can update its messages independently from the others; this leaves space for an asynchronous implementation, where each node wake-ups, independently from the others, when some event occur (as, a fixed number of new messages has arrived, or after some time) and updates the messages to send to its adjacent nodes.

The actual transmission events can be also independent from the message update, or they can occur at any time a new message has been updated. Note that for general message passing algorithms based on belief propagation, sequential updates have been observed experimentally to be better than synchronous parallel updates [43].

## 5.4 Conclusion

We presented an overview of message passing algorithms that aid in decentralized implementation of scheduling algorithms and in solving hard combinatorial optimization problems. Maximum Weighted Independent Set is one such problem. This report is intended to be a prelude for a Joint Research Activity (JRA) between CNIT-POLITO and NKUA/IASA that currently takes place. The goal of this activity is to leverage the potential of message passing algorithms to design decentralized scheduling algorithms for maximum throughput in random access CSMA/CA IEEE 802.11 networks. We present an overview of the status of this JRA in a subsequent chapter.

## **6 DISTRIBUTED OPTIMIZATION AND REPUTATION FOR MODELING RESOURCE ALLOCATION OF PEER-TO-PEER NETWORKS**

### **6.1 Introduction**

In peer-to-peer networks, resource allocation issues are and challenging to address compared with the case of classical client-server networks. The main reasons for this, are: (i) each peer is both a server and a client at the same time, and (ii) each peer operates on a voluntary basis which might result in a deviation from the agreed resource allocation protocol. In this context, it is very challenging to devise algorithms to ensure network efficient operation. The prevalent method for modeling efficiency is through peer utility maximization. That is, the maximization of each peer perceived satisfaction from participating in the network. In the following, we describe two models for peer-to-peer network operation and devise respective resource allocation schemes. The distinguishing characteristic between these models is whether the nodes are cooperating or not. In the first model, peers cooperate, that is, they comply to the protocol that is defined by the distributed optimization problem. We relax this assumption in the second model, where we use reputation mechanisms to gradually derive the extent to which a peer is selfish and is interested only in its own utility, without caring about serving provisioning to others. For both cases, we present related work and derive an analytical framework for deriving respective resource allocation algorithms. Moreover, we consider the most complicated scenario for this class of networks in which the access technology does not separate upstream and downstream traffic, and these flow through the same capacity-limited access link. For example, this is the case when the peer nodes are connected through CSMA based protocols to the backbone network, forming a wireless overlay.

In peer-to-peer networks, each peer plays the role of client and server. As server, it receives content requests made by other peers and needs to decide on what basis and to what extent it will satisfy these requests by uploading content to others. As client, it addresses its own requests to appropriate peers to download desired content after resources are granted. A valid assumption in this case, is that the bottleneck is the capacity of the access link connecting a peer to the backbone. Different peers have different utility functions which are private information and capture a peer's desire for content. The objective is to maximize the sum of peers utilities. In this setting, the following questions arise: what portions of its link capacity does each peer allocate to upload flows from other peers and download flows for itself? How does a peer decide which portion of bandwidth will be allocated to each upload flow and download flow? How can these decisions be taken in a decentralized autonomous fashion? The operation of these peer-to-peer networks can be modeled as a network utility maximization (NUM) problem, which, however, must be solved in a decentralized fashion, [46]. By employing appropriate Lagrange decomposition methods, it is proved that this problem can be solved with distributed algorithms. Hence, every peer's utility is maximized without the need for central control and coordination.

However, the previous model presumes that peers are cooperating. That is, they strive to maximize their utility, but, they do not act selfishly. Selfishness in general terms means only consuming resources and not providing resources to other peers because this would require effort and would not give any utility. In peer-to-peer networks, this behavior, known as free riding, amounts to only downloading content from others and leads to system performance degradation. In [62], we relax the assumption of cooperating peers, and devise a mechanism for providing incentives to peers for resource provisioning. In this case, a separate utility maximization problem is solved by each peer, where the peer allocates a portion of its link bandwidth to its own downloads, acting as client, and it also allocates the remaining bandwidth for serving requests made to it by other peers. The optimization is carried out under a constraint on the level of dissatisfaction the peer intends to cause by not fulfilling others' requests. This parameter is private information for each peer. The basic component of the incentive mechanism is the reputation metrics. Namely, the reputation of a peer as a server is updated based on the amount of allocated bandwidth compared to the requested one. Reputation acts towards gradually revealing hidden intentions of peers and accordingly guiding the resource allocation by rewarding or penalizing peers in subsequent bandwidth allocations.

## 6.2 Resource Allocation Models in Cooperative Peer-to-peer Networks

In this section, we discuss a model for peer-to-peer networks in which the nodes are non-selfish utility maximizers. The proposed scheme is based on the framework of Network Utility Maximization. This particular methodology, has become very attractive in the years that followed the seminal work by Kelly *et.al* [59] both for the analysis of wire-line and wireless networks for addressing and solving utility maximization problems in a distributed manner and designing novel protocols based on optimization theory. For example, in wireless networks, the decomposition is mapped to cross-layer design and placing emphasis on functionalities of a certain layer, while the circulated parameters stand for the information that needs to be exchanged among different layers [60], [61].

Protocols for resource allocation in peer-to-peer systems have been proposed in a variety of works. For example, in [52], every peer's request allocation and server selection policies are determined by local reputation values for different types of offered services. Another example is [57], where peers distribute their requests with the objective to minimize required download time, while in [48] peers organize auctions in order to allocate their serving bandwidth. On a slightly different context, the authors of [58] propose an algorithm for rate control in peer-to-peer overlays, thus extending the TCP congestion control mechanism. They formulate a network utility maximization (NUM) problem and derive a protocol based on its distributed implementation where client and server peers consider link prices and make optimal routing and bandwidth allocation decisions.

### 6.2.1 System model and problem statement

The proposed scheme differs from the above referenced work, mainly due to the fact that the proposed resource allocation strategies of every peer are derived from the decomposition of the global, network wide, utility maximization problem. In detail, we consider a set of  $N$  peers, each with some content at its disposal. The system is static for the period of peer interaction, i.e. we do not consider peers coming to or leaving the system. The case of dynamics of peer arrivals and departures may be incorporated in the formulation by allowing a certain interval for adjusting information about the system. Peers are not distinguished on the basis of specific content they possess and thus the algorithm for peer selection does not take requested content into account. Finally, we assume that the requested content by a peer is always available at other peers.

We consider peers in a star topology, where each peer  $i$  is connected to the backbone network through an access link of capacity  $C_i$  bits/sec. This can be wire-line or even wireless. In the latter case, a peer can be associated with a specific AP and is connected to the backbone network through this AP, as shown in Figure 19. The backbone network is assumed to be of high enough capacity such that it does not create in-network congestion. We assume that the last-mile wireless link between each peer  $i$  and its corresponding AP is the performance bottleneck with a capacity of  $C_i$  bits/sec that needs to be shared between upload and download flows. The allocation of capacity portions to these flows at the network layer is realized by regulation through the CSMA MAC protocol of the time portions when a peer gets access to the channel to upload content or the access point transmits such that the peer downloads. Link capacity  $C_i$  needs to be split to a portion related to peer downloads and one for peer uploads. This upload to download ratio is passed to the network layer through an application software running at each peer, such as eMule, BitTorrent clients. Then, it is communicated down to the network and MAC layers and determines wireless link usage.

Each peer as client addresses its content requests to other peers. Content requests can be directly viewed as amounts of requested bandwidth. Let us denote the requests of peer  $i$  by the resource request vector  $\mathbf{x}_i = (x_{ij} : j = 1, \dots, N, j \neq i)$ , where  $x_{ij}$  is the amount of bandwidth peer  $i$  requests from peer  $j$ . Each peer as server receives incoming requests and needs to serve them by granting them a certain amount of bandwidth. We denote the bandwidth granted by peer  $i$  by a resource provisioning vector  $\mathbf{y}_i = (y_{ij} : j = 1, \dots, N, j \neq i)$ , where  $y_{ij}$  is the amount of bandwidth that is granted from  $i$  to  $j$ . Denote by  $\tilde{\mathbf{y}}_i = (y_{ji} : j = 1, \dots, N, j \neq i)$  the amounts of bandwidth provided to peer  $i$  by other peers  $j \neq i$ . The global network decision is represented by resource request matrix  $\mathbf{X} = (\mathbf{x}_i : i = 1, \dots, N)$  and resource

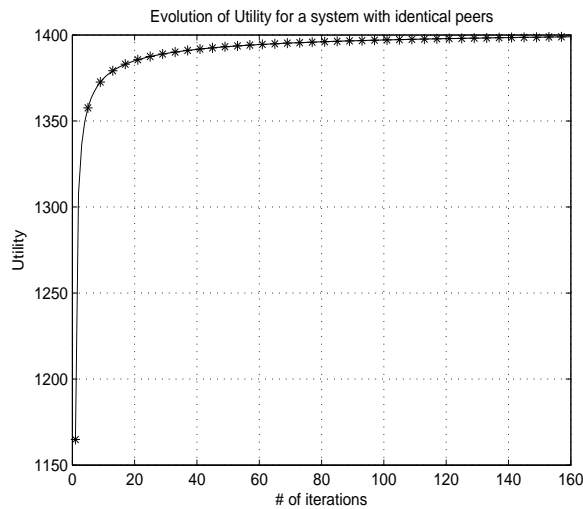


Figure 19: An instance of peer topology that is covered by our model: the backbone network consists of APs that communicate through wireline or wireless links. Each peer belongs to an AP and is connected to it through a wireless link.

provisioning matrix  $\mathbf{Y} = (\mathbf{y}_i : i = 1, \dots, N)$ . Although  $\{x_{ij}\}$  are not present in the problem formulation, we choose to define them here, as they will naturally emerge later on as auxiliary variables in the solution of the problem.

Each peer  $i$  is characterized by a differentiable utility function  $U_i(\cdot)$ , which quantifies the amount of satisfaction. In the current setup we relate it to the acquired bandwidth. In a different setup, it could also represent perceived peer delay from downloads. Hence, for a peer, the received utility,  $U_i(\cdot)$ , depends on the amounts of granted bandwidth  $y_{ji}$  by other peers  $j \neq i$  to it, (namely downloads of  $i$ ), and on the amounts of uploads  $y_{ij}$  from peer  $i$  to others. Specifically, a peer receives utility from its downloads based on a rule of diminishing marginal returns, captured by a non-decreasing, differentiable concave function  $u_i(\cdot)$  of the download bandwidth from each other peer. On the other hand, a peer experiences certain cost due to the upload bandwidth of others which is represented by a non-decreasing, differentiable convex cost function  $w_i(\cdot)$  of the upload bandwidth of each other peer. The convexity accounts for increasing marginal cost for larger amounts of uploading. A reasonable choice of utility function that captures the features above is:

$$U_i(\mathbf{y}_i, \tilde{\mathbf{y}}_i) = \sum_{j \neq i} [u_i(y_{ji}) - w_i(y_{ij})]. \quad (55)$$

Thus,  $U_i(\cdot)$  is differentiable, non-increasing concave in  $\mathbf{y}_i$  and concave non-decreasing in  $\tilde{\mathbf{y}}_i$ .

In a way,  $U_i(\cdot)$  is the net utility of a peer. This type of utility function stems partially from the theory of public goods and has been adopted in similar forms in various works [63], [64], [48]. A peer can control to a certain extent its own utility by regulating the amount of uploads of other peers. A larger value of utility component function  $u_i(\cdot)$ , of a peer in a sense denotes the peer's willingness to obtain the resource. On the other hand,  $w_i(\cdot)$  captures the cost of cooperation and hence the inability of each peer to contribute to the network. The utility function is private information for each peer.

We start from the global, network-wide goal of maximizing social welfare, namely the sum of peer utilities, subject to link capacity constraints of each peer. The selection of this objective will allow the identification of a globally optimal operating point in terms of bandwidth sharing. The problem can be formulated as:

$$\max_{\mathbf{y}_i, \tilde{\mathbf{y}}_i, i=1, \dots, N} \sum_{i=1}^N U_i(\mathbf{y}_i, \tilde{\mathbf{y}}_i), \quad (56)$$

subject to:

$$\sum_{j \neq i} y_{ij} + \sum_{j \neq i} y_{ji} \leq C_i, \quad i = 1, \dots, N. \quad (57)$$

with  $\mathbf{y}_i \geq \mathbf{0}$  and  $\tilde{\mathbf{y}}_i \geq \mathbf{0}$ . We refer to this problem as problem (P).

### 6.2.2 Distributed bandwidth allocation in cooperative peer-to-peer networks

Our aim is to devise distributed algorithms to solve this problem. We consider dual decomposition methods as most appropriate for solving the problem for reasons that will become clear in the sequel. In dual decomposition, both the primal and the dual problem are used for solving the problem. The distributed solution is attained by the circulation of implicit signals in the network about the behavior of peers, such that each peer solves separate optimization problems. By the formulation above, it can be observed first, that there exists coupling in the constraints. For each  $i$ , the function on the left-hand side of (59) depends on decisions  $\{y_{ji}\}$  of peers other than  $i$ . This fact per se does not cause any difficulty in making the problem amenable to distributed solution. In fact, relaxing link capacity constraints and assigning a Lagrange multiplier to each one of them, allows for the decomposition of the original problem to optimization problems, each of which can be solved separately by every peer. Lagrange multipliers updates enable coordination among nodes [65], [59]. Note however that in such cases, the utility of a node depends only on decisions taken by that peer (e.g. in [65] is the source rate).

The challenge in our problem lies in the fact that, besides the constraints, the objective functions of peers are coupled as well. That is, the utility function of each peer  $i$  depends on allocation decisions  $\tilde{\mathbf{y}}_i = (y_{ji} : j \neq i)$  of other peers, in addition to local decisions  $\mathbf{y}_i$ . In order to decouple peer utilities, we adopt an alternative decomposition method in the spirit of the ones presented in, [66]. For each peer  $i$ , and for each external variable  $y_{ji}$  of  $i$ , we start by introducing auxiliary variables  $z_{ij}$ , whose role is to turn the external (for peer  $i$ ) variables,  $y_{ji}$ , into local ones that can become part of the local optimization problem of peer  $i$ . Let  $\mathbf{z}_i = \tilde{\mathbf{y}}_i$  denote the vector of auxiliary variables for peer  $i$ . The introduction of these variables adds new constraints in the formulation and leads to a new maximization problem, which we refer to as problem (Q):

$$\max_{\mathbf{y}_i, \mathbf{z}_i, i=1, \dots, N} \sum_{i=1}^N U_i(\mathbf{y}_i, \mathbf{z}_i), \quad (58)$$

subject to:

$$\sum_{j \neq i} y_{ij} + \sum_{j \neq i} y_{ji} \leq C_i, \quad i = 1, \dots, N. \quad (59)$$

$$z_{ij} = y_{ji}, \quad \forall i, j, \quad \text{with } i \neq j, \quad (60)$$

with  $\mathbf{y}_i \geq \mathbf{0}$  and  $\mathbf{z}_i \geq \mathbf{0}$ .

For the problem above, let  $u^*$  denote its optimal value, namely the value of the objective function at the optimal solution. The utility of each peer becomes a function of only local variables, and the coupling has been transferred only to the constraints. Now the problem can be tackled by classical decomposition methods. To proceed, we relax only the problem's constraints. Consider the Lagrangian function for problem (Q),

$$\begin{aligned} L(\mathbf{Y}, \mathbf{Z}, \mathbf{R}, \boldsymbol{\lambda}) &= \sum_{i=1}^N U_i(\mathbf{y}_i, \mathbf{z}_i) + \sum_{i=1}^N \sum_{j=1}^N r_{ij} (y_{ji} - z_{ij}) \\ &+ \sum_{i=1}^N \lambda_i (C_i - \sum_{j \neq i} y_{ij} - \sum_{j \neq i} y_{ji}) \end{aligned} \quad (61)$$

where  $\mathbf{Z}$  denotes the matrix of auxiliary variables  $\mathbf{Z} = (\mathbf{z}_i : i = 1, \dots, N)$ , and  $\boldsymbol{\lambda} \geq \mathbf{0}$  is the vector of Lagrange multipliers corresponding to capacity constraints. Also  $\mathbf{R} = (r_{ij} : i, j = 1, \dots, N)$  is the  $N \times N$  matrix of Lagrange multipliers (dual variables)  $r_{ij}$  corresponding to the newly introduced equality

constraints. Note that  $r_{ii} = 0$  for all  $i = 1, \dots, N$ . Let  $\Omega = \{(\mathbf{Y}, \mathbf{Z}) : \mathbf{y}_i \geq \mathbf{0}, \mathbf{z}_i \geq \mathbf{0}, \forall i\}$ , and let  $\Omega_i = \{(\mathbf{y}_i, \mathbf{z}_i) \geq (\mathbf{0}, \mathbf{0})\}$ .

The dual function is defined as,

$$g(\mathbf{R}, \lambda) = \max_{(\mathbf{Y}, \mathbf{Z}) \in \Omega} L(\mathbf{Y}, \mathbf{Z}, \mathbf{R}, \lambda) \quad (62)$$

and the dual problem corresponding to the primal problem (Q) is

$$\min_{\lambda \geq \mathbf{0}, \mathbf{R}} g(\mathbf{R}, \lambda). \quad (63)$$

Attempting to solve the original problem via its dual is a suitable approach; the dual problem is always a convex optimization problem since the objective to be minimized is always convex. The dual function can be equivalently written as:

$$\begin{aligned} g(\mathbf{R}, \lambda) &= \sum_{i=1}^N \max_{(\mathbf{y}_i, \mathbf{z}_i) \in \Omega_i} \{U_i(\mathbf{y}_i, \mathbf{z}_i) \\ &+ \frac{1}{2} \sum_{j \neq i} [r_{ij}(y_{ji} - z_{ij}) + r_{ji}(y_{ij} - z_{ji})] \\ &- \lambda_i \sum_{j \neq i} y_{ij} - \sum_{j \neq i} \lambda_j y_{ij}\} + \sum_{i=1}^N \lambda_i C_i. \end{aligned} \quad (64)$$

Thus the maximization of the dual function can be decomposed into separate maximization problems, each of which can be solved by each peer  $i$  in terms of its strategy  $(\mathbf{y}_i, \mathbf{z}_i)$ . Observe also that only the  $i$ th row,  $\mathbf{r}_i = (r_{ij} : j = 1, \dots, N)$  and the  $i$ th column,  $\tilde{\mathbf{r}}_i = (r_{ji}, j = 1, \dots, N)$  of the Lagrange multiplier matrix  $\mathbf{R}$  arise in the optimization problem encountered by each peer  $i$ . For given vectors  $\mathbf{r}_i$  and  $\tilde{\mathbf{r}}_i$  and for given multiplier vector  $\lambda$ , each peer  $i$  separately solves the optimization problem,

$$\begin{aligned} \max_{(\mathbf{y}_i, \mathbf{z}_i) \in \Omega_i} \{U_i(\mathbf{y}_i, \mathbf{z}_i) + \frac{1}{2} \sum_{j \neq i} [r_{ij}(y_{ji} - z_{ij}) \\ + r_{ji}(y_{ij} - z_{ji})] - \lambda_i \sum_{j \neq i} y_{ij} - \sum_{j \neq i} \lambda_j y_{ij}\}. \end{aligned} \quad (65)$$

This is a convex optimization problem whose solution depends on the form of utility function  $U_i(\cdot)$ . Consider stage  $t$  of the algorithm, where vectors  $\mathbf{r}_i^{(t-1)}$ ,  $\tilde{\mathbf{r}}_i^{(t-1)}$  and  $\lambda^{(t-1)}$  of the previous stage are known to peer  $i$ . Peer  $i$  comes up with the optimal (for stage  $t$ ) resource provisioning vector  $\mathbf{y}_i^{(t)}$  and the optimal vector  $\mathbf{z}_i^{(t)}$ . Let us omit superscripts  $(t-1)$ . Each peer  $i$  derives the optimal solution (for stage  $t$ ) by applying the KKT conditions to obtain

$$\begin{aligned} \frac{du_i(z_{ij})}{dz_{ij}} - \frac{1}{2} r_{ij} = 0, \\ \text{and } -\frac{dw_i(y_{ij})}{dy_{ij}} + \frac{1}{2} r_{ji} - \lambda_i - \lambda_j = 0, \end{aligned} \quad (66)$$

for  $j = 1, \dots, N$ . Peer  $i$  can then determine  $\mathbf{y}_i$  and  $\mathbf{z}_i$ . These vectors for  $i = 1, \dots, N$  are then fed into the dual problem (63).

Let us fix now the values of  $(\mathbf{Y}, \mathbf{Z})$ . For given vectors  $\mathbf{y}_i^{(t)}$  and  $\mathbf{z}_i^{(t)}$ , the dual problem can be seen to simplify as follows:

$$\begin{aligned} \sum_{i=1}^N \sum_{j \neq i} \{[\min_{r_{ij}} r_{ij}(y_{ji}^{(t)} - z_{ij}^{(t)})] + \min_{r_{ji}} [r_{ji}(y_{ij}^{(t)} - z_{ji}^{(t)})]\} \\ + \sum_{i=1}^N \min_{\lambda_i} \lambda_i (C_i - \sum_{j \neq i} y_{ij}^{(t)} - \sum_{j \neq i} y_{ji}^{(t)}). \end{aligned} \quad (67)$$

Regarding multipliers  $\mathbf{R}$ , a separate problem can be solved for each pair of peers  $i, j$ . If the dual function  $g(\cdot)$  is differentiable, a typical approach is to perform one step of the iteration of a gradient-based method for  $r_{ij}$  and  $r_{ji}$ :

$$\begin{aligned} r_{ij}^{(t)} &= r_{ij}^{(t-1)} - s_t(y_{ji}^{(t)} - z_{ij}^{(t)}), \\ r_{ji}^{(t)} &= r_{ji}^{(t-1)} - s_t(y_{ij}^{(t)} - z_{ji}^{(t)}), \end{aligned} \quad (68)$$

where  $\partial g(\cdot)/\partial r_{ij} = y_{ji}^{(t)} - z_{ij}^{(t)}$ ,  $\partial g(\cdot)/\partial r_{ji} = y_{ij}^{(t)} - z_{ji}^{(t)}$  at iteration  $t$ , and  $\{s_t\}_{t \geq 0}$  is a sequence of positive steps for the gradient algorithm. Similarly, in order to update the multipliers  $\{\lambda_i\}$ , one can perform a similar type of gradient update for each  $\lambda_i$ ,

$$\lambda_i^{(t)} = \left[ \lambda_i^{(t-1)} - s_t \left( C_i - \sum_{j \neq i} y_{ij}^{(t)} - \sum_{j \neq i} y_{ji}^{(t)} \right) \right]^+ \quad (69)$$

where  $x^+ = x$  when  $x > 0$ , otherwise it is 0, and the projection accounts for maintaining non-negativity of  $\lambda_i$ .

We now proceed to the distributed algorithm for the problem in hand. We first explain various interesting attributes of our approach. Consider the auxiliary variables  $z_{ij}$  of the primal problem. The vector  $\mathbf{z}_i = (z_{ij} : j = 1, \dots, N, j \neq i)$  can be computed by each peer  $i$  separately from (66). Each variable  $z_{ij}$  can be interpreted as the amount of resource (bandwidth) that peer  $i$  requests from peer  $j$ ,  $j \neq i$ . Thus at each round of the algorithm, and for given values of Lagrange multipliers, each peer specifies the amounts of requested bandwidth  $\mathbf{z}_i$  from other peers and the amounts of granted bandwidth to other peers  $\mathbf{y}_i$  that maximize its utility. Therefore, for the auxiliary variables we have that  $\mathbf{z}_i \equiv \mathbf{x}_i$ .

Now fix attention to the updates of multipliers  $\{r_{ij}\}$  and  $\{r_{ji}\}$  for all  $(i, j)$  with  $i \neq j$  in (68). At each stage, each peer  $i$  updates the multipliers  $\{r_{ij}\}_{j \neq i}$  based on the amount of bandwidth  $z_{ij}$  that  $i$  requested from  $j$  and the amount of bandwidth  $y_{ji}$  that  $j$  granted to  $i$ . If  $y_{ji} < z_{ij}$ , that is, peer  $j$  does not fully satisfy the request of  $i$ , then  $r_{ij}$  is increased. On the other hand, if  $y_{ji} > z_{ij}$ , i.e. there is over-provisioning of resources from  $j$  to  $i$ , then  $r_{ij}$  is decreased. Intuitively,  $r_{ij}$  can be interpreted as the *reciprocal of reputation* of peer  $j$  as perceived by peer  $i$ , or in other words, the inverse of the opinion that  $i$  forms for  $j$ . The inverse reputation metric  $r_{ij}$  here is viewed as the degree to which peer  $j$  conforms to the requests of peer  $i$  and in some sense it quantifies the tendency of each peer to cooperate through resource provisioning. The dynamic update of metric  $r_{ij}$  is straightforward and does not need any other information besides the amounts of requested and provisioned bandwidth,  $z_{ij}$  and  $y_{ji}$ . The former quantity is known and the latter can be readily available by measurements of peer  $i$  on its access link.

In the same spirit with  $r_{ij}$ , multiplier  $r_{ji}$  is also updated by peer  $i$ . This metric can be interpreted as the reciprocal of reputation of peer  $i$  as perceived by  $j$ . In other words, a peer  $i$  updates its reciprocal reputation in the eyes of  $j$  based on its response  $y_{ij}$  to peer  $j$ 's request  $z_{ji}$ . Again, the update is straightforward and requires knowledge of only  $z_{ji}$  and  $y_{ij}$ . Clearly,  $r_{ij}$  depends on peer  $j$ 's response  $y_{ji}$  to peer  $i$ 's request  $z_{ij}$ . Peer  $j$  may not fully satisfy peer  $i$ 's requests due to various reasons such as different (high) reciprocal reputation metrics  $r_{ij}$  or  $r_{ji}$ , limited capacity, large amount of received requests or due to the fact that  $j$  needs to satisfy peers other than  $i$ . Naturally, peer  $i$  is agnostic of the reason it is not fully served and adjusts its reputation metrics appropriately, so that future allocations are more suitable.

However, we have to *stress that the  $r_{ij}$  are not the typical reputation metrics* introduced in the various incentive mechanisms, e.g. as in [72]. In our case,  $r_{ij}$  represents rather the *ability of the peer to contribute resources by serving others*, and not its will to conform to the agreed protocol. That is, we have assumed that peers are cooperating nodes and they do not manipulate their utility in order to increase the download rate. Nevertheless, every peer selects the most reputable peers, smaller  $r_{ij}$ , to interact with, because this will probably increase its utility.

Finally, the dual variables  $\{\lambda_i\}_{i=1, \dots, N}$  admit the (standard in literature) interpretation of prices of peer  $i$ 's access link and serve as indicators of the congestion experienced in peer  $i$ 's link. If the total load on each link increases,  $\lambda_i$  will increase to denote that it is "expensive" to use that link. In our framework,

these variables are used by the peers simply to regulate their own resource allocation decisions (both the amounts of requested and provisioned resources). They are also communicated in the network in order to signal potential congestion to other peers so that they appropriately control their own decisions. In particular, variables  $\lambda_i$  attempt to balance the demand by discouraging peers from requesting resources from peers that are very likely to be extremely popular and experience high request load. Through appropriate calibration of multipliers  $\{\lambda_i\}$ , peers are encouraged to address requests to less loaded peers. However, in a different setting with resource price advertisement and payments, these variables may represent actual link usage prices.

Each peer  $i$  has a utility function  $U_i(\cdot)$  and access link bandwidth  $C_i$ . These are kept private for each peer, so that peers other than  $i$  do not need to know this information. The basic steps of the algorithm are as follows:

- **Step 0:** Initialization. Set  $t = 0$ . Set the multipliers to initial values  $\lambda_i^{(0)} \geq 0$  and set the reciprocal reputation matrix  $\mathbf{R}^{(0)} = \alpha \mathbf{I}$ , where  $\mathbf{I}$  is the unit matrix and  $\alpha > 0$ .
- **Step 1:** Each peer  $i$ , independently of others, solves locally its separate optimization problem in (66) and computes the optimal (for stage  $j$ ) vectors  $\mathbf{y}_i^{(t)}$  and  $\mathbf{z}_i^{(t)}$  with the help of (66). Subsequently, it communicates each  $z_{ij}^{(t)}$  to peers  $j : z_{ij}^{(t)} > 0$  and grants bandwidth  $y_{ij}^{(t)}$  to other peers.
- **Step 2:** Each peer  $i$  measures  $\{y_{ji}^{(t)}\}_{j \neq i}$  and updates the reciprocal reputation metrics  $\{r_{ij}\}$  and  $\{r_{ji}\}$  in (68). These are kept as private information.
- **Step 3:** Each peer  $i$  updates its multiplier  $\lambda_i$  according to (69) and broadcasts it to the network.
- **Step 4:**  $t \leftarrow t + 1$ . If a termination condition is satisfied, STOP. Else, go to Step 1.

While in usual distributed optimization methods the signals that are circulated in the network are the Lagrange multipliers, in our formulation, the multipliers  $\{r_{ij}\}$  are not circulated. Instead, it is the auxiliary variables  $\{z_{ij}\}$  that are naturally circulated, as they denote resource requests of peers. In addition, a peer  $j$  needs to know only the amounts of resource requests  $\{z_{ij}\}_{i \neq j}$  addressed to itself by other peers and not the amounts  $\{z_{ik}\}$ ,  $i, k \neq j$  requested from other peers. As mentioned above, vectors  $\mathbf{z}_i = (z_{ij} : j \neq i)$  and  $\tilde{\mathbf{y}}_i = (y_{ji} : j \neq i)$  are readily available or easily measurable on the access link of a peer  $i$ . Interestingly, Lagrange multipliers  $\{r_{ij}\}$  and  $\{r_{ji}\}$  that correspond to the auxiliary variable constraints can be maintained as private information stored locally at each peer and used for a peer's own resource allocation decisions. This attribute is highly desirable in our case, as these multipliers can be interpreted as pairwise reputation metrics that should not be revealed in a network. If the utility functions  $U_i(\cdot)$  are strictly concave, differentiable and bounded, and the step size  $s_t$  for multiplier updates is appropriately chosen, the algorithm above converges to the optimal solution of the original problem (P).

We evaluate the performance of our approach in a simulated system of 10 peers. We consider two different scenarios for the utility  $U(\cdot)$ . First one, each peer differs from others in its function  $u_i(\cdot)$ . We consider  $u_i(x) = G_i \log(1+x)$  where  $G_i > 0$  is a private parameter that captures the valuation of bandwidth by each peer  $i$ . This choice of utility function models peers with different bandwidth needs that places more emphasis on the amount of download. Secondly, each peer differs in its function  $w_i(\cdot)$ . We consider  $w_i(y) = G_i y^2$ , where  $G_i > 0$ . In a sense, this choice models various peer behavior profiles, with different degree of "ability" to contribute to the network.

For these choices of utility functions, we obtain from (66),

$$z_{ij} = \left( \frac{2G_i}{r_{ij}} - 1 \right)^+,$$

$$\text{and } y_{ij} = \frac{1}{2G_i} \left( \frac{1}{2} r_{ji} - \lambda_i - \lambda_j \right)^+. \quad (70)$$

We observe that a peer  $i$  aims at placing more requests to peers  $j$  with low  $r_{ij}$ . This accounts for an intuitive selection of peers as servers based on how much reputable (i.e. capable) they are in the eyes of peer  $i$ . Also note that, the higher the value of  $G_i$  of a peer  $i$ , the larger the amount of requests of that peer. On the other hand, in deciding the amounts of granted bandwidth, a peer  $i$  wishes to do that so that

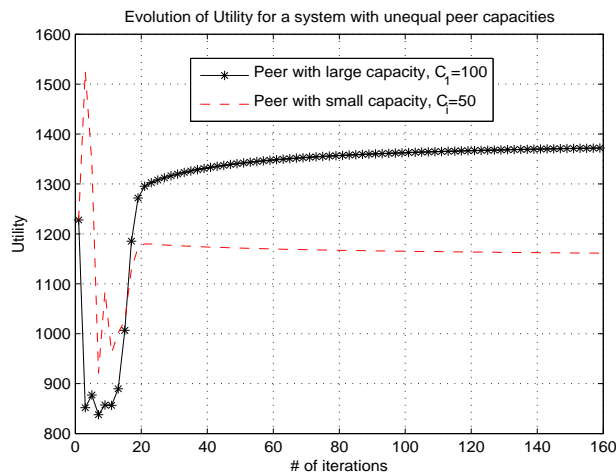


Figure 20: Utility vs. number of iterations in a system with different link capacities

it satisfies (and gains the attention of) peers which, according to its perception, do not consider peer  $i$  to be reputable. This can be seen from the fact that  $y_{ij}$  is proportional to  $r_{ji}$ , the reciprocal reputation that of  $i$  in the eyes of  $j$ . Note also, that a peer refrains from providing large amount of bandwidth if its link or peer  $j$ 's link are signaled as being congested, i.e the values of  $\lambda_i$  and  $\lambda_j$  are large.

The simulation model consists of  $N = 10$  peers which interact in successive rounds according to the proposed protocol. We assume that the communication is synchronous. Thus, in each round, every peer's requests and allocations are successfully communicated to the intended receivers (peers) before the next round takes place. The basic attributes of each peer are the capacity  $C_i$  of the access link through which it is connected to the network and the parameter  $G_i$  which differentiates, either through  $u_i(\cdot)$  or through  $w_i(\cdot)$ , its utility function. We consider the two different concave utility functions:

$$(A) : U_i(\mathbf{z}_i, \mathbf{y}_i) = G_i \sum_{j \neq i} \log(1 + z_{ij}) - \alpha_1 \sum_{j \neq i} y_{ij}^2,$$

and

$$(B) : U_i(\mathbf{z}_i, \mathbf{y}_i) = \alpha_2 \sum_{j \neq i} \log(1 + z_{ij}) - G_i \sum_{j \neq i} y_{ij}^2,$$

where  $\alpha_1$  and  $\alpha_2$  are scaling parameters and do not affect the results and the conclusions.

First, we simulate a system in which all peers are described by identical utility functions of type (A),  $G_i = 100$ . Nine of them, have equal link capacities,  $C_i = 100$  units, and one peer has link capacity equal to 50 units, lower than the capacity of the rest. The results are depicted in figure 20 and we observe that the system is gradually driven to a steady state while the utilization of each link is approximately 100%. Moreover, the peer with the lower capacity, submits smaller requests, grants less bandwidth to other peers, has worse reputation and eventually obtains less utility. The case where different peers have different utility functions is studied in figure 21. We show the evolution of utility for a system where peers have utility functions of type (A), equal link capacities,  $C_i = 100$ , but different values of  $G_i$ . Specifically,  $G_1 = 80$ ,  $G_2 = 120$ , and  $G_i = 100$  for every other peer. We observe that the utility is proportional to the value of the  $G$  parameter. Similar results hold for the case where the peer utility functions are of type (B). From the figure above, we observe that the peers with the largest utility functions, i.e. larger  $G$  for type (A) or smaller  $G$  for type (B), obtain more resources and finally higher perceived utility. This is expected for our problem formulation, (P), as social welfare maximization.

### 6.3 Resource Allocation Models in Non-Cooperative Peer-to-peer Networks

The algorithm in the previous section assumes that nodes are cooperating and optimize their strategy according with their needs. Namely, they do not act selfishly by manipulating their utility function in

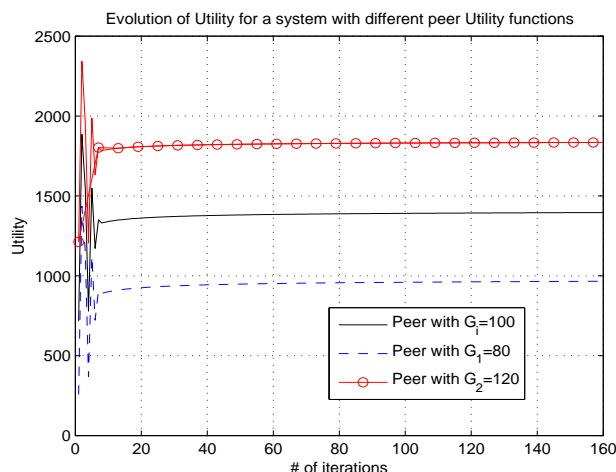


Figure 21: Utility vs. number of iterations in a system where nodes are described by utility functions with different  $G$  parameters.

order to increase their benefits. Nevertheless, in the majority of the peer-to-peer networks the nodes are non-cooperating selfish agents which avoid sharing their resources. That is, they tend to disallow others to share their content since they can only obtain perceivable utility as clients. This selfish behavior leads to the phenomenon of free riding, congestion at the nodes that are willing to share content, and subsequent performance degradation of the network. In order to address this critical issue, many researchers have proposed a variety of incentive mechanisms and some of these, already have been incorporated in existing systems. For example, such mechanisms are implemented in eDonkey/eMule or BitTorrent where each peer uploads to peers that provide him the best download rates. One way of providing incentives is through a *reputation* mechanism, which attempts to specify or estimate the behavioral profile of a peer in its transactions with other peers and impose certain resource allocation regimes based on that. The first category of works in this context study issues directly related to reputation. In [72], peers use direct and second-hand information to assess the behavior of other peers. With a statistical approach, erroneous or incompatible reputation rankings are prevented from inclusion in reputation updates. In [50], the reputation of a peer is based on its past interactions and on indirect information from a selected subset of peers through a weighted voting scheme. Finally, in the model of [51], each peer is characterized by its reputation that models its past transaction behavior, as well as by its inherent tendency to cooperate. The reputation of a peer converges to its true inclination to cooperate.

The second category of works deals with resource allocation problems that implicitly use reputation or similar concepts. In [57], peers are selected for downloading so as to minimize the required download time and the monetary cost for downloading if a bandwidth pricing function is advertised. In [56], the download bandwidth offered by a server is allocated across clients based on their connection type and their tendency to allow sharing of their resources, thereby enforcing cooperation. Finally, the work [52] proposes a protocol for enabling distributed trust-based policies and regulating the exchange of different type of services in a peer-to-peer system. The resource allocation and server selection policies are based on local reputation vectors whose elements are reputations of peers for providing each service to the system. It is shown that peers tend to form coalitions and to cooperate by exchanging resources and services while free riding behavior is discouraged.

Most of existing works focus on resource sharing by considering only the point of view of client or server. However, both these situations are interrelated, since the upload decisions of a peer as a server should be related to the grade of download service it has received as a client. This coupling is more profound, when upstream and downstream traffic takes place over the same capacity-limited link that connects the peer to the network. This case reflects better the interplay between the amount of resource dedicated to downloads from others and resource granted to uploads to others. In this work, we focus

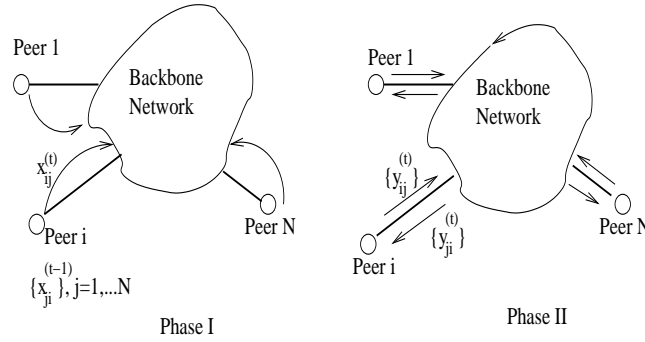


Figure 22: Peer interactions at time  $t$  take place in two phases. **Phase I:** Each peer  $i$  has stored incoming request vector  $\tilde{\mathbf{x}}_i^{(t-1)} = \{x_{ji}^{(t-1)}, j = 1, \dots, N, j \neq i\}$ . By solving the optimization problem outlined in section III.B, it decides on resource request vector  $\mathbf{x}_i^{(t)} = \{x_{ij}^{(t)}, j = 1, \dots, N, j \neq i\}$  and demand satisfaction vector  $\mathbf{y}_i^{(t)} = \{y_{ij}^{(t)}, j = 1, \dots, N, j \neq i\}$ . At the end of phase I, it sends new resource requests  $\{x_{ij}^{(t)}, j = 1, \dots, N, j \neq i\}$ . **Phase II:** Each peer  $i$  receives amounts  $\{y_{ji}^{(t)}, j = 1, \dots, N, j \neq i\}$  from other peers (in response to its requests at  $t - 1$ ) and sends  $\{y_{ij}^{(t)}, j = 1, \dots, N, j \neq i\}$  to other peers (in response to their requests at  $t - 1$ ).

on this completed scenario and adopt an optimization theory framework where each peer aims at maximizing a generic utility function. That is, each peer allocates a portion of its link bandwidth to its own downloads, acting as client, and it also allocates the remaining bandwidth across requests from other peers, acting as a server. The optimization by each peer is carried out under an implicit constraint on the level of dissatisfaction it intends to cause by not fulfilling others' requests. This parameter is private information for each peer, it quantifies its behavioral profile from selfishness to altruism and is not circulated in the network. For an incentive mechanism we propose a reputation scheme, where reputation of a peer as a server is updated based on the allocated bandwidth compared to the requested one.

### 6.3.1 System model and problem statement

We consider a set of  $N$  peers, each with some content at its disposal. The system model is the same with the one in the previous section and it is depicted in figure 22. Fix attention to peer  $i$ . The system resource request matrix is denoted by matrix  $\mathbf{X}$ . The  $i$ -th row of  $\mathbf{X}$ ,  $\mathbf{x}_i = (x_{ij} : j = 1, \dots, N, j \neq i)$  is the *resource request vector* of peer  $i$ ,  $\mathbf{x}_i$  that captures strategy of peer  $i$  as a client and denotes the amount of resource (which we abstract here by bandwidth) that peer  $i$  requests from each server  $j \neq i$ . The  $i$ -th column of  $\mathbf{X}$ ,  $\tilde{\mathbf{x}}_i$  denotes the incoming request vector to peer  $i$  from others, i.e.,  $\tilde{\mathbf{x}}_i = (x_{ji} : j = 1, \dots, N, j \neq i)$ . As a server, peer  $i$  considers incoming requests of other peers and controls the amount of bandwidth it provides to each one of them. This is specified by the *demand satisfaction vector*  $\mathbf{y}_i = (y_{ij} : j = 1, \dots, N, j \neq i)$ , where  $y_{ij}$  is the amount of bandwidth provided by  $i$  to  $j$ . We assume absence of congestion and therefore of any delay caused by the backbone network, so that the precise allocated bandwidth  $y_{ij}$  by peer  $i$  is received by peer each  $j$ .

We assume that the allocation protocol takes place in consecutive time periods (which we call slots). All peers act in sync with each other. At the beginning of each slot  $t$ , peer  $i$  has at its disposal the incoming request vector  $\tilde{\mathbf{x}}_i^{(t-1)}$  from the previous slot. At slot  $t$ , it determines resource request vector  $\mathbf{x}_i^{(t)}$  and demand satisfaction vector  $\mathbf{y}_i^{(t)}$ . These decisions emerge from solving an optimization problem to be outlined in the sequel. The allocated amount of bandwidth to each client peer does not exceed the requested one, that is constraint

$$\mathbf{y}_i^{(t)} \leq \tilde{\mathbf{x}}_i^{(t-1)}, \text{ for all } t \quad (71)$$

holds component-wise, or equivalently  $y_{ij}^{(t)} \leq x_{ji}^{(t-1)}$  for all  $j \neq i$ . Furthermore, the link capacity constraint

is taken into account, that is,

$$\sum_{j \neq i} x_{ij}^{(t)} + \sum_{j \neq i} y_{ij}^{(t)} \leq C_i \quad (72)$$

Each peer is characterized by a non-decreasing concave utility function  $U_i(\cdot)$ . The utility functions of all peers are assumed to be common information to the system. The case of incomplete knowledge at a peer about perceived utilities of others or even its own has interesting repercussions and is worth investigating. In this work, we will assume common utility function for all peers.

The fundamental tradeoff encountered by a peer is the following. On the one hand, the peer would like to assign as much capacity as possible to its own downloads, since in that case it obtains large utility. However, this results in reduced amount of allocated resource that it uploads to client peers, and has implications in subsequent obtained utility. In the absence of incentives, a peer may simply attempt to maximize its utility by allocating the entire link capacity to its own downloads and by not providing any capacity to uploads of other peers. That is, it completely disregards other peer requests and asks for  $\sum_{j \neq i} x_{ij}^{(t)} = C$ . Clearly, this is not a viable solution and leads to the problem of free riding and tragedy of commons.

The inherent tendency of a peer  $i$  to comply with the protocol and voluntarily offer its resources by allowing downloads from others is modeled by a parameter  $K_i$ . This parameter is hidden information to other peers and is only known by peer  $i$ . Parameter  $K_i$  is connected to the maximum amount of dissatisfaction that peer  $i$  tends to cause to other peers by not fulfilling their resource requirements. A larger  $K_i$  denotes a peer that is willing to dissatisfy others more, while peers with a small  $K_i$  tend to be more altruistic by allowing others to download content. Hence a larger  $K_i$  denotes a misbehaving peer. The dissatisfaction  $D_{ij}^{(t)}$  caused by peer  $i$  to peer  $j$  at time  $t$  occurs if  $i$  does not allocate the requested resources to  $j$ . Hence, it is given as the following difference in perceived utility of the requesting peer:

$$D_{ij}^{(t)} = U_j(x_{ji}^{(t-1)}) - U_j(y_{ij}^{(t)}) \quad (73)$$

and is always a non-negative quantity due to constraint (71). Parameter  $K_i$  denotes the maximum amount of dissatisfaction that peer  $i$  causes to others by not fulfilling their requests. Thus, each peer operates under the constraint:

$$\sum_{j \neq i} D_{ij} \leq K_i. \quad (74)$$

The fundamental challenge encountered by an incentive mechanism is to impose a resource allocation regime such that free riding is avoided. Ideally, each peer should end up with perceived utility that is in accordance with its inclination to share its resources or not, captured by  $K_i$ . That is, peers that inherently do not satisfy requests should ultimately obtain less utility than peers that tend to satisfy other peers' requests.

### 6.3.2 Reputation-assisted utility maximization algorithms

We introduce a simple reputation mechanism to provide incentives to peers to share their resources. Each peer maintains a vector of reputation rankings  $\mathbf{r}_i = (r_{ij} : j \neq i, j = 1, \dots, N)$  of all peers with which it is involved in transactions. Metric  $r_{ij}$  denotes reputation of  $j$  in the eyes of  $i$ . With each transaction iteration, this metric is updated, depending on the amount of allocated resources from  $j$  to  $i$  in relation to requested amount from  $i$  to  $j$ , otherwise the reputation remains unchanged. That is

$$r_{ij}^{(t+1)} = r_{ij}^{(t)} + a \frac{y_{ji}^{(t)}}{x_{ij}^{(t-1)}}, \text{ if } x_{ij}^{(t-1)} > 0 \quad (75)$$

otherwise,  $r_{ij}^{(t+1)} = r_{ij}^{(t)}$ . In the above update equation,  $a$  is a positive constant. Clearly, the maximum amount by which reputation can be increased is  $a$ . It is important to note that reputation update is realized independently by each peer and it relies only on direct peer interaction and not on third party provided

information. Furthermore, it does not need a centralized authority that keeps track of all transactions. A peer can have different behavioral profiles towards different peers and hence different reputation in their eyes. Since reputation can only increase, peers that are more willing to serve others gain more reputation, while selfish peers are limited to their initial reputation values. Parameter  $a$  needs to be appropriately selected, since it denotes in a sense the rate of increase of reputation: large values of  $a$  denote rapidly changing reputation values, while smaller values correspond to more conservative views. Reputation values can be initialized after each completion of the peers group interaction or may be normalized similarly to what is proposed in [51]. The latter is important so as to prevent constant increase of reputation values, which would render entrance and content acquisition difficult for newcomers in the system. Reputation initialization and appropriate newcomer treatment needs to be addressed in order to also avoid the white-washing phenomenon, namely that of peers purposefully leaving and entering the system under new identities [78].

We now explain the rationale of incorporating reputation to the proposed model. The reputation values in possession of a peer about others determine the behavior of this peer as a server, namely the portion of resources a server peer devotes to satisfying requests. We do not use the reputation mechanism for designating the strategy of a peer as a client, namely selecting the servers from which the download will take place, although such an extension is certainly possible. Thus, reputation is used *only* for assigning resources to requesting peers. Reputation values are used for weighting the dissatisfaction caused to serving peers. In other words, the implicit constraint faced by a server peer when allocating bandwidth for uploads is:

$$\sum_{j \neq i} r_{ij} D_{ij} \leq K_i. \quad (76)$$

This way, the dissatisfaction that peer  $i$  invokes to peer  $j$  is inversely proportional to reputation  $r_{ij}$ . The incentive mechanism is simple. By serving other peers, a peer improves its reputation relative to others and therefore it will be more satisfied from uploading, namely it will obtain larger utility. If a peer mostly downloads for its own benefit, its reputation does not grow and thus it ends up obtaining smaller utility. With this simple mechanism, peers are discouraged from free-riding and are encouraged instead to allocate portion of their bandwidth for uploading of others.

The aforementioned reputation mechanism can be incorporated in the optimization problem that each peer solves to determine its resource allocation decisions. Specifically, each peer decides on its allocation strategy  $(\mathbf{x}_i, \mathbf{y}_i)$  by solving the following optimization problem:

$$\max_{\mathbf{x}_i, \mathbf{y}_i} \sum_{j \neq i} U_i(x_{ij}) \quad (77)$$

subject to:

$$\sum_{j \neq i} x_{ij} + \sum_{j \neq i} y_{ij} \leq C_i \quad (78)$$

$$\sum_{j \neq i} r_{ij} \left[ U_j \left( x_{ji}^{(t-1)} \right) - U_j(y_{ij}) \right] \leq K_i \quad (79)$$

$$y_{ij} \leq x_{ji}^{(t-1)}, \forall j \quad (80)$$

and also  $x_{ij}, y_{ij} \geq 0$ . Constraint (78) represents bandwidth limitations, constraint (79) focuses on the amount of dissatisfaction caused to others as outlined above and constraint (80) specifies that the granted amount of resource is upper bounded by the requested one.

The only information that needs to be passed from one peer to another is the requested amount of resources. Each peer decides the portion of link bandwidth  $Y_i = \sum_{j \neq i} y_{ij}$  that will be dedicated to uploads and the amount of the upload bandwidth  $y_{ij}$  that will be allocated to each requesting peer individually. The constraint of total incurred dissatisfaction needs to be satisfied. The peer also finds the amount of bandwidth  $X_i$  allocated to requests for its own downloads. This can be equally split among other peers, namely  $x_{ij} = X_i / (N - 1)$ , since the policy does not use reputation to differentiate among requested

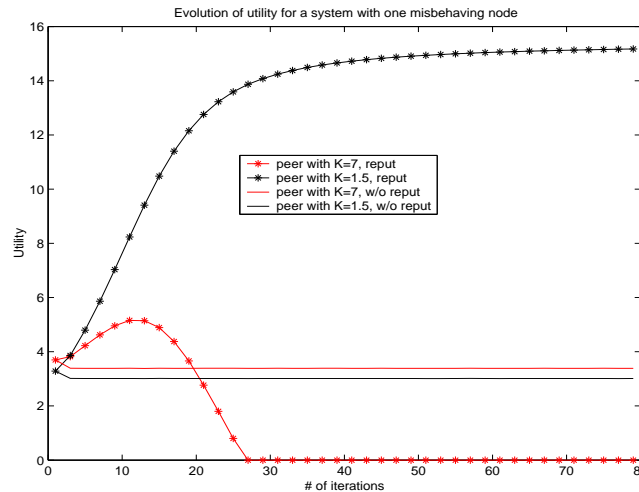


Figure 23: Actual utility vs. number of iterations in a system with one misbehaving peer.

amounts from different peers. By adopting a simple utility function, e.g.  $U(x) = \log(1+x)$  and applying the Karush-Kuhn Tucker optimality condition, one can see the dependence of the analytic solution on parameters  $K_i$  and  $C_i$  and can verify that the allocated upload bandwidth by a peer  $i$  to other peers is proportional to their reputation, i.e.  $(y_{ij} + 1)/(y_{ik} + 1) = r_{ij}/r_{ik}$ . The optimization problem has  $2(N-1)$  unknown variables, however the effective number is  $N$ , ( $N-1$  for individual granted bandwidth to a requesting peer and one for the total download bandwidth  $X_i$ ).

The important thing here is that each peer solves a separate optimization problem and makes its allocation decisions independently from others. Note however that the utility function that each peer attempts to maximize does not reflect the *actual* utility (which is still unknown, since it depends on allocation decisions of other peers) but the *anticipated* utility. After solving the problem above at each time  $t$ , each peer communicates each component of the request vector  $\mathbf{x}_i$  and the demand satisfaction vector  $\mathbf{y}_i$  to other peers. In turn, the peer receives requests by other client peers and allocated resources by servers in response to its own requests. Then it computes the actual obtained utility that depends on the amount bandwidth allocated to it by other peers,  $U_{\text{act},i} = \sum_{j \neq i} U_i(y_{ji})$ . The algorithm can be incorporated in a light-weight fashion in a resource allocation protocol in a client/server application software. It is implemented in consecutive iteration rounds, each of which consists of three stages. Each iteration round denotes an instance of interaction of peers which adjust their allocation strategy to maximize their utility. Peers need to readjust their strategy since they are not aware of the actual behavior of other peers. They attempt to deduce that behavior by observing the successive allocations that pertain to them and updating reputation values.

The performance of the proposed scheme is depicted in Figure 23. We apply the simulation set up of the previous section. The basic attributes of each peer  $i$  are the capacity  $C_i$  of the access link through which it is connected to the network and the dissatisfaction factor  $K_i$  that models its resource allocation intentions. We use the logarithmic utility function  $U(x) = \log(1+x)$  for all peers. The performance metric is the perceived actual utility of each peer. The simulation is performed with or without reputation update, where the latter corresponds to the case where each peer solves the optimization problem without the reputation weights. The system consists of 10 peers. Nine of them have  $K$ -factor equal to 1.5 and one peer notably misbehaves by having  $K = 7$ . All of them have identical capacity of  $C_i = 100$  units. We see that the inclusion of the reputation update mechanism has decisive impact on peer utilities and regulates them according to peer resource allocation intentions. The selfish peer is penalized by being forced to operate at a point where it does not obtain utility. On the other hand, peers that voluntarily share their resources are rewarded by the algorithm and obtain high utility. Actually, the absence of a reputation mechanism results in slightly higher utilities for peers with intention to misbehave, which is not in accordance with desired fair system operation.

## 7 IMPACT OF STOCHASTIC GEOMETRY ON FADING AND INTERFERENCE MODELING IN WIRELESS NETWORKS

### 7.1 Introduction

The question of what is the maximally achievable scaling of the total throughput with the system size in an ad hoc wireless network has been first tackled by Gupta and Kumar in [81] where, considering  $n$  nodes, randomly located in the unit disk and wishing to communicate each to a random destination at rate  $R(n)$ , it is showed that multihop communication with conventional single-user decoding cannot achieve a scaling better than  $\mathcal{O}(\sqrt{n})$ . This landmark contribution, which is on its own an interference limited result, has stimulated also the scientific community in providing a quantification of what is the fundamental (i.e. independent on the communication paradigm, for instance channel codes, protocols...) limit of throughput scaling in such networks. A substantial amount of works has then appeared, dealing with the scaling evaluation problem under different assumptions on the electromagnetic propagation process, which led to (very) different lower and upper bounds on the overall information rate scaling. The most optimistic results rely on (almost) full cooperation between nodes and/or nodes clusters, and promise scaling of  $\mathcal{O}(n^{2/3})$  [82] and even  $\mathcal{O}(n^{1-\epsilon})$  [83]. The information-theoretic capacity of a random ad hoc network seems, thus, to well approximate that of a single-user MIMO system, where cooperation between transmit and receive antennas can be fully exploited. The network effect<sup>6</sup> appears as a *panacea* against the interference impairments, and a suitable upper bound on the aggregate rate turns out to be of order  $\mathcal{O}(n \log n)$  [83, Th. 3.1]. However, an analysis exploiting spectral behavior of the electromagnetic field showed that, for the assumed geometry, a scaling better than  $\mathcal{O}(\sqrt{n} \log n)$  is forbidden by physical limitations [84], since the degrees of freedom of the radiating field, namely, the number of available dimensions in the space whom the radiation operator (i.e. the functional representing the radiated field from the nodes in the *transmit side* of the network) belongs to [85], is bounded by  $\sqrt{n} \log n$ , as  $n$  grows large.

Such a result relies on pure physical (geometric) structure analysis of the communication system under consideration, and shows that more optimistic scenarios are somewhat unrealistic. Usefulness and effectiveness of stochastic channel models cannot be, however, denied at once. The question arise, rather, of how to find a link between the optimistic, stochastic channel based result of linear scaling and the actual square root decay law, dictated by functional analysis.

A first step is made here by both taking into account some stochastic geometry aspects usually neglected in the common approach, as well as exploiting in our network framework some mutual information expansions, widely adopted in the single-user multi-antenna systems analysis.

Here, we present the results obtained in [86] and [87]. We first embody spatial randomness, borrowing results from [88], in the characterization of a MIMO communication between geometry-dependent clusters of the networks, providing explicit expressions for some functions of the eigenvalues of the newly defined channel matrix which are useful in the information theoretical analysis. Then, using tools from random matrix theory already proven to be effective in the single-user multiple antenna scenario, we provide the evaluation of the cut-set bound for a large wireless network with Rayleigh faded long-range links, noticing that such an approach allows to recover both the  $\mathcal{O}(\sqrt{n} \log n)$  as well as the linear scaling as particular cases.

This section is organized as follows: Section 7.2 contains the system model description, and a list of assumptions on the stochastic propagation process is therein reported. The MIMO Wishart-Poisson model for the wireless channel is defined and analyzed. In Section 7.3 a basic SIMO upper bound on the capacity scaling is evaluated under different choices of the path-loss exponent, while a cut-set result is presented and discussed in Section 7.4.

<sup>6</sup>We use the locution to refer to the diversity achievable through the full cooperation among the nodes, as in [83].

## 7.2 System Model and Assumptions

Let  $\mathcal{N}$  be a two-dimensional stationary Poisson point process over  $\mathfrak{R}^2$ , defined on a probability space  $(\Omega, \mathcal{F}, P)$ . We denote by  $E[\cdot]$  the expectation taken with respect to the measure induced by  $P$ . The points of the process represent the (fixed) locations of the devices. The process is assumed to have intensity  $0 < \lambda < +\infty$ , where  $\lambda$  is defined as the expected number of points in the unit square. Given a finite Borel subset  $A \in \mathfrak{R}^2$ , the number of points of  $\mathcal{N}$  in  $A$ , denoted by  $\mathcal{N}(A)$ , is then a Poisson random variable of intensity  $\lambda v(A)$ , where  $v(A)$  is the Lebesgue measure of the set  $A$ . White Gaussian noise of power  $N_0$  is assumed to be present at the receiver, and each node transmits at a prescribed power level  $P_{tx}$ .

We assume that the channel gain between any nodes pair is subject to random phase changes, and that each node is in far-field zone with respect to any randomly picked one. The model closely follows the assumptions in [83], and the only difference consists in explicitly taking into account the spatial randomness of the devices locations in the fading. The probability density functions (pdfs) of the ordered distances are provided in [88].

Our aim is to analytically characterize the communication protocol proposed in [83]; a first step consists of the distribution of the bits to be sent from the source to its first  $m$  neighbors, then, a traditional MIMO communication between the two clusters which source and destinations, respectively, belong to, takes place, and finally a joint decoding of the received bits, sent back from its neighbors to the intended destination, is performed. The impact of nodes stochastic geometry on the first and third step will be analyzed, while a deeper analysis of the random distances impact on the inter-cluster transmission would require exploitation of some results in [89, and references therein] and is subject of ongoing work.

### 7.2.1 Spatial gain matrix

Let us consider the information sharing between the source and its  $m$  neighbors. The point-to-point channel from the source node, sending symbol  $x$  to its  $k$ -th neighbor can be represented as

$$z_k = \sqrt{G} e^{j\theta_k} r_k^{-\alpha/2} x + n_k \quad (81)$$

where the received signal is indicated as  $z_k$ , the gain  $G$  can be assumed to be either a deterministic constant (see, e.g., [83]) or a random variable<sup>7</sup>,  $r_k$  follows the *generalized* Gamma distribution given in [88, Eq. (2)],  $\alpha \geq 2$  is the path loss exponent, and  $\theta_k$  is the random phase on the channel between the source and its  $k$ -th neighbor. The random variables  $r_k$  and  $\theta_k$  are assumed to be independent.

In two dimensional random networks with the considered Poisson point node distribution, the pdf of the distance from the source to its  $k$ -th nearest neighbor<sup>8</sup> can be written as

$$f_{r_k}(r) = e^{-\lambda\pi r^2} \frac{2(\lambda\pi r^2)^k}{r(k-1)!}, \quad (82)$$

and, in turn, denoting by  $y_k = Gr_k^{-\alpha}$  the fading amplitude seen from such neighbor<sup>9</sup>,

$$f_{y_k}(y) = \left(\frac{2}{\alpha}\right) \frac{e^{-\lambda\pi(G/y)^{2/\alpha}}}{y(k-1)!} (\lambda\pi)^k \left(\frac{G}{y}\right)^{2k/\alpha}. \quad (83)$$

The  $m$ -th moment of the random variable  $y_k$  has thus the following expression:

$$E[y_k^m] = \frac{G^m (\lambda\pi)^{\frac{\alpha m}{2}}}{(k-1)!} \Gamma\left(k - \frac{\alpha m}{2}\right). \quad (84)$$

<sup>7</sup>In this case, we will assume a unit-mean distribution for  $G$ , following [88]

<sup>8</sup>There is no loss of generality assuming the source located at the origin *for each* cluster, due to the homogeneous Poisson distribution of the nodes. In fact, it is well known that the spatial nodes distribution conditioned on having a node in the origin is the same as the original one for a homogeneous Poisson point process.

<sup>9</sup>We remark that expression (82) refers explicitly to the case of deterministic  $G$ , while it can be viewed as a conditional distribution if  $G$  is assumed to randomly vary.

Such a general model may, however, suffer from the singularity of the path loss function with respect to distance if the network is very dense. A way to cope with such problem is to consider a regularized version of the path loss function (see, e.g. [90]), namely to model the channel through

$$z_k = \sqrt{G} e^{j\theta_k} \max\{r_0, r_k\}^{-\alpha/2} x_k + n_k, \quad (85)$$

with  $r_0$  a prescribed constant, representing the minimum distance between two nodes, which regularizes the unbounded behavior of the attenuation function close to the origin. The Cumulative Distribution Function (CDF) of the random variable  $u_k = \max\{r_0, r_k\}$  can be written as

$$F_{u_k}(x) = \left[ 1 - e^{-\lambda \pi x} \sum_{\ell=0}^{n-1} \frac{(\lambda \pi x)^\ell}{\ell!} \right] \mathbf{1}_{r_0 \leq x},$$

and its pdf as

$$f_{u_k}(x) = \gamma(k, \lambda \pi x) \delta(x - r_0) + \mathbf{1}_{r_0 \leq x} \lambda \pi e^{\lambda \pi x} \frac{(\lambda \pi x)^{k-1}}{(k-1)!}, \quad (86)$$

with  $\gamma(k, x) = \int_0^x t^{k-1} e^{-t} dt$  the lower incomplete Gamma function. With that,

$$E[u_k^{-\alpha}] = r_0^{-\alpha} \gamma(k, \lambda \pi r_0) + \frac{(\lambda \pi)^\alpha}{(k-1)!} \Gamma(k - \alpha, \lambda \pi r_0),$$

where  $\Gamma(k, x) = \int_x^\infty t^{k-1} e^{-t} dt$  is the Incomplete Gamma function. The first step of information sharing among the source and its neighbors can be then modeled through a diagonal random matrix  $\mathbf{G}$ , which we refer to as the spatial gain matrix from now on, whose squared nonzero entries marginally follow, depending on the chosen attenuation model, either the law (83) or (86).

To additionally take into account channel randomness due to amplitude fluctuations and not just to stochastic distances, we model  $G$  as exponentially distributed with unit mean, i.e.  $f_G(x) = e^{-x}$ . The random variable  $Y_k = G r_k^{-\alpha}$  pdf can be evaluated through

$$f_{Y_k|r_k}(y) = e^{-y r_k^\alpha} r_k^\alpha,$$

so that

$$f_{Y_k}(y) = \frac{2(\lambda \pi)^k}{(k-1)!} \int_0^\infty e^{-y r_k^\alpha - \lambda \pi r_k^2} r_k^{2k+\alpha-1} dr_k,$$

which for  $\alpha = 2$  leads to  $f_{Y_k}(y) = \frac{k(\lambda \pi)^k}{(y + \lambda \pi)^{k+1}}$ . Notice that this distribution has finite moments up to the order  $m = k - 1$ , according to previous results in [88].

A general expression for  $f_{Y_k}(y)$  when  $\alpha > 2$  can be more easily evaluated via  $f_{Y_k}(y) = \int_0^\infty f_{Y_k|G}(y|x) e^{-x} dx$ , with  $f_{Y_k|G}(y|x)$  given by (83). Following this way, we finally get

$$f_{Y_k}(y) = \left( \frac{2}{\alpha} \right) \frac{(\lambda \pi)^k}{(k-1)!} \frac{\Gamma(\beta)}{[y(1 + y^{-2/\alpha} \lambda \pi)]^\beta}, \quad (87)$$

with  $\beta = \frac{2k}{\alpha} + 1$ .

### 7.2.2 The MIMO Wishart-Poisson model

The second step of the communication can be modeled as a MIMO communication on the linear channel

$$\mathbf{z} = \mathbf{H} \mathbf{G} \mathbf{x} + \mathbf{n}$$

where  $\mathbf{x}$  and  $\mathbf{z}$  are, respectively, the input and output vectors while  $\mathbf{n}$  is white Gaussian noise. The channel between the two clusters is represented by the  $m \times m$  zero-mean random matrix  $\mathbf{H}$ , with i.i.d. Gaussian

entries, where  $m$  is the (common) size of the clusters, while the diagonal matrix  $\mathbf{G}$  accounts for the additional randomness due to the intra-cluster information sharing and, in particular,  $\mathbf{G}_{k,k} = \sqrt{G}e^{j\theta_k}r_k^{-\alpha/2}$ .

The information-theoretic analysis of the above channel subsumes the statistical characterization of the grammian channel matrix  $\mathbf{H}\mathbf{G}\mathbf{G}^\dagger\mathbf{H}^\dagger$ , which will be the main subject of the present Section. We will study in particular the positive definite matrix  $\mathbf{T} = \mathbf{G}\mathbf{G}^\dagger$ , whose main diagonal contains strongly correlated entries, due to the distances ordering. A way to get rid of the correlation and deal with independent entries is to condition the process on having a certain number of nodes in a given interval, or, equivalently, conditioning on the value of  $r_{m+1}^\alpha = a$ .

With that, following again [88] one can then evaluate the marginal density distribution of an unordered nonzero entry of  $\mathbf{T}$  obtaining

$$f_{y_k}^{(a)}(y) = \frac{2}{y\alpha} \left(\frac{1}{ay}\right)^{2/\alpha} \Gamma\left(\beta', \frac{1}{a}\right) \quad (88)$$

with  $\beta' = \frac{2}{\alpha} + 1$  and, as a consequence, the moments of the trace of the matrix related to the spatial randomness. In particular, when the channel between the source and the neighbors is unfaded, one can evaluate for the matrix  $\mathbf{T}$  both the Shannon and the  $\eta$ -transforms, whose expressions will be helpful in evaluating the information flow between the two clusters.

### 7.2.3 Shannon Transform

Following [91, (2.47) and (2.49)], we evaluate the transforms for the law in eq. (88), obtaining,

$$\eta_{\mathbf{T}}(\gamma) = \left(\frac{a}{\gamma}\right) \frac{{}_2F_1\left(1, \beta'; \beta' + 1; -\frac{a}{\gamma}\right)}{\beta'}, \quad (89)$$

with  ${}_2F_1$  the Gauss Hypergeometric function [92], and, respectively,

$$\begin{aligned} v_{\mathbf{T}}(\gamma) = \left(\frac{\alpha}{2\gamma}\right) \left[ a^{\beta'} \left( \frac{\gamma}{\alpha} \left( \frac{\gamma}{\alpha} \frac{{}_2F_1\left(1, 2 - \beta'; 3 - \beta'; -\frac{\gamma}{a}\right)}{\frac{2}{\alpha} - 1} + \right. \right. \right. \\ \left. \left. \left. \log\left(1 + \frac{\gamma}{a}\right)\right) - \left(\frac{\gamma}{a}\right)^{\beta'} \pi \csc(\pi\beta') \right) \right]. \quad (90) \end{aligned}$$

From the expressions above, moreover, we can evaluate the Shannon transform for the compound channel matrix as [91]

$$v_{\mathbf{HTH}^\dagger}(\gamma) = \tilde{\beta} v_{\mathbf{T}}(\eta\gamma) + \log \frac{1}{\eta} + (\eta - 1) \log e, \quad (91)$$

with  $\eta$  the solution to

$$\tilde{\beta} = \frac{1 - \eta}{1 - \eta_{\mathbf{T}}(\eta\gamma)}.$$

## 7.3 Scaling laws analysis: SIMO upper bound

Before evaluating the cut-set rate scaling of the network, we may evaluate the scaling achievable in the general case by exploiting the underlying spatial random structure of the node process. We remark that after random source-destination matching and the consideration of the actual power regimes experienced by the nodes, such scaling will strongly change, as shown in Section 7.4.

**Theorem 1** [87] *The average aggregate throughput in a network with  $n$  nodes distributed according to a two-dimensional homogeneous Poisson process is bounded above by*

$$T(n) \leq Kn \log \log n, \quad (92)$$

where  $K$  is a constant.

The proof of the theorem is as follows. Along the lines of [83], we can upper bound the transmission rate  $R(n)$  from a source node  $s$  to the destination  $d$  by the capacity of the single-input multiple-output (SIMO) channel between the source and the remaining nodes. In our case, specifically, the bound turns out to be, for  $\alpha = 2$  and exploiting (84),

$$\begin{aligned} \mathbf{E} \left[ \log \left( 1 + \frac{P}{N_0} \sum_{i \neq s} \frac{G}{r_{i,s}^\alpha} \right) \right] &\leq \log \left( 1 + \frac{P}{N_0} \sum_{i \neq s} \mathbf{E} \left[ \frac{G}{r_{i,s}^\alpha} \right] \right) \\ &\leq \log \left( 1 + \frac{PG}{N_0} \lambda \pi \sum_{\ell=2}^n \frac{1}{\ell-1} \right), \end{aligned}$$

which for large  $n$  tends to  $R(n) \leq K' \log \log n$  by [92]. We explicitly note that, for  $\alpha > 2$ , expression (84) is singular at least for the closest neighbors. In this case, we resort to the regularized attenuation function with first moment given by (86), noticing that

$$\frac{x^n E_{1+\alpha/2-n}(x) + \Gamma(n) - \Gamma(n, x)}{\Gamma(n)} \leq \frac{1}{n-1}$$

and, then, still

$$\begin{aligned} \mathbf{E} \left[ \log \left( 1 + \frac{P}{N_0} \sum_{i \neq s} \frac{G}{\max\{r, r_0\}_{i,s}^\alpha} \right) \right] &\leq \\ \log \left( 1 + \frac{P}{N_0} \sum_{i \neq s} \mathbf{E} \left[ \frac{G}{\max\{r, r_0\}_{i,s}^\alpha} \right] \right) &= \\ \log \left( 1 + \frac{PG}{2N_0 r_0^\alpha} \sum_{\ell=2}^n \frac{1}{n-1} \right), & \end{aligned} \tag{93}$$

i.e. we obtain an upper bound of the same form, albeit with a different constant.

#### 7.4 Cut-set bound

The elegant derivation in [84] aims at obtaining an upper bound to the mutual information between the nodes contained within a circular region of area proportional to the node number and those placed in a circular crown surrounding the first one. The information flow is split into two contributions, a first one concerning the communication between the inner nodes and those placed within an annulus of width  $\delta$ , and a second one coming from the information transfer to the remaining outer nodes. While the first contribution analysis can be carried out without resorting to electromagnetic theory, a careful analysis of the degrees of freedom dictating the maximum number of available independent channels (and thus, basically, the achievable scaling) requires tools from functional analysis [84, 85, and references therein]. Specifically, the rank of the radiation operator (i.e. of the channel matrix) is evaluated performing a singular value decomposition of the radiated field, which leads to the remarkable result that the effective number of independent MISO channels between the inner nodes and the farthest nodes is of order of  $\sqrt{n}$ , rather than proportional to  $n$ , thus forbidding a linear scaling.

In this section, we aim at providing an upper bound on aggregate rate sustainable by a large random network through some compact information-theoretic performance indexes already proven to be very effective in the design and analysis of single and multi-user wireless communications systems. To bound the achievable information flow we resort to the classical cut-set argument. Our study relies on the high Signal to Noise Ratio (SNR) affine expansion of the mutual information in coherent MIMO channels [93] as to the near-to-cut region, and on the low-power approximation [94], respectively, for the remaining nodes.

Before proceeding further in the analysis, we briefly recall the low and high-power expansions to be exploited in the following, and their expressions as a function of the involved channel matrices.

### 7.4.1 High and low-power mutual information analysis

In the high-SNR regime, one can expand the mutual information as a function of the SNR<sup>10</sup> as [93]

$$\mathcal{J}(\text{SNR}) = S_\infty \left[ \frac{\text{SNR}|_{\text{dB}}}{3 \text{ dB}} - \mathcal{L}_\infty \right] + o(1),$$

where

$$S_\infty = \lim_{\text{SNR} \rightarrow \infty} \frac{\mathcal{J}(\text{SNR})}{\log_2 \text{SNR}} \quad (94)$$

and  $\mathcal{L}_\infty$ , whose value is not of direct interest as long as just the scaling is to be investigated, is defined in [93].

In the low-SNR regime instead [95], the key performance measures are  $\frac{E_b}{N_0 \min}$  (the minimum energy per information bit required to convey any positive rate reliably) and  $S_0$ , the capacity slope in bits/s/Hz/(3 dB), such that

$$\mathcal{C}\left(\frac{E_b}{N_0}\right) = \frac{S_0}{3 \text{ dB}} \left( \frac{E_b}{N_0} |_{\text{dB}} - \frac{E_b}{N_0 \min} |_{\text{dB}} \right) + \varepsilon \quad (95)$$

with  $\varepsilon$  vanishing faster than the main term as  $\frac{E_b}{N_0}$  approaches  $\frac{E_b}{N_0 \min}$ . In the following, we will be mainly concerned with the evaluation of the low-power slope  $S_0$ , since  $\frac{E_b}{N_0 \min} = \ln 2$  for AWGN noise, irrespectively on the adopted transmission scheme.

### 7.4.2 Upper bounding the information flow

We start from a square portion of the plane of linear dimension  $\sqrt{n}$ , where  $n$  nodes are randomly deployed, and consider a cut dividing the area into two equal halves. The maximum achievable sum-rate between the randomly chosen source-destination pairs is bounded above by the capacity of the MIMO channel between nodes  $S$  located to the left of the cut and nodes  $D$  located to its right. Under fast fading assumption, such sum-rate can be upper bounded by  $E[\log \det(\mathbf{I} + \mathbf{H}\mathbf{H}^\dagger)]$ , with  $\mathbf{H}$  the channel matrix of the overall MIMO system<sup>11</sup>.

We further consider the domain  $D$  to be sub-divided into a rectangular strip of area  $1 \times \sqrt{n}$  close to the border of the cut, which contains no more than  $\sqrt{n} \log n$  nodes [83, Lemma (5.1.a)]. By Hadamard's inequality we can write

$$\log \det(\mathbf{I} + \mathbf{H}\mathbf{H}^\dagger) \leq \log \det(\mathbf{I} + \mathbf{H}_1\mathbf{H}_1^\dagger) + \log \det(\mathbf{I} + \mathbf{H}_2\mathbf{H}_2^\dagger), \quad (96)$$

where  $\mathbf{H}_1$  is the channel matrix modeling the communication between the nodes on the left of the cut, and those in the little strip, say the region  $V_D$  and, in turn,  $\mathbf{H}_2$  is the matrix modeling the communication between the nodes on the left and the remaining ones on the right  $D - V_D$ . Nodes placed in the strip  $V_D$ , thus, are experiencing a communication in high-SNR regime, while the remaining nodes communication takes place in the low-power regime. From [93],  $S_\infty \leq \min\{n_{tx}, n_{rx}\}$ , with  $n_{tx}$  the number of transmit antennas and, respectively,  $n_{rx}$  the number of receiving antennas. For our channel,  $n_{tx} = O(n)$  and  $n_{rx} = O(\sqrt{n} \log n)$ ,  $S_\infty \leq \sqrt{n} \log n$ , confirming the  $\sqrt{n}$  law for the near-to-cut region to which both purely stochastic and purely electromagnetic approach end up [83, 84]. As to  $\mathcal{L}_\infty$ , its value can be approximated by [93, Eq. (15)] (this is tantamount to assume the entries of  $\mathbf{H}_1$  be i.i.d.). Finally, by [94, eq. (19)],

$$S_0 = \frac{2n_{eqtx}n_{eqrx}}{n_{eqtx} + n_{eqrx}},$$

<sup>10</sup>In our case of fixed transmit power and thermal noise at the receiver,  $\text{SNR} = P_{tx}/N_0$ .

<sup>11</sup>We remark that a careful analysis of the network would require to adopt a (conditionally on the fading) Euclidean random matrix model for  $\mathbf{H}$  [89]. We will, instead, make a simplifying assumption keeping  $\mathbf{H}$  zero-mean Gaussian with possibly correlated entries.

where  $n_{eqtx}$  and  $n_{eqrx}$  are *equivalent* number of transmit and receive antennas, which take into account a reduction in the effective number of spatial degrees of freedom due to phenomena impairing the transmit or, respectively, the receive side of the channel. The work in [84], in particular, has revealed by inspection of the radiation operator that the number of independent channels crossing the cut toward the low-power region<sup>12</sup> is  $O(\sqrt{n} \log n)$ , and that this phenomenon can be interpreted as an effective reduction of the number of independent receiving nodes within the above mentioned region. A more qualitative analysis [96, Proposition I], comprehensive of both stochastic as well as electromagnetic aspects, still shows such an impact on the spatial degrees of freedom, reducible at the definition of  $n_{eqtx}$  and  $n_{eqrx}$  on the basis of electromagnetic considerations in the region close to the transmitter and the receiver, separately. Finally, we notice that if a separable correlation model can be identified for the channel under consideration, due to [94, Property I],  $O(1) \leq n_{eqrx} \leq O(n)$ , and thus  $1 \leq S_0 \leq n$  (in order sense), encompassing different scenarios, ranging from constant to linear throughput scaling with  $n$ , and comprehensive of the  $\sqrt{n}$  law.

### 7.4.3 On specific spatial correlation models

Linear scaling could be, following previous Section, achieved only in case  $n_T^{eq}$  and  $n_R^{eq}$  are of the same order of magnitude. This is in contradiction with the electromagnetic argument of counting independent channels in the low-power region [84], and the aim of this Section is to detail a framework where stochastic and electromagnetic arguments offer closer results.

A simplistic, though suitable, way to enhance channel non-ideality effects is to express the random channel matrix following the Kronecker or *separable correlation* model, i.e.

$$\mathbf{H}_2 = \Theta_R^{1/2} \mathbf{W} \Theta_T^{1/2} \quad (97)$$

where  $\mathbf{W}$  is composed of independent unit-variance complex Gaussian random entries. This model implies that the covariance matrix of each row of  $\mathbf{H}$  is thus given by  $\Theta_T$  while the covariance matrix of each column is given by  $\Theta_R$ . From a physical point of view, in single-user MIMO systems this means that the immediate surroundings to each array are responsible for the correlation between its antennas but have no impact on the correlation between the antennas at the other end of the link. Such a model could be questionable in the case of spatially distributed nodes, due to the further geometric aspects to be managed in order to verify whether the spatial distribution of the nodes in a region of the network does impact on the correlation structure on the other side, but we choose as a starting point of the analysis, and for ease of exposition, to keep it as far as no multiple-polarizations and/or other signalling strategies, usually known as breaking the Kronecker model, are not exploited.

In terms of the spatial correlation matrices, the equivalent number of antennas can be expressed as [94, Corollary 2]

$$n_T^{eq} = \frac{n_T}{\zeta(\Theta_T)} \quad n_R^{eq} = \frac{n_R}{\zeta(\Theta_R)}. \quad (98)$$

with  $n_T$  and  $n_R$  the actual number of transmit (respectively, receive) antennas, and the function  $\zeta(\cdot)$ , often referred to as the *dispersion* of the (random) square matrix of dimension  $m$  in the argument, defined as [94, Eq.(8)],

$$\zeta(\mathbf{A}) = m \frac{E[\text{Tr}\{\mathbf{A}^2\}]}{E^2[\text{Tr}\{\mathbf{A}\}]}. \quad (99)$$

Notice that, since a correlation matrix has unit diagonal elements, expression (99) particularizes to

$$\zeta(\Theta) = \frac{E[\text{Tr}\{\Theta^2\}]}{n}. \quad (100)$$

which is usually referred to as *correlation number*, and whose value is bounded, being

$$1 \leq \zeta(\Theta) \leq n \quad (101)$$

<sup>12</sup>The analysis is carried out in a region with circular symmetry, however as far as asymptotic scaling is concerned the conclusions can be transferred also to a square geometry.

with the lower bound achieved if and only if the sensor nodes are uncorrelated and the upper bound achieved if and only if they are fully correlated.

The evaluation of  $S_0$  in our framework essentially boils down to the evaluation of  $E[\text{Tr}\{\Theta^2\}]$  for  $\Theta$  a suitable (random) spatial correlation matrix in a wireless network.

As a first step to deeper understanding the random network behavior, we analyze some among the most commonly adopted spatial correlation models, namely

- *Constant correlation model* [98, Example IV]  
Given  $\rho \in (0, 1)$ ,  $\Theta_{Ri,j}(\rho) = \rho \forall i, j$  such that  $i \neq j$ .
- *Jakes' model* [99]  
 $\Theta_{Ri,j} = \mathcal{J}_0\left(\frac{2\pi}{\lambda}d_{i,j}\right)$ , with  $d_{i,j}$  the inter-node distances for an HPPP and  $\lambda$  the carrier wavelength.
- *Random Toeplitz*  
The  $n$  elements of the first row of  $\Theta_R$ , say  $\vartheta_{1,j}$ ,  $j = 1, \dots, n$  are independent random variables which form a Toeplitz matrix.

For simplicity, and in order to allow comparison with previous results such as [83, 84], we make the optimistic assumption w.r.t. transmit correlation that  $\Theta_T = \mathbf{I}$ , hence  $\zeta(\Theta_T) = 1$  and  $n_T^{eq} = n_T$ .

**Proposition 1** *The correlation number of a constant correlation matrix  $\Theta_R(\rho)$  can be written as  $\zeta(\Theta_R(\rho)) = 1 + (n-1)\rho^2$ .*

**Proposition 2** *The correlation number for the random Jakes' model when nodes locations follow a HPPP pattern can be written as*

$$\zeta(\Theta_R) = 1 + \sum_{\ell=2}^n \binom{n}{\ell} \sum_{t=0}^{n-\ell} \frac{(-1)^t}{\ell+t} \binom{n-\ell}{t} \cdot {}_2F_3\left(\ell+t, 1/2; 1, 1, \ell+t+1; -\left(\frac{2\pi\sqrt{n}}{\lambda}\right)^2\right), \quad (102)$$

where  ${}_pF_q$  is the generalized hypergeometric series [100].

**Proposition 3** *The correlation number when the entries of  $\Theta_R$  are independent, nonzero mean<sup>13</sup>, subgaussian random variables<sup>14</sup>, with common mean  $\mu$ , forming a Toeplitz matrix, can be lower bounded by*

$$\zeta(\Theta_R) \geq \mu.$$

The listed results are worth some comments; notice that, since the number of nodes in  $S$  and that in  $D - V_D$  are of the same order, one can write as for the single-user MIMO channel with both receiver and transmitter equipped with the same number of nodes [94, Corollary 3]

$$S_0 = \frac{2n}{1 + \zeta(\Theta_R)}. \quad (103)$$

Particularizing the above equation to the constant correlation model, it is evident that it offers a very poor low power scaling, namely a per-node decay of the throughput as fast as  $O(n^{-1})$ . Constant correlation suitably models a scenario where receive nodes are so closely spaced as to not to experience any anisotropy in the received signal behavior. One should then be very careful in stating that co-located

<sup>13</sup>We cannot assume the mean of all elements to be zero since at least for the diagonal elements we should ensure them to have unit mean, in order to comply with the definition of correlation number.

<sup>14</sup>A random variable  $X$  is called *subgaussian* if

$$\mathbf{P}[|X| \leq t] \leq 2e^{-at^2} \quad \forall t \geq 0$$

and for some constant  $a > 0$ .

nodes are most likely to well cooperate and offer higher throughput, since also such spatial impairments, like in the single-user MIMO case, have to be taken into account.

Things significantly change when putting into (103) the Jakes based correlation number. Indeed, one can numerically verify that the summation of hypergeometric functions does not cause a substantial increase of the correlation number. However, such a parameter has been evaluated under overoptimistic hypotheses, namely assuming that inter-nodes distances are scattered as randomly as a HPPP dictates, and that the sensors are omnidirectional. A numerical investigation of a generalized Jakes model, keeping fixed the angular beam of interest for the received signal, and relying on distance statistics tailored on a non-isotropic node radiation pattern (see e.g. [88, Corollary 3]) would offer more significant results.

The Toeplitz scenario is the more challenging from a mathematical point of view. Indeed, the given bound is trivial when  $\mu = 1$ , which indeed should be at least on the main diagonal. Consider, however, that an actual evaluation of the correlation number would involve nonlinear statistics of the noncentral Toeplitz matrix entries, while we are herein exploiting results on the spectral norm, i.e. the square of the maximum eigenvalue of the matrix under exam. Notice further that the given result is based on approximating the elements of the random correlation matrix to have all the same first moment, which clearly does not apply to a real world scenario.

The *brute-force* generalization (and, even, adoption without any adaptation) of the correlation models of the point-to-point scenario is questionable, though, it suggests further lines of investigations. Mostly, the question arises of how to refine the stochastic channel model in order to embody the system geometry, while keeping it still analytically tractable. We believe that a good alternative to separable correlation models, actually subject of ongoing work, is the adoption of Vandermonde-like channel matrices ([101]) in order to accounting for the randomness of phases relationships between the receive sensors

## 7.5 Planned developments

Summarizing, the proposed approach to model the channel impairments in wireless networks with randomly deployed nodes consists of two stages, a macroscopic one, aimed at evaluating the overall scaling through a cut-set argument by exploiting some recent results in non-Gaussian large random matrices characterization, and a microscopic one, whose potentiality have not yet been fully exploited, and that we plan to investigate in the near future. Actually, while the macroscopic model is more suitable for fully ad-hoc networks (i.e. total absence of coordination and centralization), the latter one would offer more insight in the structured case, allowing for the analytical characterization of the channel between nodes belonging to a single cluster or, more in general, to properly chosen (on the basis of the communication paradigm and of the structure hypotheses) nodes' subsets. Relying on both the above mentioned results as well as on more recent studies (see e.g. [102], where the case of a finite number of nodes in the point process is considered, or further developments in the stochastic geometry impact on the communication performance like in [103]), we plan to obtain developments on scaling laws for the following cases:

- Given an ad-hoc network where each node is able to perfectly null, decode or cancel the interference transmitted by its  $K$  nearest neighbors, we may achieve the goal of evaluating the capacity scaling based on the order statistics of the distance between the nodes, following the approach in [104]; See section 7.5.1 below.
- Given a dense network provided of some infrastructure, no relaying of the information (like in the ad-hoc paradigm) is necessary, and only the interference must be modeled through random matrix tools. This could be given through a characterization of the Signal-to-Interference plus Noise Ratio based on the tools in [102].

The starting point of our approach is the mitigation of short-range interference, as described below.

### 7.5.1 Short-Range Interference Mitigation

Interference alignment has been proposed recently [105] as an approach for coding for the K-user interference channel.

Considering  $K$  pairs of users trying to establish one-to-one communications, and assuming flat-fading MIMO channels remaining constant during the time of transmission, the received signal for user  $k$  can be written in vector notation at a given time instant as

$$\underline{y}_k = \sqrt{\gamma_{kk}} \mathbf{H}_{kk} \mathbf{V}_k \underline{s}_k + \sum_{j=1, j \neq k}^N \sqrt{\gamma_{kj}} \mathbf{H}_{kj} \mathbf{V}_j \underline{s}_j + \underline{n}_k, \quad (104)$$

where  $\underline{s}_k \in \mathbb{C}^{d_k \times 1}$  is the  $k^{\text{th}}$  transmit signal,  $\mathbf{V}_k \in \mathbb{C}^{n_T \times d_k}$  is a precoding matrix, and  $\mathbf{H}_{kk}$  and  $\mathbf{H}_{kj} \in \mathbb{C}^{n_R \times n_T}$  are MIMO channels matrices.  $\underline{n}_k \sim \mathcal{CN}(0, \mathbf{I}_{n_R})$  accounts for the thermal noise generated in the radio frequency front-end of the receiver.  $\gamma_{kj}$  is the path loss coefficient and a power budget is usually given, i.e.,  $\text{Tr}(\mathbf{Q}_{\underline{s}_k \underline{s}_k}) = \text{Tr}(\mathbb{E}_{\underline{s}_k}[\underline{s}_k \underline{s}_k^H]) = \rho_k$  for  $k = 1 \dots N$ .

In this system of  $K$  transmitter-receiver pairs, interference alignment with multiplexing gains  $(d_1, \dots, d_K)$  is achievable if there exists  $n_T \times d_k$  truncated unitary matrices (precoding matrices)  $\mathbf{V}_k$  and  $n_R \times d_k$  truncated unitary matrices (ZF interference suppression matrices)  $\mathbf{U}_k$  such that, for  $k = 1, \dots, K$

$$\begin{aligned} \mathbf{U}_k^H \mathbf{H}_{kj} \mathbf{V}_j &= 0, \forall j \neq k \\ \text{rank}(\mathbf{U}_k^H \mathbf{H}_{kk} \mathbf{V}_k) &= d_k. \end{aligned} \quad (105)$$

The achievable performance of this scheme in the case where the considered  $K$  nodes form an isolated cluster (i.e. there is no source of interference outside of the  $N - 1$  cooperating transmitters) has been analyzed in [106]. The resulting equations (including pre-coding and zero-forcing at the receivers) can be interpreted as an equivalent  $d_k \times d_k$ -MIMO system. Performance analysis is facilitated by the fact that  $\mathbf{H}_{kk}$  is independent from  $(\mathbf{U}_k, \mathbf{V}_k)$ , and that if  $\mathbf{H}_{kk}$  is Gaussian i.i.d., then  $\mathbf{U}_k^H \mathbf{H}_{kk} \mathbf{V}_k$  is Gaussian i.i.d. as well. Furthermore, bounds on the average mutual information for the case of interference alignment based on imperfect channel knowledge are provided in [106].

If the number of antennas per node is fixed, interference alignment is only achievable among a finite number of nodes [107]. Therefore, when considering large networks (with a number of nodes  $n \rightarrow +\infty$ ), interference alignment over constant channels is only possible among a finite subset of nodes. Therefore, it is necessary to account for interference from transmitters which are not collaborating in the alignment. We address this by considering clusters comprising a finite number of nodes, among which interference alignment is performed. Nodes outside the cluster contribute interference in the classical sense, i.e. whose statistical properties are uncorrelated with what happens inside the considered cluster.

Furthermore, we assume that nodes inside a cluster are able to exchange channel state information and implement interference alignment. Using the above notations, the received signal of user  $k$  inside the cluster after (zero-forcing) interference suppression yields

$$\begin{aligned} \bar{y}_k &= \sqrt{\gamma_{kk}} \mathbf{U}_k^H \mathbf{H}_{kk} \mathbf{V}_k \underline{s}_k + \sum_{j \neq k \in (\Omega \cup \Omega^c)} \sqrt{\gamma_{kj}} \mathbf{U}_k^H \mathbf{H}_{kj} \mathbf{V}_j \underline{s}_j + \mathbf{U}_k^H \underline{n}_k \\ &= \sqrt{\gamma_{kk}} \mathbf{U}_k^H \mathbf{H}_{kk} \mathbf{V}_k \underline{s}_k + \sum_{j \neq k \in \Omega^c} \sqrt{\gamma_{kj}} \mathbf{U}_k^H \mathbf{H}_{kj} \mathbf{V}_j \underline{s}_j + \bar{n}_k, \end{aligned} \quad (106)$$

where we used the fact that all interference from transmitters inside the cluster  $\Omega$  is perfectly suppressed, due to (105).

In future, we plan to propose a performance analysis of (106), based on a clustered wireless ad hoc network. The clustering of nodes may be due to geographical factors or may also be induced by MAC protocols. In particular we consider a stochastic geometry based on [104]. In [104], the authors consider single antenna nodes, path loss model and fading model. They show that clustering of transmitters is beneficial for large link distances, while the success probability of communication at smaller link distances

is lower than in a network with transmitter positions governed by a homogeneous Poisson process with the same intensity. This loss is caused by the the dominant interference arising from nodes in the cluster around the transmitter, which cause maximum "damage". We plan to adopt a geometric model based on the Neyman-Scott cluster process. We focus our attention at the cluster which includes transmitter  $k$  and assume that the number of daughter points in the Neyman-Scott cluster process is fixed. By considering order statistics on the distances, we separate interference from inside the cluster from the interference coming from the rest of the network. We plan characterize the statistics of the out-of-cluster interference, since intra-cluster interference can be nulled perfectly as per (106).

## 8 STATUS OF JRAS

### 8.1 JRA 1: Distributed implementations of backpressure protocols in wireless networks

**Involved partners:** CNIT-POLITO, NKUA/IASA.

The objective of this JRA is to research, design and implement decentralized scheduling algorithms that lead to maximum throughput in wireless networks. The backpressure scheduling policy requires to compute the solution of a linear-programming (LP) problem based on the centralized knowledge of all queue sizes in the entire network. Fortunately, the policy is based on a metric which refers only to neighboring nodes. Indeed, the weight of a queue, considered on the LP problem, depends only on the size of the queue at the node and on the size of the downstream queue. Hence, a local interaction between neighboring nodes is required to compute the weight.

Let each node be characterized by a weight, representing its queue size. We would like to activate the subset of nodes that form an eligible schedulable set such that the total weight of this set is maximum. This is equivalent to determining the Maximum Weight Independent Set (MWIS) in a graph. This hard combinatorial optimization problem can be solved quite efficiently with the so called message passing algorithms. This class of algorithms relies on iterative message passing among nodes until convergence to a solution. For the maximum weighted matching problem, it has been shown that these algorithms converge to an optimal solution under some mild assumptions.

We would like to exploit this local interaction among neighboring nodes to devise a distributed scheduling algorithm, based on a message-passing approach. Thus, we will be able to approximate the optimal policy in an efficient way. In particular we intend to apply the rationale of message passing approaches to IEEE 802.11 CSMA/CA based wireless networks.

The research road map for this JRA goes as follows:

- Research and understand message passing algorithms for solving the the MWM or MWIS problems.
- Turn these algorithms into appropriate message passing protocols that take into account the specifics of CSMA/CA.
- Implement these message passing access control protocols in a realistic wireless test-bed.

For IEEE 802.11 based networks that are based on random access, it seems that MWIS is a better suited approach to consider and thus we will focus our approaches toward this optimization problem.

Regarding the second step in the road map we are currently investigating the specifics of CSMA/CA. CSMA/CA is a randomized means of medium access, where channel access is regulated through the probabilistic backoff algorithm. Nodes that (randomly) select smaller backoff instances according to a uniform distribution within a certain contention window intervals are granted channel access. The idea for taking into account the specifics of the CSMA/CA protocol while incorporating message passing approach is as follows.

We divide time into successive control intervals and data transmission intervals. A period is defined to consist of a control and a data transmission interval. During the control interval, nodes are let to execute a message passing algorithm until they converge to some solution. The messages are essentially functions of the local weights (namely the queue sizes) and the previously received weights of others. Suppose nodes converge to an independent set. Then, during the data transmission interval, they need to transmit their data. Each transmission interval consists of a certain number of (virtual) time slots. These time slots may be formed through a slight change in the backoff algorithm. That is, nodes that are included in the solution that emerged from the message passing algorithm decide on a backoff vector that will effectively define a round robin slot allocation to each one of them. We are currently contemplating on potential alternatives. The next step would be to implement this protocol in a realistic test-bed consisting of 802.11 mesh nodes.

## 8.2 JRA 2: On the Interplay between MAC Protocols and Data Fusion in Wireless Sensor Networks

**Involved partners:** CNIT-UniBo, CTTC.

Among the applications of Wireless Sensor Networks (WSNs) research emerged in recent years, environmental monitoring and event detection are attracting a growing attention.

In the most basic configuration, a group of sensors is in charge of taking samples of some parameter of interest (e.g., pressure, humidity, etc. . . ) and wirelessly communicating the readings to a fusion center. Due to limitations of sensing devices, the collected measurements are affected by noise. The fundamental issue in such a system is to optimize the number of sensors to be deployed. In fact, in order to have an accurate estimation, it is desirable to have as many measurements as possible. However, the finite channel capacity imposes a limitation on the overall data rate from sensors to fusion center. Consequently, each sensor must encode its observation with a finite number of bits and, thus, this results in a quantization noise added to the measurement to be transmitted to the fusion center.

The work performed within the present JRA aims at extending the model introduced in [108] and is mainly focused on two aspects.

On the one hand, the network model could be improved by considering a more sophisticated network architecture and accounting for MAC losses occurring during transmissions. In particular, when a large amount of sensors transmit their measurements to a relay node or to the fusion center, packet collision is very likely to happen, this resulting in a decimation of the information gathered at the endpoint and, consequently, in a poor quality estimation. Moreover, the analysis carried out in [110, 111] on the performance of IEEE 802.15.4 MAC protocol may easily be applied to the current model and the effects of changing the parameters of the standard may be evaluated. For example, by considering the 802.15.4 Beacon Enabled mode, different values of beacon interval, superframe order and duration and packet size will lead to potentially various network behaviors and, in turn, quality of estimation.

On the other hand, the target estimate to be performed could be generalized into a spatial field estimation. In this case, each sensor observes a different point of a bi-dimensional process (e.g., temperature over a large area) and sends its reading to the fusion center. The accuracy in reconstruction of the underlying process may then be computed by means of random sampling theory. To this end, the approach of [109] is taken as a starting point. A field of sensors is uniformly and randomly deployed over the monitoring area. According to random sampling theory, reconstruction of the process depends on nodes density: the greater it is, the more the aliasing noise can be reduced. However, limited bandwidth once again requires quantization which, in turn, adds noise to the transmitted samples and make estimation quality poorer.

## 8.3 JRA 3: Network entity behavioral modeling as a dynamic game

**Involved partners:** CNIT-UniCT, NKUA/IASA

The objective of this JRA is to develop a generic model for network entity behavioral modeling and identification of malicious behavior. We intend to make use of a Markov chain model consisting of two or more states for each node. Each state will denote the different degree of goodness or badness that will be exhibited by each node. For simplicity, assume there exist two states for each node. Now suppose that there are  $N$  behavioral states in total in the network. These states span the entire range of possible behavioral profiles. Each node behavior is characterized by a subset  $\mathcal{S}_i$  of these  $N$  states (say  $|\mathcal{S}_i| = 2$  for each  $i$  for simplicity and let  $\mathcal{S}_i = \{S_{i1}, S_{i2}$ . Also each node is characterized by a transition probability  $p_i$  for transition from  $S_{i1}$  to  $S_{i2}$  and a transition probability  $p'_i$  for transition from  $S_{i2}$  to  $S_{i1}$ . For each node the state subset  $\mathcal{S}_i$  and transition probabilities are private information, which model its behavioral profile and dynamic behavior among these states.

Nodes engage in contacts and make some type of abstract transactions. The output of each transaction is an observation  $y$ . Suppose again for simplicity that we have encounters and transactions only among pairs of nodes. After the transaction, say between nodes  $i$  and  $i$  nodes observe  $y_i$  and  $y_j$  respectively. These observations are statistically connected with each of the  $N$  states, namely there exist given distributions

$\Pr(y|s)$  for each state  $s$ . For instance a transaction outcome  $y$  that is connected with a good behavior has more probability weight for these states  $s$  that indicate good behavior.

Each transaction incurs a payoff vector  $(u_i, u_j)$  for each node pair. Each node updates its belief about the behavioral profile of others after each transaction. Ideally each node would like to encounter only good nodes and make transactions with them. One issue here is that good nodes are always popular and can make only a limited amount of transactions. We can model this constraint through an upper bound on the utility or some other constraint. The objective is to study the interactions of these nodes, see how opinions are formed, how is learning achieved amidst a stochastic environment where no prior knowledge is assumed.

The ultimate objective is to see what are the network operating points  $\mathbf{u}$  to which the system is driven. A network operating point consists of the per transaction or the total utilities of all nodes (in the long run). Next, we would like to explore potential ways in which nodes can actually affect this operation point.

#### 8.4 JRA 4: Connectivity and MAC issues and the impact of different node spatial distributions

**Involved partners:** CNIT-UniBo, RWTH

The aim of this JRA is to study the impact of different node spatial distributions on connectivity and MAC issues. By considering a set of scenarios, briefly described in the sequel, we intend to develop a mathematical framework which allows us to study the network performance from the connectivity and MAC viewpoints.

Sensors and sinks could be distributed over bounded or unbounded regions according to a given distribution. Therefore, we intend to study single-sink and multi-sink scenarios, where nodes are distributed according to different distributions, over infinite or finite areas, with different shapes. In particular, we will consider square or rectangular areas, or areas composed of various rectangles, with different values of node densities in each of them. Two different topologies will be studied, namely star and tree-based. In the first one, sensors transmit to the selected sink (that could be the sink providing the strongest signal strength) through a direct link; in the latter case, instead, sensors are organized in trees having a sink as root. We assume that sensors access the channel through a CSMA based protocol, like the IEEE802.15.4 MAC protocol.

This JRA will have the following two main objectives:

- Devise a mathematical framework that takes CSMA and connectivity issues into account under a joint approach;
- Exploit different sensors and sinks distributions in order to study their impact on network performance.

We will develop a mathematical model to derive, for all scenarios mentioned above, the probability that a given sensor node is connected to at least one sink, and that it succeeds in transmitting its packet, considering different CSMA based protocols.

#### 8.5 JRA 5: Scaling laws in wireless networks

**Involved partners:** FTW, CNRS.

In a previous chapter, we have outlined the background and objectives of this JRA. Here, we summarize the main roadmap for this JRA. The proposed approach to model the channel impairments in wireless networks with randomly deployed nodes consists of two stages, a macroscopic one, aims at evaluating the overall scaling through a cut-set argument by exploiting some recent results in non-Gaussian large random matrices characterization, and a microscopic one, whose potentiality have not yet been fully exploited, and that we plan to investigate in the near future. Actually, while the macroscopic model is more suitable for fully ad-hoc networks (i.e. total absence of coordination and centralization), the latter one would offer more insight in the structured case, allowing for the analytical characterization of the channel between nodes belonging to a single cluster or, more in general, to properly chosen (on the basis of the communication paradigm and of the structure hypotheses) nodes' subsets. Relying on both the above

mentioned results as well as on more recent studies where the case of a finite number of nodes in the point process is considered, or further developments in the stochastic geometry impact on the communication performance like in [103]), we plan to obtain developments on scaling laws for the following cases:

- Given an ad-hoc network where each node is able to perfectly null, decode or cancel the interference transmitted by its  $K$  nearest neighbors, we may achieve the goal of evaluating the capacity scaling based on the order statistics of the distance between the nodes, following the approach in [104]; See section 7.5.1 below.
- Given a dense network provided of some infrastructure, no relaying of the information (like in the ad-hoc paradigm) is necessary, and only the interference must be modeled through random matrix tools. This could be given through a characterization of the Signal-to-Interference plus Noise Ratio based on the tools in [102].

The starting point of our approach is the mitigation of short-range interference, as described above. Specifically we intent to leverage the proposed technique of interference alignment towards this goal.

In future, we plan to propose a performance analysis of based on a clustered wireless ad hoc network. The clustering of nodes may be due to geographical factors or may also be induced by MAC protocols. In particular we consider a stochastic geometry based on [104]. In [104], the authors consider single antenna nodes, path loss model and fading model. We plan to adopt a geometric model based on the Neyman-Scott cluster process. We focus our attention at the cluster which includes transmitter  $k$  and assume that the number of daughter points in the Neyman-Scott cluster process is fixed. By considering order statistics on the distances, we separate interference from inside the cluster from the interference coming from the rest of the network. We plan characterize the statistics of the out-of-cluster interference, since intra-cluster interference can be nulled perfectly as discussed above.

## 8.6 JRA 6: Cooperative multi-casting algorithms in wireless networks

**Involved partners:** CTTC, NKUA/IASA.

In this JRA we plan to explore cooperative algorithms and techniques to boost the capacity of wireless networks. We assume a wireless adhoc network consisting of a set of nodes, each of which is equipped with an adaptive antenna array capable of spatial multiplexing and beamforming according to IEEE 802.11n. In previous work of CTTC an NKUA/IASA, we have researched cooperative protocols and techniques for wireless networks of nodes with omnidirectional antennas. The main idea there was to take advantage of message overhearing by other nodes to improve either transmission quality or the amount of successful transmissions from sender to receiver. We now ask the question: how can these techniques be extended, or new ones be designed in the context of networks where nodes can control also the directionality of transmission through beamforming.

We plan to exploit the background research of both partners and further integrate it. NKUA/IASA has already proposed a new approach to describe physical layer multicast transmission using cross-layer approach, enabling techniques as beamforming, MIMO antennas, OFDM and low latency MAC operation. The obtained simulation results show a substantial improvement in network performance for the proposed strategy in IEEE802.11n wireless access networks.

On the other hand, CTTC has focused on practical solutions to implement multiuser downlink transmission in infrastructure 802.11n based WLANs. A low-complexity beamforming transmission technique is employed at the physical layer and four MAC schemes that vary in complexity and efficiency have been presented. Moreover, some preliminary results through computer simulations have been shown. The directions of research for this recently introduced JRA are the following:

- Include advanced multiuser MAC protocols in 802.11n based systems.
- Study and analyze opportunistic schemes based on SNIR thresholds in the feedback channel.

In the near future, we expect at least one and perhaps two planned researcher or student exchanges to take place between NKUA/IASA and CTTC in order to materialize the objectives of the JRA.

## 9 CONCLUSIONS

In this report we have presented an overview of recent advances accomplished in the context of WPR.10 partners. The research contributions spanned the area of Network Theory, with particular emphasis on autonomous operations of peer-to-peer networks, distributed resource allocation, scaling laws and sensor networks. The results presented in these areas aid in enhancing our understanding about fundamental performance limits of networks in terms of derived utility versus incurred cost, utility from content sharing, throughput and energy efficiency, or estimation quality. Each chapter focuses on a different aspect of network theory with corresponding ramifications on advances in understanding performance limits of networks. We considered cooperation in autonomous wireless and peer-to-peer networks, distributed scheduling algorithms through message passing and optimization of wireless sensor networks performance were the main topics that we focused. We derived both analytical and numerical results and proofs of our findings.

We also presented the status of six JRAs through which research integration among partners is realized. The six different ongoing JRAs span the areas of decentralized resource allocation, cooperative communications, impact of access control and connectivity on performance of WSNs, asymptotic scaling laws of wireless networks, as well as behavioral modeling and detection of misbehavior in wireless networks. Through these JRAs that will hopefully end up with successful collaboration and joint publications, we aim at addressing the WP objectives.

**REFERENCES**

- [1] L. Buttyan and J.-P. Hubaux, “Security and cooperation in wireless networks”, *Cambridge University Press*, 2008.
- [2] L. Galluccio, “A game-theoretic approach to prioritized transmission in wireless CSMA/CA Networks,” *IEEE VTC 2009, Barcelona, Spain*, April 2009.
- [3] J. Zander, “Jamming in slotted ALOHA multihop packet radio networks,” *IEEE Trans. on Comm.*, Vol. 39, No. 10, Oct. 1991.
- [4] A. B. MacKenzie and S. Wicker, “Stability of multipacket slotted ALOHA with selfish users and perfect information,” *IEEE Infocom 2003, S. Francisco, CA*, Apr. 2003.
- [5] M. Cagalj, S. Ganeriwal, I. Aad, and J.-P. Hubaux, “On selfish behavior in CSMA/CA networks,” *IEEE Infocom 2005, Miami, FL*, Mar. 2005.
- [6] Y. Zhang, H. Hu, and M. Fujise, “Resource, Mobility and Security Management in Wireless Networks and Mobile Communications”, Auerbach Publications.
- [7] M. Felegyhazi and J. P. Hubaux, “Game theory in wireless networks: a tutorial,” *EPFL Technical report LCA-Report-2006-002*, Feb. 2006.
- [8] G. Bianchi, “Performance analysis of the IEEE 802.11 distributed coordination function,” *IEEE Journ. on Sel. Areas in Comm.*, Vol. 18, No. 3, Mar. 2000.
- [9] I. F. Akyildiz *et al.*, “A survey on sensor networks,” *IEEE Comm. Mag.*, vol. 40, no. 8, pp. 102-114, Aug. 2002.
- [10] Standard, “IEEE 802.15.4: Wireless medium access control (MAC) and physical layer (PHY) specifications for low-rate wireless personal area networks (lr-wpans),” *IEEE*, 2003.
- [11] J. Riihijärvi, P. Mähönen, and M. Rubsamen, “Characterizing wireless networks by spatial correlations,” *Communications Letters, IEEE*, vol. 11, no. 1, pp. 37-39, 2007.
- [12] P. Stuedi, O. Chinellato, and G. Alonso, “Connectivity in the presence of shadowing in 802.11 ad hoc networks,” in *IEEE WCNC 2005*, vol. 4, 13-17 March 2005.
- [13] C. Bettstetter, “On the minimum node degree and connectivity of a wireless multihop network,” in *Mobile Ad Hoc Networks and Comp.(Mobihoc), Proc. ACM Symp. on*, Jun. 2002.
- [14] Z. Vincze, R. Vida, and A. Vidacs, “Deploying multiple sinks in multi-hop wireless sensor networks,” in *IEEE International Conference on Pervasive Services*, 15-20 July 2007, pp. 55–63.
- [15] P. Santi, “Topology control in wireless ad hoc and sensor networks,” *ACM Comp. Surveys*, vol. 37, no. 2, pp. 164–194, 2005.
- [16] P. Mähönen, M. Petrova, and J. Riihijärvi, “Applications of topology information for cognitive radios and networks,” in *Proc. of IEEE DySPAN*, 2007.
- [17] M. Petrova, P. Mähönen, and J. Riihijärvi, “Connectivity analysis of clustered ad hoc and mesh networks,” in *IEEE GLOBECOM '07*, 2007.
- [18] M. Thomas, “A generalization of poisson’s binomial limit for use in ecology,” *Biometrika*, vol. 36, pp. 18–25, 1949.
- [19] J. Hoydis, M. Petrova, and P. Mähönen, “Effects of topology on local throughput-capacity of ad hoc networks,” in *Proc. of IEEE PIMRC 2008*, Cannes, France, September 2008.

- [20] R. Verdone, F. Fabbri, and C. Buratti, "Area throughput for CSMA based wireless sensor networks," in *Proc. of IEEE PIMRC 2008*, Cannes, France, September 2008.
- [21] C. Buratti and R. Verdone, "A mathematical model for performance analysis of IEEE 802.15.4 Non Beacon-Enabled mode," in *Proc. of European Wireless 2008*, Prague, Czech Republic, 2008.
- [22] —, "Performance analysis of IEEE 802.15.4 non-beacon enabled mode," accepted for publication on *IEEE Transaction on Vehicular Technology*, 2009.
- [23] A. Ribeiro and G.B. Giannakis, "Bandwidth-constrained distributed estimation for wireless sensor networks part I: Gaussian case," *IEEE Trans. on Signal Proc.*, vol. 54, no. 3, pp. 1131-1143, Apr. 2005.
- [24] J.-J. Xiao, S. Cui, Z.-Q. Luo, and A. J. Goldsmith, "Power scheduling of universal decentralized estimation in sensor networks," *IEEE Trans. on Signal Proc.*, vol. 54, no. 2, pp. 431-422, Feb. 2006.
- [25] M. Gastpar and M. Vetterli, "Source-channel communication in sensor networks," in *Lecture Notes in Computer Science*, April 2003, pp. 162-177.
- [26] S. Cui, J. Xiao, A. Goldsmith, Z.-Q. Luo, and H. V. Poor, "Estimation diversity and energy efficiency in distributed sensing," *IEEE Trans. on Signal Proc.*, vol. 55, no. 9, pp. 4683 – 4695, Sept. 2007.
- [27] R. Knopp and P. A. Humblet, "Information capacity and power control in single-cell multiuser communications," in *IEEE ICC*, vol. 1, June 1995, pp. 331-335.
- [28] D. N. C. Tse, "Optimal power allocation over parallel gaussian broadcast channels," in *Proc. of International Symp. Inform. Theory*, June 1997, p. 27.
- [29] D. Gesbert and M.-S. Alouini, "How much feedback is multi-user diversity really worth?" in *IEEE Int'l Conference on Communications*, June 2004, pp. 234–238.
- [30] S. Sanayei and A. Nosratinia, "Opportunistic downlink transmission with limited feedback," *IEEE Trans. on Informtion Theory*, vol. 53, no. 11, pp. 4363–4372, Nov. 2007.
- [31] W. Yu and M. Cioffi, "Constant-power waterfilling: Performance bound and low-complexity implementation," *IEEE Trans. on Communications*, vol. 54, no. 1, pp. 23-28, Jan. 2006.
- [32] Y. Chen, Q. Zao, V. Krishnamurthy, and D. Djonin, "Transmission scheduling for optimizing sensor network lifetime: A stochastic shortest path approach," *IEEE Transaction on Signal Processing*, no. 5, pp. 2294–2309, May 2007.
- [33] S. Cui, J. Xiao, A. Goldsmith, Z.-Q. Luo, and H. V. Poor, "Energy-efficient joint estimation in sensor networks: Analog vs. digital," *IEEE ICASSP*, 2005.
- [34] S. Sanayei and A. Nosratinia, "Opportunistic beamforming with limited feedback," *IEEE Trans. on Wireless Communications*, vol. 6, no. 8, pp. 2765-2771, Aug. 2007.
- [35] J. Matamoros and C. Antón-Haro, "Opportunistic power allocation schemes for wireless sensor networks," in *Proc. IEEE ISSPIT*, December 2007, pp. 220-224.
- [36] J. Matamoros and C. Antón-Haro, "Opportunistic power allocation schemes for the maximization of network lifetime in wireless sensor networks," in *IEEE ICASSP 2008*, April 2008, pp. 2273-2276.
- [37] S. M. Kay, *Fundamentals of Statistical Signal Processing: Estimation Theory*.
- [38] J. Matamoros and C. Antón-Haro, "Opportunistic power allocation in wireless sensor networks with imperfect channel state information," in *in Proceedings of the ICT-Mobile Summit 2008*, June 2008.

- [39] Y. Chen and Q. Zao, "On the lifetime of wireless sensor networks," *IEEE Comm. Letters*, no. 1, pp. 976-978, Nov. 2005.
- [40] L. Tassiulas, and A. Ephremides, "Stability properties of constrained queueing systems and scheduling policies for maximum throughput in multihop radio networks," *IEEE Transactions on Automatic Control*, no. 12, pp. 1936-1948, 1992.
- [41] S. Sanghavi, D. Shah, and A. S. Willsky, "Message Passing for Max-weight Independent Set," in *Proceedings of NIPS*, 2007.
- [42] K. Jain, J. Padhye, V. N. Padmanabhan and Lili Qiu, "Impact of interference on multi-hop wireless network performance," in *Springer, Wireless Networks*, no. 11, pp. 471-487, 2005.
- [43] M. F. Tappen, and W. T. Freeman, "Comparison of Graph Cuts with Belief Propagation for Stereo, using Identical MRF Parameters," in *Proceedings of ICCV*, 2003.
- [44] R. Gummadi, K. Jung, D. Shah and R. Sreenivas, "Feasible Rate Allocation in Wireless Networks," in *Proceedings of INFOCOM*, 2008.
- [45] R. Gummadi, K. Jung, D. Shah and R. Sreenivas, "Computing the Capacity Region of a Wireless Network," in *INFOCOM*, 2009.
- [46] I. Koutsopoulos, and G. Iosifidis, "Distributed Resource Allocation Algorithms for Peer-to-peer Networks", *In Proc. ACM ValueTools*, 2008.
- [47] N. Laoutaris, P. Rodriguez and L. Massoulie, "ECHOS: Edge Capacity Hosting Overlays of Nano data centers", *ACM SIGCOMM Comp. Comm. Review*, vol.38, no.1, pp.51-54, Jan. 2008.
- [48] M. Meo, and F. Milan, "A Rational Model for Service Rate Allocation in Peer-to-Peer Networks", *In Proc. of 8th IEEE Global Internet Symp., 2005*) March 2005.
- [49] <http://www.fon.com>.
- [50] S. Marti, and H. Garcia-Molina, "Limited reputation sharing in P2P systems", *In Proc. of 5th ACM Conf. on Electr. Commerce*, 2004.
- [51] B. Mortazavi, and G. Kesidis, "Incentive-compatible cumulative reputation systems for peer-to-peer file-swapping", *In Proc. IEEE CISS*, 2006.
- [52] A. Satsiou, and L. Tassiulas, "A Trust-Based Exchange Framework for Multiple Services in P2P Systems", *In Proc. of 7th Intern. Conf. on P2P Comp.*, 2007.
- [53] S. Marti, T. J. Giuli, K. Lai, and M. Baker, "Mitigating Routing Misbehavior in Mobile Ad hoc Networks", *In Proc. of 6th MobiCom*, 2000.
- [54] F. Milan, J. J. Jaramilo, and R. Srikant, "Achieving cooperation in multihop wireless networks of selfish nodes", *In Workshop GameNets*, 2006.
- [55] J. J. Jaramilo, and R. Srikant, "DARWIN: Distributed and Adaptive Reputation Mechanism for Wireless Adhoc Networks", *Proc. of 13th MobiCom*, 2007.
- [56] R.T.B. Ma, S.C.M. Lee, J.C.S. Lui, and D.K.Y. Yau, "An Incentive Mechanism for P2P Networks", *In Proc. Intern. Confer. Distr. Comp. Systems (ICDCS)*, pp.516-523, 2004.
- [57] M. Adler, R. Kumar, K. Ross, D. Rubenstein, T. Suel and D.D. Yao, "Optimal peer selection for P2P downloading and streaming", *In Proc. INFOCOM*, 2005.

- [58] K. Eger, and U. Killat, "TCPeer: Rate Control in P2P over IP Networks", *LNCS 4516, In 20th ITC20*, 2007.
- [59] F.P. Kelly, A. Maulloo, and D. Tan, "Rate Control for communication networks: Shadow prices, proportional fairness and stability", *J. Oper. Res. Soc.*, vol.49, no.3, pp.237-252, 1998.
- [60] M. Chiang, S. H. Low, A. R. Calderbank, and J. C. Doyle, "Layering as optimization decomposition: A mathematical theory of network architectures", *Proc. IEEE*, vol. 95, no. 1, pp. 255-312, Jan. 2007.
- [61] B. Johansson, P. Soldati and M. Johansson, "Mathematical decomposition techniques for distributed cross-layer optimization of data networks", *IEEE J. Select. Areas Commun.*, vol. 24, no. 8, pp. 1535-1547, Aug. 2006.
- [62] G. Iosifidis and I. Koutsopoulos, "Reputation-assisted utility maximization algorithms for peer-to-peer networks", *In Proc. IEEE IWQoS*, 2008.
- [63] C. Courcoubetis, and R. Weber, "Incentives for large peer-to-peer systems", *IEEE J. on Select. Areas Commun.*, vol.24, no.5, pp.1034-1050, May 2006.
- [64] D. R. Figueiredo, J. K. Shapiro, and D. Towsley, "A public good model of availability in peer to peer systems", *Tech. Rep. 04-27, CSE Dept*, Michigan State University, 2004.
- [65] S. Low, D.E. Lapsley, "Optimization-based flow control I: Basic algorithms and convergence", *IEEE/ACM Trans. Networking*, vol.7, no.6, pp.861-874, Dec. 1999.
- [66] D. Palomar, and M. Chiang, "Alternative decompositions for distributed maximization of network utility: framework and applications", *In Proc. INFOCOM*, 2006.
- [67] D.P. Bertsekas, *Non-linear Programming*, Athena Scientific, 2003.
- [68] S. Boyd and L. Vandenberghe, *Convex Optimization*, Cambridge, U.K.: Cambridge Univ. Press, 2004
- [69] E.K. Lua, J. Crowcroft, M. Pias, R. Sharma and S. Lim, "A survey and comparison of peer-to-peer overlay network schemes", *IEEE Comm. Survey and Tutorial*, March 2004.
- [70] <http://www.joost.com>.
- [71] D. Qu and R. Srikant, "Modeling and performance analysis of BitTorrent-like peer-to-peer networks", *Proc. ACM SIGCOMM*, 2004.
- [72] S. Buchegger and J.-Y.L. Boudec, "A Robust Reputation system for P2P and mobile ad-hoc networks", *Second Workshop on Economics of Peer-to-Peer Systems*, 2004.
- [73] S.D. Kamvar, M.T. Schlosser, and H. Garcia-Molina, "The eigentrust algorithm for reputation management in P2P Networks", *Proc. 12th International Conference on WWW*, 2003.
- [74] T.G. Papaioannou and G.D. Stamoulis, "Effective use of reputation in peer-to-peer environments", *Proc. 4th International Scientific Workshop on Global and Peer-to-Peer Computing*, 2004.
- [75] R.T.B. Ma, S.C.M. Lee, J.C.S. Lui, and D.K.Y. Yau, "Incentive and Service Differentiation in P2P networks: A Game theoretic approach", *IEEE/ACM Trans. Networking*, vol. 14, no. 5, pp. 978-991, Oct. 2006.
- [76] M. Feldman, K. Lai, and L. Zhang, "A Price-Anticipating Resource Allocation Mechanism for Distributed Shared Clusters", *Proc. 6th ACM Conference on Electronic Commerce*, Jun. 2005.

- [77] M. Feldman, K. Lai, J. Chuang, and I. Stoica, “Quantifying Disincentives in Peer-to-Peer Networks”, *In 1st Workshop on Economics of Peer-to-Peer Systems*, 2003.
- [78] M. Feldman, C. Papadimitriou, I. Stoica, and J. Chuang, “Free-Riding and Whitewashing in Peer-to-Peer Systems”, *Proc. SIGCOMM Workshop on Practise and Theory of Incentives and Game Theory in Networked Systems*, 2004.
- [79] A. Bharambe, C. Herley, and V. Padmanabhan, “Analyzing and improving a BitTorrent Network’s Performance Mechanisms”, *Proc. IEEE INFOCOM*, 2006.
- [80] G. Neglia, G. L. Presti, H. Zhang, and D. Towsley, “A network formation game approach to study BitTorrent Tit-for-Tat”, *In EuroFGI International Conference on Network Control and Optimization*, 2007.
- [81] P. Gupta and P. R. Kumar, “The Capacity of Wireless Networks”, *IEEE Trans. on Inf. Th.*, vol. 46, pp.,388-407, 2000.
- [82] S. Aeron S. and V. Saligrama, “Wireless ad-hoc networks: Strategies and Scaling laws for the fixed SNR regime ”, *IEEE Trans. on Inf. Th.*, vol. 53 , no. 6 , 2007.
- [83] Özgür, Ayfer and Lévêque, Olivier and Tse, David , “Exact Capacity Scaling of Extended Wireless Networks”, *IEEE Int. Symp. on Inf. Theory*, 2007.
- [84] Franceschetti, Massimo and Minero, Paolo and Migliore, Marco D., “The Capacity of Wireless Networks: Information-Theoretic and Physical Limits”, *Proc. of 45-th Allerton Conference*, 2007.
- [85] Bucci, Ovidio M. and Franceschetti, Giorgio , “n the degrees of freedom of scattered fields ”, *IEEE Trans. on Antennas and Prop.* , vol. 37 , no. 7, pp.918-926, 1989.
- [86] Giuseppa Alfano and Antonia Tulino and Maxime Guillaud , “High and Low-SNR Regimes for Stochastic Networks ”, *Proc. International Symposium on Information Theory and its Applications (ISITA)*, 2008.
- [87] G. Alfano, M. Guillaud, A. M. Tulino , “Scaling laws for large ad-hoc wireless networks with Wishart-Poisson fading ”, *ISSSTA 2008*, 2008.
- [88] , “A Geometry Inclusive Fading Model for Random Wireless Networks”, *Proc. of IEEE Int. Symp. on Inf. Theory*, 2006.
- [89] Charles Bordenave, “ Eigenvalues of Euclidean Random Matrices”, <http://www.citebase.org/abstract?id=oai:arXiv.org:math/0606624>, 2006.
- [90] O. Dousse and F. Baccelli and P. Thiran , “Impact of Interferences on connectivity in ad-hoc networks”, *IEEE/ACM Trans. Networking*, vol.13 , no.2 , pp.,425-436, 2005.
- [91] A. M. Tulino and S. Verdú, “Random Matrices and Wireless Communications”, *Foundations and Trends in Communications and Information Theory*, vol. 1 , no.1 , 2004.
- [92] M. Abramowitz and I. A. Stegun, “Handbook of Mathematical Functions with Formulas, Graphs, and Mathematical Tables”, *Dover Publications*, 1995.
- [93] A. Tulino, and A. Lozano, and S. Verdú, “High-SNR power offset of multiantenna communication ”, *IEEE Trans. on Information Theory*, vol. 51, no. 12, pp. 1019-1030, 2005.
- [94] A. Tulino, and A. Lozano, and S. Verdú, “Multiple antenna capacity in the low-power regime ”, *IEEE Trans. on Information Theory*, vol. 49 , no. 10 , pp. 1019-1030, 2003.

- [95] S. Verdú, "Spectral efficiency in the wideband regime", *IEEE Trans. Inform. Theory*, vol. 48 , no. 6 , pp. 1319-1343, 2002.
- [96] Abhayapala, T.D. and Pollock, T.S., and Kennedy, R.A., "Spatial decomposition of the MIMO wireless channels", *Proc. of 7th ISSPA*, 2003.
- [97] D. Gesbert and H. Bölcskei and D. Gore and A. J. Paulraj, " ", *MIMO Wireless Channels: Capacity and Performance Prediction*, 2000 .
- [98] Hyundong Shin and Jae Hong Lee, "Capacity of multiple-antenna fading channels: spatial fading correlation, double scattering, and keyhole ", *IEEE Transactions on Information Theory*, vol. 49 , no. 10, pp.,2636-2647, 2003.
- [99] W.C.Jakes, "Microwave mobile communications", *Journal of Information Technology Education*, vol. 1 , pp. 53-63, 1974.
- [100] I. S. Gradshteyn and I. M. Ryzhik, "Table of integrals, series, and products", *Academic Press* , 1983.
- [101] Ralf R. Müller, " A Random Matrix Model of Communication via Antenna Arrays ", 2001.
- [102] S. Srinivasa and M. Haenggi, "Distance Distributions in Finite Uniformly Random Networks: Theory and Applications", *IEEE Transactions on Vehicular Technology*, 2009.
- [103] R. K. Ganti and M. Haenggi, "Spatial and Temporal Correlation of the Interference in ALOHA Ad Hoc Networks", *IEEE Communications Letters*, 2009.
- [104] R. K. Ganti and M. Haenggi, "Interference and Outage in Clustered Wireless Ad Hoc Networks ", *IEEE Trans. on Information Theory* , 2009.
- [105] K. Gomadam and Viveck R. Cadambe and Syed A. Jafar , "Approaching the Capacity of Wireless Networks through Distributed Interference Alignment ", *submitted*, 2008.
- [106] R. Tresch and M. Guillaud, "Cellular Interference Alignment with Imperfect Channel Knowledge ", *International Workshop on LTE Evolution, Proc. IEEE International Conference on Communications (ICC)*, 2009.
- [107] R. Tresch and M. Guillaud and E. Riegler, "On the Achievability of Interference Alignment in the K-User Constant MIMO Interference Channel ", *Proc. IEEE Workshop on Statistical Signal Processing (SSP)*, 2009.
- [108] J. Matamoros and C. Anton-Haro, "Bandwidth Constraints in Wireless Sensor-Based Decentralized Estimation Schemes for Gaussian Channels," in *Global Telecommunications Conference, 2008. IEEE GLOBECOM 2008. IEEE* , vol., no., pp.1-5, Nov. 30 2008-Dec. 4 2008.
- [109] D. Dardari, A. Conti, C. Buratti and R. Verdone, "Mathematical Evaluation of Environmental Monitoring Estimation Error through Energy-Efficient Wireless Sensor Networks," in *IEEE Transactions on Mobile Computing*, vol. 6, no. 7, pp. 790-802, July 2007.
- [110] C. Buratti and R. Verdone, "Performance Analysis of IEEE 802.15.4 Non Beacon-Enabled Mode," in *IEEE Transactions on Vehicular Technology* (to appear).
- [111] C. Buratti, "Performance Analysis of IEEE 802.15.4 Beacon-Enabled Mode," submitted to *IEEE Transaction on Vehicular Technology*.